PACIFIC EARTHQUAKE ENGINEERING
RESEARCH CENTER

U.S.-Japan Workshop on the Effects of Near-Field Earthquake Shaking

March 20–21, 2000
San Francisco, California

Andrew S. Whittaker
Editor

Sponsors
Pacific Earthquake Engineering Research Center
Applied Technology Council
Japan Ministry of Education, Science, Sports, and Culture
U.S. National Science Foundation

PEER 2000/02
JULY 2000

U.S.-Japan Workshop on the Effects of Near-Field Earthquake Shaking

March 20 – 21, 2000
San Francisco, California

Andrew S. Whittaker
Editor

Organizers

Kenzo Toki and Hirokazu Iemura
Kyoto University

Andrew S. Whittaker
Pacific Earthquake Engineering Research Center
University of California, Berkeley

Sponsors

Pacific Earthquake Engineering Research Center
Applied Technology Council
Japan Ministry of Education, Science, Sports, and Culture
U.S. National Science Foundation

PEER Report 2000/02
Pacific Earthquake Engineering Research Center
College of Engineering
University of California, Berkeley
July 2000

FOREWORD

The January 1995, Hyogoken Nanbu earthquake devastated the port city of Kobe, Japan, with widespread damage to the built environment and great loss of life. The earthquake damaged buildings, bridges, industrial and transportation infrastructure, ports and harbors, and telecommunications systems. The direct and indirect losses from this earthquake were felt around the world.

Following the 1995 earthquake, the Japanese Ministry of Education, Science, Sports, and Culture initiated a five-year research program that addressed a wide variety of issues relating to the impact of a near-field earthquake on a major urban center. The issues addressed public policy, human response, risk assessment and management, response planning and disaster recovery, geotechnical and structural engineering, and engineering seismology. The five-year research endeavor was completed in March 2000. Much new information was gathered and promulgated in Japan. The results of the Japanese research are summarized in a 700+ page report entitled *Confronting Urban Earthquakes*[1].

The Pacific Earthquake Engineering Research (PEER) Center was formed in 1997 to develop, validate, and disseminate performance-based seismic design technologies for buildings and infrastructure to meet the diverse economic and safety needs of owners and society. The nine universities that constitute the core institutions of the Center are all based in major urban centers on the West Coast of the United States, a region vulnerable to severe earthquake shaking. A moderate or major earthquake in or near one of these urban centers would have dramatic state, national, and international social and fiscal implications, as demonstrated by the disaster in Japan in January 1995. As such, characterizing the effects of near-field shaking and understanding the effects of such shaking on the response of buildings, bridges, and other components of the built environment is an essential part of PEER's mission.

In mid-1999, the Pacific Earthquake Engineering Research Center was asked by representatives of the Japanese Ministry of Education, Science, Sports, and Culture to help organize a workshop in the United States to present the results of the Japanese five-year research program. The Center was approached because of its work on the effects of near-field earthquake shaking on the built environment. The Center proposed to host a joint U.S.-Japan workshop to present state-of-the-art information from both sides of the Pacific Rim's so-called Ring of Fire to design professionals, regulatory officials, researchers, faculty, and graduate students in the United States. The Japanese researchers accepted this proposal, and the workshop was held at the Radisson Miyako Hotel, San

---

[1] Toki, K. (*ed.*) 2000. *Confronting Urban Earthquakes.* Report of Fundamental Research on the Mitigation of Urban Disasters caused by Near-Field Earthquakes, Japanese Ministry of Education, Science, Sports and Culture. Tokyo.

Francisco, California, on March 20 and 21, 2000. More than 150 people, including 24 participants from Japan, attended the workshop. Professor Kenzo Toki of Kyoto University headed the Japanese delegation. Dr. Andrew Whittaker and Professor Jack Moehle of the Center led the U.S. delegation. Each paper presented at the workshop is included in these proceedings. The papers are organized in the order of presentation. Summary comments from the breakout sessions that were held in the late afternoon on March 21 are included following the acknowledgments. The Japanese papers that were presented at the poster session are not included; information on this work can be found in Toki (2000).

Near-field earthquake shaking in major urban centers will pose problems and challenges to all involved in earthquake risk mitigation for the foreseeable future. Nonetheless, the advances in knowledge and design practice that are presented in these proceedings will, if widely implemented, serve to reduce the great risk posed to Japan and the West Coast of the United States. Our collective challenge is to implement these advances in a timely manner.

Dr. Andrew Whittaker
Associate Director
Pacific Earthquake Engineering Research Center
University of California, Berkeley

ACKNOWLEDGMENTS

The U.S.-Japan Workshop on the Effects of Near-Field Earthquake Shaking was sponsored by the Pacific Earthquake Engineering Research Center, the Applied Technology Council, the Japanese Ministry of Education, Science, Sports, and Culture, and the U.S. National Science Foundation. Special thanks are due to Mr. Chris Rojahn, Dr. Gerry Brady, and Ms. Bernadette Mosby of the Applied Technology Council; Professors Kenzo Toki (Kyoto University), Hirokazu Iemura (Kyoto University) and Shunsuke Otani (University of Tokyo) representing the Japanese Ministry of Education, Science, Sports, and Culture; and Drs. Joy Pauschke and Shi-Chi Liu of the U.S. National Science Foundation.

Ms. Darlene Wright, Janet Cooks, and Barbara Mauk, and Mr. Ken Wong of the Pacific Earthquake Engineering Research Center worked with the staff of the Applied Technology Council to make local arrangements and finalize the workshop program. These significant contributions to the success of the workshop are gratefully acknowledged. Ms. Janine Hannel of the Center organized the submission of the manuscripts and finalized the publication of these proceedings.

The workshop and these proceedings were supported in part by the Pacific Earthquake Engineering Research Center through the Earthquake Engineering Centers Program of the National Science Foundation under Award Number EEC-9701568.

BREAKOUT SESSIONS ON MARCH 21, 2000

Three concurrent breakout sessions were held in the afternoon of March 21, 2000, to discuss socio-economic issues; hazard assessment; and methodologies, demand assessment, and capacity assessment. The sessions were co-chaired by Professors Mary Comerio and Kiyoshi Kobayashi (Socio-Economic Issues), Professors Scott Ashford and Fumio Yamazaki (Hazard Assessment), and Dr. Andrew Whittaker and Professor Shunsuke Otani (Methodologies, Demand Assessment, and Capacity Assessment). The discussions in each session were recorded. A summary of these records follows. Thanks are due to Professors Ashford and Ms. Carrie Barnecut for summarizing the discussions in the Socio-Economic and Demand Assessment breakout sessions.

Five subjects were identified for discussion in each breakout session, namely, (1) key impacts of near-field earthquakes, (2) gaps in current knowledge, (3) opportunities for research that could substantially impact current practice or policy, (4) possible changes to practice and policy in the short term, and (5) impediments to change in current practice or policy.

Summary remarks are enumerated below. Due to time constraints, not all subjects were discussed in each breakout session.

Socio-Economic Issues

Key impacts

1. Multifamily, low-income residential construction is often hardest hit by major urban earthquakes.
2. Social fabric is often badly damaged by urban earthquakes.
3. Closure of primary and secondary schools occurs because earthquake damage has a large impact on the community.
4. Redundant transportation systems contribute substantially to rapid recovery.

Gaps in current knowledge

1. Systematic procedures are needed for gathering post-earthquake socio-economic data.
2. Socio-economic data on recovery following urban earthquakes are needed.

Opportunities for research

1. Integration of socio-economic losses into loss-estimation models.
2. Development of cost/benefit analysis tools for mitigation.
3. Improvement of methods of communicating direct and indirect loss estimates to the public.

Short-term changes to practice and policy

1. Include socio-economic impact in recovery planning.
2. Improve and better fund recovery planning at the local level.
3. Implement and subsidize low-cost, high-impact mitigation measures such as retrofitting of residential construction.

Impediments to changes in practice and policy

1. Planning, environmental, and historic issues.
2. Risk of loss due to earthquakes perceived as smaller than other natural and man-made risks.

Hazard Assessment

Key impacts

1. Much more is to be learned regarding ground motion in the near field, including the relationships between the fling step and the directivity pulse, and between pulse period and earthquake magnitude.
2. Significant damage to structures and lifelines has resulted from fault rupture and ground distortion immediately adjacent to the line of rupture.

Gaps in current knowledge

1. Impacts of the directivity pulse and the fling step on the demand on and the resistance of structures.
2. No robust procedures for characterizing the directivity pulse and the fling step as a function of factors that could include earthquake magnitude, site conditions, distance to the fault, fault type, and rupture type (surface or subsurface).
3. Influence of simultaneous fault-parallel and fault-normal shaking on site response.
4. Effect of the directivity pulse on liquefaction potential.
5. Effect of near-field shaking on slope stability.

Opportunities for research

1. Parameterization of the directivity pulse and fling step (static displacement).
2. Effect of the directivity pulse and fling step on the response of structures.
3. Effect of simultaneous fault-parallel and fault-normal shaking on site response in the near field.

Short-term changes to practice and policy

1. Improved technology transfer to design professionals and regulators

Impediments to changes in practice and policy

1. Lack of understanding among educators, practitioners, and policy makers regarding the damaging effects of near-field earthquakes.
2. The code-change process (especially in the United States) is not conducive to rapid implementation of new knowledge.

Methodologies, Demand Assessment, and Capacity Assessment

Key impacts

1. The codes of design practice are not producing buildings that meet the expectations of the public.
2. New performance-oriented evaluation and design procedures should be developed and implemented in codes of design practice.

Gaps in current knowledge

1. The risks (exposure to loss) associated with code-compliant buildings in design earthquake shaking are unknown. [Such risks must be established before substantial changes are made to codes of practice such as requirements for strength and stiffness.]
2. The relationships between component failures and building collapse.
3. The lack of clearly defined qualitative performance levels for buildings (e.g., collapse prevention, life safety, and immediate occupancy), the corresponding structural damage states (e.g., cracking, concrete spalling, and rebar fracture), and the associated design values (e.g., concrete strain at spalling).
4. Robust mathematical models of steel and concrete components that can capture strength and stiffness degradation and fracture.

Opportunities for research

1. Gravity-load collapse of nonductile building components, frames, and systems.
2. Load redistribution in building frames following component failures.
3. Performance-oriented procedures for the evaluation and design of nonstructural building components.
4. Fragility curves for nonductile components in buildings and bridges.

5. Fragility curves for buildings and bridges to aid in post-earthquake network analysis and response and recovery.
6. Performance objectives for buildings based on rational benefit-cost analysis.

CONTENTS

CONFRONTING URBAN EARTHQUAKES

Kenzo TOKI [1]

"Confronting Urban Earthquakes" is the short expression for the title of the research project "Fundamental Research on Mitigation of Urban Disasters caused by Near-Field Earthquakes" that has been conducted under the auspices of the Japan Ministry of Education, Science, Sports and Culture as a four years program from fiscal years 1996 to 1999. The research group consists of Japanese researchers engaged in earthquake engineering and relevant fields, mainly from universities.

The Ministry suggested emphasis on particular fields rather than covering wide areas related to earthquake disasters because of the definition of the Grant in Aid for Scientific Research on Priority Areas. The main part of the research project is the core projects for which the research program for the entire period was designed beforehand and for which research funding had been assured for four years. This part comprises 8 research teams in three major categories such as strong ground motion due to inland active faults, structural response to a killer pulse induced by strong shaking and the postearthquake management of seismic disasters. The members of each team are basically fixed and the total number of researchers engaged in this part of the project is 84.

The other part of the project is the individual research that is selected by reviewers from proposals submitted by individual applicants. The total number of approved research projects is 149 for four years thus making the total number of researchers involved in this program more than 230. The annual grant is about US $30,000, and one third of them has been assigned to the individual research program.

The following are the titles and coordinators of the core programs, which are subdivided into the above three major categories.

Ground Motion

(A-1) Strong Motion Estimation for Active Faults with High Earthquake Potential. —K. Irikura

(A-2) Evaluation of Ground Motion for Urban Structures by Near Field Earthquakes. —T. Ohmachi

Structural Effects

(B-1) Macro-zonation of Potential Seismic Risk in Urban Cities. —S. Murakami

(B-2) Improvement of Structural Safety against Near-field Earthquakes in Urban Areas. —S. Otani

[1] *Graduate School of Civil Engineering, Kyoto University, Kyoto, Japan*
Email: toki@quake.kuciv.kyoto-u.ac.jp

(B-3) Disaster Mitigation Function by Transportation and/or Telecommunication System under Catastrophic Earthquakes. —H. Kameda, Y. Iida

Social Effects

(C-1) Real-Time Control System for Civil Infrastructure during Earthquake Disaster. —F. Yamazaki

(C-2) Information Management for Urban Earthquake Disaster Mitigation. —H. Kagami

C-3) Human Response under Densely Populated Space during Earthquakes Disaster. —O. Hiroi

When the project started, the coordinators expected to disseminate the outcome of the project to the researchers engaged in earthquake engineering of the world. As an implementation of this idea, a workshop was held in Taipei, Taiwan, on February 28 to 29, 2000. The papers of this report were compiled from the second workshop held in San Francisco, March 20 to 21, 2000.

RECIPE FOR STRONG MOTION ESTIMATION FROM ACTIVE FAULT EARTHQUAKES

Kojiro Irikura[1], Katsuhiro Kamae[2], and Tomotaka Iwata[3]

ABSTRACT

Recipes for estimating strong ground motion from large earthquakes caused to active faults are proposed based on the product of the Monbusho Scientific Research Program (Tokutei-A, Strong Motion Estimation for Active Faults with High Earthquake Potential). This program successfully developed the following four topics for establishing a methodology of strong motion prediction: assessments of active faults for evaluating hazard potentials of active faults and geometries of source fauls for estimating strong ground motions, source characterization based on inversion analysis of seismic recordings and theoretical modeling of dynamic rupture process, numerical techniques for modeling of subsurface structures from source to site from geophysical surveys and calculating seismic wave propagation in irregular layers, prediction of strong ground motions taking into account heterogeneous source, propagation-path and surface geology effects. Source characterizations are made based on the scaling relations of heterogeneous rupture processes obtained by a statistical analysis of the source inversion results of crustal earthquakes. For strong motion estimation we adopt a asperity model satisfying scaling relations for the heterogeneity of slip on the fault surface in a deterministic manner. The validity and applicability of strong ground prediction are examined in comparison with the observed records and actual damage from recent large earthquakes such as the 1995 Hyogo-ken Nanbu (Kobe) earthquake, the 1994 Northridge earthquake, and 1999 Kacaeli earthquake.

1. INTRODUCTION

Recent large earthquakes, such as the 1995 Hyogo-ken Nanbu (Kobe, Japan) earthqauke, the 1999 Kacaeli (Turkey) earthquake, and the Chi-chi earthquake occurred on well-mapped active faults. However, no obvious precursory evidences appeared even near the faults before the events. Damage caused by the events showed characteristic distributions depending on rupture process as well as geological conditions. For example, heavy damage in Kobe area larger than in the Awaji area during the 1995 Hyogo-ken Nanbu earthquake is explained by source effects such as slip heterogeneity and forward rupture directivity and basin-edge effects due to basin structures. In the Awaji area there was less damage although surface breaks appeared along the Nojima faults. This means the importance of strong ground motion prediction from earthquake faults to mitigate disaster for future earthquakes.

Scenario earthquakes for subject areas have gradually been popular to make seismic disaster prevention measures by some governmental agencies and municipalities. However, most of strong motion estimations in earthquake hazard analysis are still inclined to empirical methods. Peak ground acceleration and velocity and response spectrum for earthquake-resistant design are given by empirical methods as a function of magnitude, fault distance, ground condition. They have not been taken into account yet developments in seismology, such as source processes in earthquake faults and 3-D simulation in complex structures.

We attempted to make a recipe to popularize the prediction of ground motions for engineering purpose based on seismological fruits. Most of the uncertainties in predicting strong ground motion are to specify the proper methods of characterizing the source models of future earthquakes.

[1] *PI , Disaster Prevention Research Institute, Kyoto University, Uji, Kyoto 611-0011, Japan, Email: irikura@egmdpri01.dpri.kyoto-u.ac.jp*

[2] *Research Reactor Institute, Kyoto University, Kumatori, Osaka 590-0494*

[3] *Disaster Prevention Research Institute, Kyoto University, Uji, Kyoto 611-0011, Japan*

There are two important aspects of characterizing the earthquake sources, global and local source parameters. The global parameters such as total fault length, width, seismic moment and so on are obtained based on geological investigations of capable earthquake faults and seismological studies of source models. The local source parameters are slip heterogeneity on fault plane determined from the source inversion of crustal earthquakes. Based on the statistical analysis of the inverted results, we have studied the scaling relations of asperities satisfying the spatial heterogeneity of slip and its two-dimensional Fourier transform on the fault surface. Source modeling should be given on self-similar scaling relations of asperities and the k-squared model of the slip distributions on the fault surface.

The validity and applicability of strong ground prediction are examined in comparison with the observed records and actual damage during the 1995 Hyogo-ken Nanbu (Kobe) earthquake, the 1994 Northridge earthquake.

2. SOURCE CHARACTERIZATION

Another important issue for strong motion prediction is source process for a future earthquake. We take into account earthquakes caused by active faults. A question is "Do earthquakes due to a specific active fault have repeatedly a similar source process ?". If yes, it is possible to make source modeling for future earthquakes. One answer would be obtained follows from geological and geographical investigations so far done. Long-term evaluation of earthquake prediction has been made based extensive research of segmentation and grouping of active faults. They found that slip distributions along fault segments have similar features to the results from the source inversion using seismic data, e. g. slip is largest in the middle of the segment and decreases towards the edge as shown in Fig. 1(Nakata, et al.,1998). The other possible answer would be fault dynamics estimated by the waveform inversion of strong motion records. Bouchon et al. (1998) studied the characteristics of stress field before and after the 1995 Hyogoken Nanbu earthquake based on the results of the source inversion using near-field recordings. There is a relatively strong correlation between the initial and final stress distribution, which suggests that intrinsic fault properties, not modified by the earthquake, control the spatial distribution of tectonic stress over fault. Those results suggest the possibility that earthquakes originating in the same active faults have a similar source process repeatedly.

For estimating strong ground motions in a deterministic approach, we need to have two kinds of source parameters, global and local ones.

2.1 Global Source Parameters

The global source parameters are total fault length and width, average slip and slip duration, rupture velocity and so on, which are to characterize the macroscopic pictures of given source faults. They are inferred , based on geological investigations of capable earthquake faults and seismological studies of source models.

Total fault lengths (L) of scenario earthquakes would be evaluated as one of the long-term seismic hazard evaluation. Some attempts have been making to estimate segmentation and grouping of active faults based on branching features of seismic surface ruptures (Matsuda, 1998). Such surveys give us **strike (ϕ)** and **slip type** of every segment consisting of the fault system. **Dip angle (δ)** is inferred from seismic reflection profile.

Fault width cannot be directly determined from the geological survey but mostly from source modeling for waveform simulations compared with observed records. Watanabe et al. (1998) made a plot (Fig. 2) to show the relation of fault width (W) vs. length (L), compiling 87 inland earthquakes from the source parameter catalog by Wells and Coppersmith (1994) and 5 large earthquakes by Abe (1990). The saturation of the width yields for events larger than M 6.8, corresponding the thickness of seismogenic zones. The seismogenic zones are infered from the depth-frequency distribution of small earthquakes (Ito, 1990). Recent study by Ito (1999) shows that The seismogenic zones seem to have upper cutoff depth as well as lower cutoff depth derived from the seimic-aseismic boundary in the mid-crust dependent on regions.

The **seismic moment** of the capable faults are estimated by the empirical relationship between the source areas and seismic source(A = LW), then average slips are automatically constrained by the seismic moment and source area (e.g. Somerville et al. 1999).

It is also very important source parameters where rupture start on the fault, to which directions, and where terminate. Rupture nucleate at the bottom of the seismogenic zones because of stress concentration in the seismic-aseismic boundary (Sibson, 1992). The starting point and propagation direction of rupture is identified from the patterns of surface traces from geographical investigations and theoretical modeling. Nakata et al. (1998) proposed a method to identify the direction of rupture propagation, the termination of rupture and in some cases, the epicenter location based on the branching features of active faults as shown in Fig. 3. Such ideas were examined by the dynamic theory of earthquake faulting. Kame and Yamashita (1998) numerically studied the effect of medium fracturing on the dynamic growth of earthquake rupture, suggesting that the faulting is needed to bend in the arresting of rupture or to make branching near its termination.

2.2 Local Source Parameters – Fault Heterogeneity or Roughness –

The slip and slip velocity have been found not to be uniform in the source areas, in particular for large earthquakes more than 7 as clarified from the waveform inversion of rupture process (Wald, 1996). We need to know slip and slip velocity distribution in the source area as well as the average slip to estimate strong ground motions. We call here such source parameters local source parameters that express fault heterogeneity or roughness. So far slip models have been derived from longer period ground motions using the waveform inversion. Direct application of such long-period source models to strong ground motion estimation is not always available because higher ground motions than 1 Hz cannot be generated. Nevertheless, we found that the asperity models derived from the heterogeneous slip distribution using the waveform inversion of longer-period ground-motion recordings are available for estimating broad-band ground motions of engineering interest (e.g. Kamae and Irikura, 1998).

Somerville et al. (1999) analyzed the characteristics of slip models of totally fifteen crustal earthquakes ranging from about 6 to 7 in moment magnitude (Mw) for use in the prediction of strong ground motion. They used two approaches, deterministic and stochastic, in characterizing the slip models.

First they define **fault asperities** in a deterministic manner to quantify the properties of heterogeneous slip models. The asperities are areas on the fault rupture surface that have large slip relative to the average slip on the fault. An asperity is defined to enclose fault elements whose slip is 1.5 or more times larger than the average slip in the fault as shown in Fig. 4 (in detail refer to Somerville et al.,1999). The number of asperities in the slip models of those events is 2.6 on average. The slip contrast, the average slip on the asperities over average slip is about 2. The combined area of asperities on average occupies about 22 % of the total rupture area.

Total rupture area (A), combined area of asperities (Aa), and area of largest asperity (Am) scale in a self-similar manner with increasing seismic moment.

$$A(\mathrm{km}^2) = 2.23 \times 10^{-15} \times Mo^{2/3}(\mathrm{dyne \cdot cm}) \qquad (1)$$

$$Aa(\mathrm{km}^2) = 5.00 \times 10^{-16} \times Mo^{2/3}(\mathrm{dyne \cdot cm}) \qquad (2)$$

$$Am(\mathrm{km}^2) = 3.64 \times 10^{-16} \times Mo^{2/3}(\mathrm{dyne \cdot cm}) \qquad (3)$$

Other parameters such as average asperity slip, hypocentral distance to closest asperities, slip duration also scale with seismic moment in the self-similar way.

Second, they used the stochastic approach to quantify the heterogeneity of slip on the fault surface by its two-dimensional Fourier transform (the wavenumber spectrum). They derived a model for **the wavenumber spectrum of spatial slip distribution** on the fault which falls off as the inverse of the k-squared at high wavenumbers, consistent with the model of Herrero and Barnard(1994). The k-squared model is consistent with the fractal model of Frankel (1991) when the fractal dimension is 2, resulting in a kinematic source model with the omega-squared model (Aki, 1967).

The validity and applicability of strong ground prediction and the relation between strong ground motions and structure damage should be examined in comparison with the observed records and actual damage during the 1995 Hyogo-ken Nanbu (Kobe) earthquake. We find that the source model with three asperities for the 1995 Hyogo-ken Nanbu (Kobe) earthquake by Kamae and Irikura (1998) also follows the k-squared model.

3. SIMULATION OF STRONG GROUND MOTION BASED ON HETEROGENEOUS SOURCE MODEL

3.1 The 1995 Hyogo-ken Nanbu Earthquake (Mw=6.9)

We attempt to make up the source model for broadband ground motions from the 1995 Hyogo-ken Nanbu earthquake taking into account heterogeneous source model, i.e. asperity model using the empirical Green's function model (Kamae and Irikura, 1998). The source slip model of this earthquake was determined from the inversion of strong ground motion records by several authors. The slip distribution on the fault plane is roughly similar each other, although there are clear differences depending on frequency ranges of the data, smoothing techniques used there and etc. Even if the inverted source model is almost uniquely determined, it is not always available for strong motion simulation. The inversion is usually done using only low frequency motions less than 1 Hz., therefore it might not be useful for higher frequency motions of engineering interest. Fortunately, recent studies from high frequency envelop inversion of source suggests that variable slip models derived from low-frequency ground motions are related to the radiation of high frequency motions from inland earthquakes (Kakehi et al, 1996; Hartzell et al., 1996).

We then assume the initial source model with the asperities based on the rupture process obtained from the inversion of strong ground motion records by Sekiguchi et al. (1996). For simplicity, we consider each asperity as a subevent with uniform stress drop in a finite extent. Then, the initial model was revised by the forward modeling, i.e. comparison between the synthetic and observed ground motions. The final model consists of three subevents as shown in Ref. Kamae and Irikura (1998). Asperity 1 with stress drop of 163 bars lies under the Akashi Strait around the rupture starting point, Asperity 2 with stress drop of 86 bars, under the Nojima Fault in Awaji Island, and Asperity 3 with stress drop of 86 bars, under Kobe. The synthesized motions at KBU and MOT very close to the causative faults show a good fitting to the observed ones.

The total area of the asperities occupies about 25 % of the total rupture area, coinciding well with the averaged slip model of compiled 15 earthquakes. We obtained the wavenumber spectrum for the final slip model fitting to the k-squared model.

3.2 The 1994 Northridge Earthquake (Mw=6.7)

Strong ground motions from the 1994 Northridge earthquake were widely recorded in the San Fernando valley and the Los Angeles basin. The locations of stations near the source area and the epicenters of the mainshock and aftershock used as the empirical Green's function are shown in Fig. 5. The rupture process of the Northridge earthquake was determined from the inversion of strong motion data by Wald et al. (1996) as shown in Fig. 6a. Simplifying the slip distribution we assume the initial source models with two and three asperities. The best-fit model to observed records is shown in Fig. 6b. The stress drop in each asperity is assumed to be 300 bars in Asperity 1 and 3 and 400 bars in Asperity 2. The synthesized motions, acceleration, velocity and displacement, at SPVA and NEWH are compared with the observed in Fig. 7. We found that the velocity and displacement agree well even in each phase between the synthesized and observed, and the acceleration does in amplitude level and duration.

4. CONCLUSION

We summarized the procedure for predicting strong ground motions from future earthquakes caused by inland active faults as a recipe. The source characterization for the future earthquakes is made by the statistical analysis of the source inversion using strong motion and teleseismic data. Referring to Somerville et al. (1999) we find that the combined area of asperities as well as total rupture area follows the self-similar scaling and the wave-number spectra for the final slip model fit to the k-squared model at high-wavenumbers. The validity and applicability of the source characterization for strong ground prediction are examined in comparison with the observed records and actual damage from recent large earthquakes such as the 1995 Hyogo-ken Nanbu (Kobe) earthquake, the 1994 Northridge earthquake, and the 1999 Kacaeli earthquake.

This study was partially supported by a grant-in-Aid for Scientific Research, Number

09044079, from the Ministry of Education, Science, Sports, and Culture.

5. REFERENCES

Abe, K.. (1990), "Seismological aspects of Luzon, Philippines earthquake of July 16, 1990", *Bull. Earthq. Res. Inst.*, 65, pp851-874 (in Japanese)

Aki, K. (1967), "Scaling law of seismic spectrum", *J. Geophys. Res.*, 72, pp217-231.

Bouchon, M., H. Sekiguchi, K. Irikura, and T. Iwata (1998), "Some characteristics of the stress field of the 1995 Hyogo-ken Nanbu (Kobe) earthquake", *J. Geophys. Res.*, 103, pp24,271-24,282.

Frankel, A. (1991), High-frequency spectral fall-off of earthquakes, fractal dimension of complex rupture, b value, and the scaling strength on Fault", *J. Geophys. Res.*, 96, pp6,291-6,302.

Hartzel, S. H., P. Liu, and C. Mendoza (1996), "The 1994 Northridge California earthquake: Investigation of rupture velocity, rise time, and high-frequency radiation, *J. Geophys. Res.* 101, pp20091-20108.

Herrero, A. and P. Bernard (1994), "A kinematic self-similar rupture process for earthquakes", *Bull. Seism. Soc. Am.*, 84, pp1216-1228 .

Irikura, K. (1986), "Prediction of strong acceleration motion using empirical Green's function", *Proc. 7th Japan Earthq. Eng. Symp.*, pp151-156.

Irikura and Kamae (1999), "Strong ground motions during the 1948 Fukui earthquake", *Zisin (J. Seism. Soc. Japan)*, 52, pp129-150 (in Japanese).

Ito, K. (1990), "Regional variations of the cutoff depth of seismicity in the crust and their relation to heat flow and large inland-earthquakes", *J. Phys. Earth.*, 38, pp223-250.

Ito, K. (1999), "Seismogenic layer, reflective lower crust, surface heat flow and large inland-earthquakes", *Tectonophysics*, 306, pp423-433.

Kakehi, Y. K., K. Irikura, and M. Hoshiba (1996), "Estimation of high-frequency wave radiation areas on the fault plane of the 1995 Hyogo-ken Nanbu earthquake by the envelope inversion of acceleration seismograms, *J. Phys. Earth*, 44, pp505-517.

Kame, N. and T. Yamashita (1998), "Why are the numeber of small earthquakes larger than that of large earthquakes ? –spontaneous arresting of earthquake rupture –", *KAGAKU*. 68: 702-709 (in Japanese).

Kamae, K. and K. Irikura (1998), "Source model of the 1995 Hyogo-ken Nanbu earthquake and simulation of near-source ground motion", *Bull. Seism. Soc. Am.* , 88, pp400-412.

Matsuda, T. (1998), "Present state of long-term prediction of earthquakes based on active fault data in Japan, *Zisin (J. Seism. Soc. Japan)*, 50, pp23-34 (in Japanese).

Nakata, T., K. Shimazaki, Y. Suzuki, and E. Tsukuda (1998), "Fault branching and directivity of rupture propagation", *Journal of Geography*, 107, pp512-528 (in Japanese).

Sekiguchi, H., K. Irikura, T. Iwata, Y. Kakehi, and M. Hoshiba (1996), "Minute locating of faulting beneath Kobe and the waveform inversion of the source process during the Hyogo-ken Nanbu, Japan, earthquake using strong ground motion records", *J. Physics of the Earth*. 44, pp473-488.

Sibson, R. H. (1992), "Implications of fault-valve behaviour for rupture nucleation and recurrence", *Tectonophysics*, 211, pp283-293.

Somerville, P., K. Irikura, R. Graves, S. Sawada, D.Wald, N. Abrahamson, Y. Iwasaki, T. Kagawa, N. Smith, and A. Kowada (1998), "Characterizing earthquake slip models for the prediction of strong ground motion", *Seismological Research Letters*, 70, pp59-80.

Tsurugi, M., M. Tai, K. Irikura, and A. Kowada (1997), "Estimation of empirical site amplification effects using observed records", *Zisin (J. Seism. Soc. Japan)*, 50, 215-228 (in Japanese).

Wald, D. J., T. H. Heaton, and K. W. Hudnut (1996), "The slip history of the Northridge, California earthquake determined from strong-motion, teleseismic, GPS and leveling data", *Bull. Seism. Soc. Am.*, 86, ppS49-S70.

Wald, D. J. (1996), "Slip history of the 1995 Kobe, Japan, earthquake determined from strong motion, teleseismic, and geodetic data", J. Phys. Earth, 44, pp489-503.

Watanabe, M., T. Sato, and K. Dan (1998), "Scaling relations of fault parameters for inland earthquakes", *Proc. 10th Japan Earth. Eng. Symp.*, 1, pp583-588.

Wells, D. L. and K. L. Coppersmith, 1994, New empirical relationships among magnitude, rupture width, rupture area, and surface displacement", *Bull. Seism. Soc. Am.* , 84, pp974-1002.

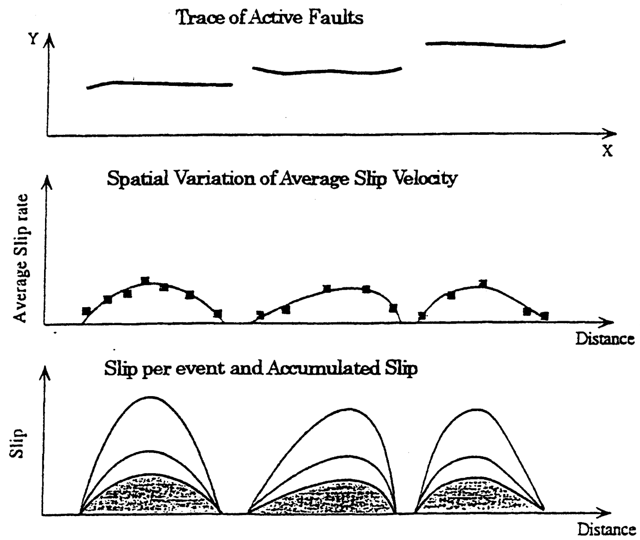

Fig. 1. Spatial distribution of fault traces, average slip velocity, and accumulated slip.

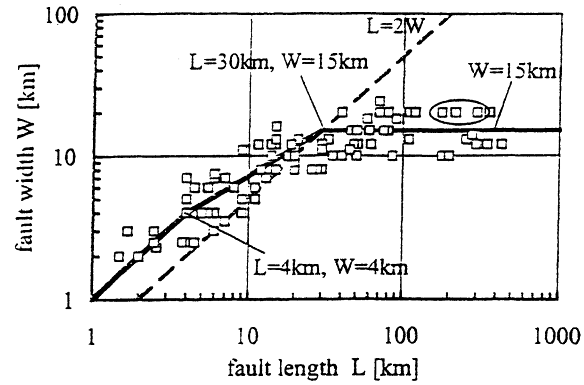

Fig. 2. Relation of fault width versus fault length for inland crustal earthquakes.

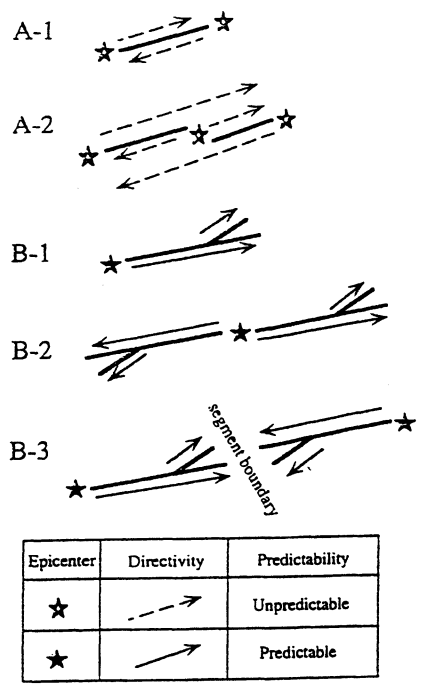

Fig. 3. Illustrative models of fault branching and rupture propagation (After Nakata et al., 1998)

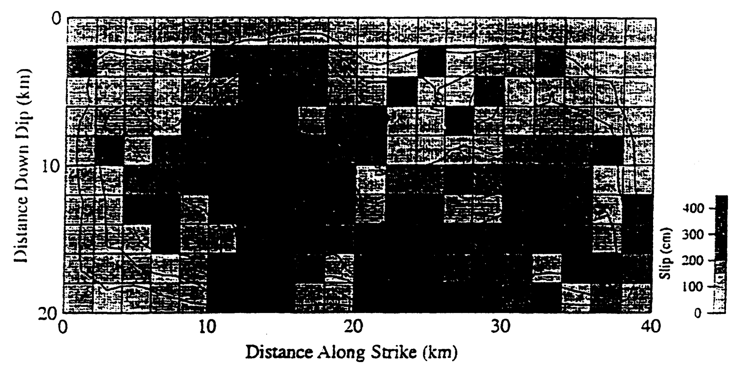

0	0	0	0	0	0	0	0	0	0	0	0	0	0	0	0	0	0	0	0
172	84	70	98	11	191	202	156	386	107	0	17	213	21	121	108	172	41	41	69
52	64	145	43	83	119	279	248	303	146	147	206	85	0	402	44	87	88	50	39
85	106	127	0	178	246	210	327	102	177	238	81	80	213	101	80	134	124	75	70
125	208	98	174	166	372	412	237	297	188	175	92	68	125	113	159	169	164	250	56
131	62	184	180	234	512	370	496	297	234	77	169	166	312	163	223	218	189	63	89
102	71	252	227	81	308	324	219	476	321	142	240	312	101	146	203	311	176	68	304
104	99	86	415	56	129	444	219	346	169	289	304	229	212	399	370	214	189	102	208
130	69	147	34	144	267	215	273	196	98	336	462	283	188	349	152	69	211	260	176
147	10	56	106	136	215	245	261	148	121	301	267	331	318	306	167	237	78	178	148

Distance Down Dip (km): 0, 10, 20
Distance Along Strike (km): 0, 10, 20, 30, 40

Trim Line

Asperity

148 Slip in cm

Fig. 4. Slip model of the 1989 Loma Prieta earthquake (Somerville et al., 1994, based on Wald et al., 1991) and identification of asperities.

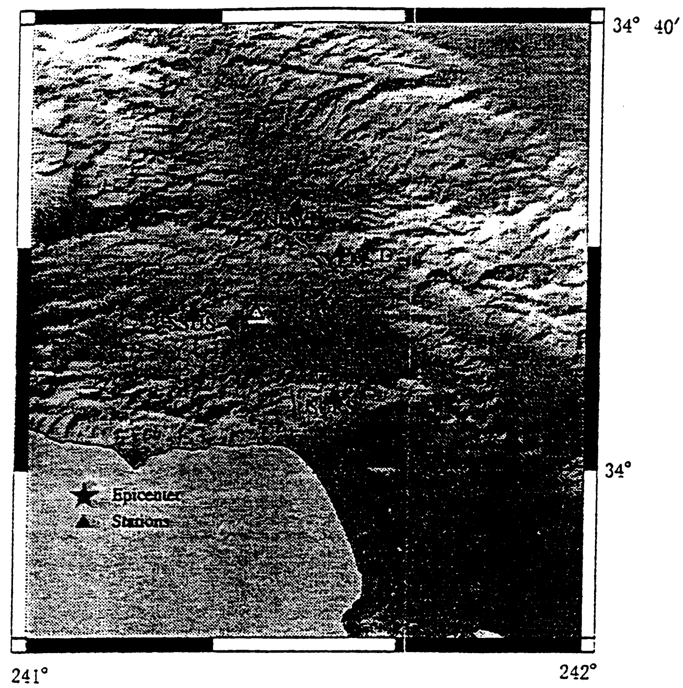

Fig. 5. Locations of the stations and epicenters of the mainshock (★) and the aftershock (▲) used as the empirical Green's function.

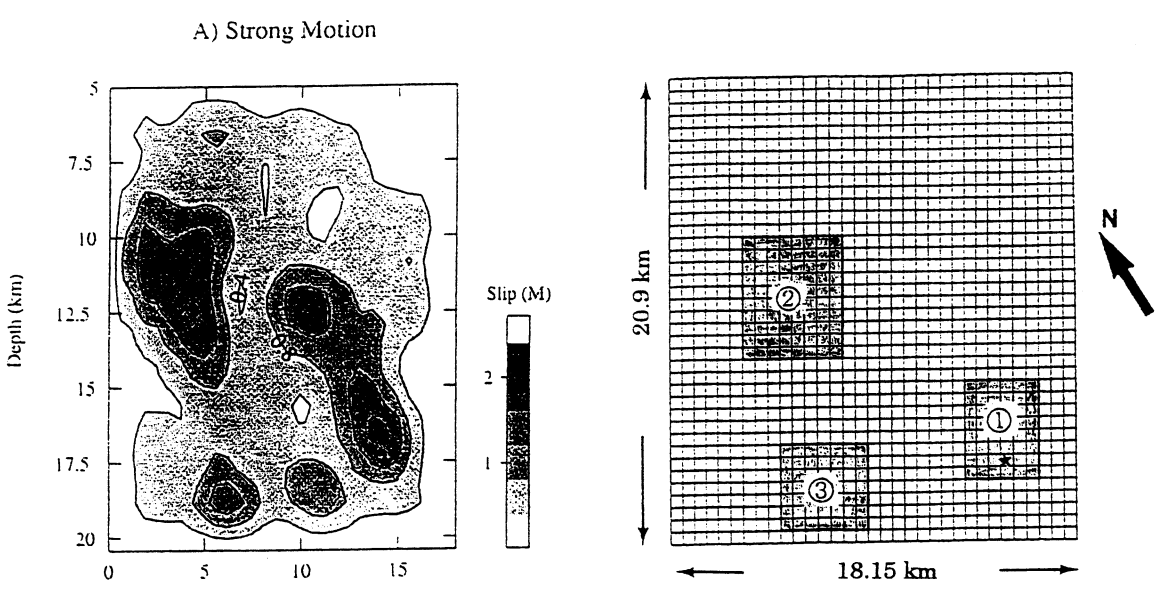

Fig. 6. (a) Slip distribution on the fault plane inverted from strong motion data for the 1994 Northridge earthquake. (b) Source model for simulating strong ground motions with three asperities. The starting point is indicated by ★. The rupture extends radially from the starting point with rupture velocity of 2.8 km/s. The rise time is assumed to be 0.6 sec for No. 1 and 3 and 1.0 sec for No.2.

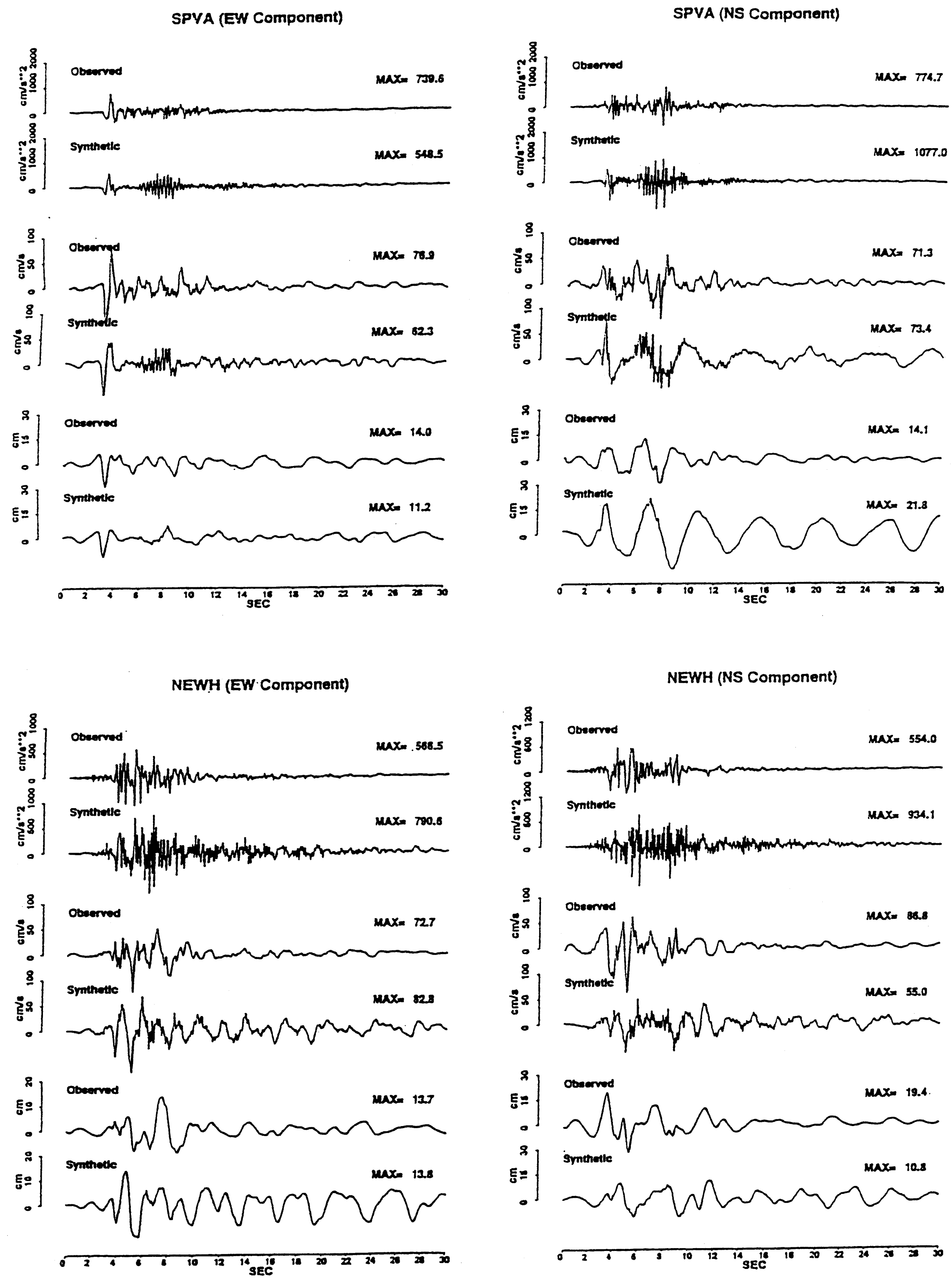

Fig. 7. Comparison between the synthetics by the empirical Green's function method and the observed records of the mainshock of the 1994 Northridge earthquake at SPVA and NEWH.

NEAR-FAULT GROUND MOTIONS FROM THE 1999 CHI-CHI EARTHQUAKE

Norman ABRAHAMSON[1]

INTRODUCTION

The near-fault ground motions recorded during the 1999 Chi-Chi earthquake provide a tremendous increase in the number of recordings close to large earthquakes. Prior to the Turkey earhtquakes, there were a total of 8 recordings world-wide recorded at distances less than 20 km from crustal earthquakes with magnitude greater than 7.0. The August 199 Turkey earthquake added an additional 5 recordings. The Chi-Chi earthquake added in additional 68 recordings.

A key aspect of this type of extensive data set is that the spatial variability of the ground motion can be seen and measured. In the past, we have often had only a few recordings close to a large earthquake. As a result, the features of the few recorded ground motions were extrapolated to the entire fault. The data from the Chi-Chi earthquake show the tremendous variability in the amplitude and characteristic of the time histories.

GROUND MOTION AMPLITUDES

At periods less the 2 seconds, the ground motions from the Chi-Chi earthquake were significantly lower than the median ground motion from standard attenuation relations used in the United States. The mean residuals of recordings within 20 km of the fault were computed using the Abrahamson and Silva (1997) attenuation model as a reference. At short periods, the recorded ground motions are a factor of 2 lower than the median predicted ground motions. At long periods (T>4 seconds), the ground motions become similar to the median predicted ground motions from the attenuation relation.

There are two ways to interpret these low ground motions: these data are typical and our current magnitude scaling is wrong, or these data are anomalous and the current magnitude scaling is reasonable. If these data are representative of ground motions from future large magnitude earthquakes, then there needs to be significant revision to the magnitude scaling of attenuation relations. In particular, should the median ground motion be required to increase monotonically with magnitude? Is there something fundamentally different in the way very large earthquakes behave?

Clearly, existing ground motion attenuation relations need to be updated to incorporate the new ground motion data from the Turkey and Taiwan earthquakes. The assumptions made in constraining the attenuation relation (e.g., require monotonic increase with magnitude or allow over-saturation with magnitude) will have a large impact on the resulting attenuation model.

[1]Senior Seismological Engineer, Pacific Gas and Electric Company, San Francisco, California

Velocity Pulses

There are two causes of velocity pulses in near fault ground motions: rupture directivity and permanent fault offset. In this paper, the terms directivity pulse and fling-step are used for these two effects.

Directivity Pulse

The dynamic rupture of an earthquake results in constructive interference of the long period ground motions from different parts of the faults. In the forward rupture directions, the rupture velocity is generally about 80 percent of the shear-wave velocity. As a result, there is a near shock wave condition. The ground motions from different parts of the fault pile up upon each other to produce a large velocity pulse. This pulse is two-sided in that it is related to dyanamic shaking and not permanent deformation.

For strike-slip and dip-slip faults, the directivity pulse appears on the horizontal component that is perpendicular to the fault strike. For strike-slip faults is observed at stations located along strike away from the epicenter. For dip-slip faults, the directivity pulse also occurs on the fault perpendicular component but it is observed at sites located up-dip from the hypocenter (not down strike)

Fling-Step

The permanent tectonic deformation of the ground will result in a step in displacement. The amount of time that it takes for the slip to occur at a point on the fault is called the rise-time. The permanent movement of the ground will result in a velocity pulse that is one-sided. The width of the velocity pulse (e.g. about one-half the period) should be approximately the rise-time. The amplitude of the velocity will be related to the ratio of the amplitude of tectonic deformation to the rise-time.

For strike-slip faults, the fling-step pulse occurs on the component parallel to the strike whereas for dip-slip faults it is occurs on the component perpendicular to the strike. The fling-step is observed at all locations along the strike at which there was significant permanent tectonic displacement. That is, it is controlled by the local fault displacement.

Chi-Chi Velocity Pulses

The Chi-Chi data contain the largest peak velocities every recorded. At station TCU068, located a the northern end of the rupture, the peak velocity was about 300 cm/s. In many papers, this has been referred to as directivity effects. Since the Chi-Chi earthquake is a dip-slip earthquake, the fling-step and directivity are both expected to occur on the fault perpendicular component. By examining the character of the velocity pulse and the location relative to the hypocenter, we can determine if the large velocity pulses are due to directivity or fling-step. These very large pulses are one-sided velocity pulses that are due to the fling-step and not due to the rupture directivity.

The fling-step can be removed from the recorded ground motions to produce a dynamic shaking component and a permanent displacement component. If this is done, then the peak velocity at TCU068 is reduced from 300 cm/s to about 100 cm/s which is much more typical of previous recorded ground motions. It also becomes similar to the peak velocities observed nearby on the other side of the fault (on the footwall).

These large velocities associated with the fling-step are not representative of the ground motions that have been used to develop the attenuation relations in the past. The fling-step pulse and the directivity pulse attenuate at very different rates from the fault. It is not appropriate to simply combine these two very different ground motions into a single attenuation relation. Separate models for ground motion due to dynamic shaking and fling-step need to be developed.

TOPIC A-2: EVALUATION OF NEAR-FIELD GROUND MOTION FOR DESIGN OF STRUCTURES IN URBAN AREAS

Tatsuo OHMACHI[1]
Professor, Tokyo Institute of Technology

ABSTRACT

Our four-year research activity on the A-2 topic entitled "Evaluation of Near-Field Ground Motion for Design of Structures in Urban Area" is outlined first. As a matter of fact, this topic is closely related to Level 2 (L2) Motion in the Proposal, issued by the Japan Society for Civil Engineers (JSCE) following the 1995 Hyogoken-nanbu earthquake, and most seismic codes for civil engineering structures in Japan have been revised in accordance with the proposal. Hence, the L2 motion is briefly introduced next, including definitions and features of the motion.

1. OBJECTIVE

To mitigate urban earthquake disaster, we have to take in account the effects of near-field ground motion in the earthquake resistant design of urban facilities and urban planning. For those purposes, we need to specify design earthquake motion and/or seismic loading, and to obtain seismic microzoning maps. The research topic of our group aims to facilitate such processes from engineering points of view.

2. SUBTOPICS AND MEMBERS

The main topic of this group was subdivided into the following three subtopics.

(1) Input Ground Motion and Seismic Loading.

This includes near-field ground motion and its effects on earth pressure, liquefaction potential and ground displacement, specifically used for structural design in general.

(2) Worst Near-Field Motion and Its Effects

In structural design and disaster management, we have to pay attention to special cases where standard design motion and loading are exceeded somehow or other. Causes and effects of such worst cases are studied under this subtopic.

(3) Seismic Microzonation

Since ground motion intensity varies due to local site effects, we should bear this in mind in urban planning. The effects are often attributed to topographical and/or geological irregularities, and detected by microtremor measurement.

Each subtopic was originally allocated to the researchers numbered in parentheses in the following members list, in which * indicates the research coordinator.

[1]*Department of Built Environment, Tokyo Institute of Technology, Yokohama, Japan*
Email: ohmachi@enveng.titech.ac.jp

Masanori HAMADA, School of Science and Engineering, Waseda University (1)
Toshimi KABEYASAWA, Earthquake Research Institute, University of Tokyo (1)
Tadao MINAMI, Earthquake Research Institute, University of Tokyo (1)
Tadanobu SATO, Disaster Prevention Research Institute, Kyoto University (1)
Takeshi TAMURA, Graduate School of Civil Engineering, Tokyo University (1)
Ikuo TOWHATA, Department of Civil Engineering, University of Tokyo (1)
Kazue WAKAMATSU, Association for Earthquake Disaster Prevention (1) Satoshi KURITA, School of Engineering, Tohoku Univeristy (2)
Motohiko HAKUNO, Department of Civil and Environmental Engineering,Tokyo University (2)
*Tatsuo OHMACHI, Interdisciplinary Graduate School of Science and Engineering, Tokyo Institute of Technology (2)
Masanori HORIKE, Architecture Department, Osaka University (3)
Saburoh MIDORIKAWA, Interdisciplinary Graduate School of Science and Engineering, Tokyo Institute of Technology (3)

3. COMMENTS ON MEMBERS' ACTIVITITIES

During the period of this research project, especially for the last academic year, there was a small change in the members of this group. Dr. Wakamatsu and Dr. Tamura joined us to make contribution in the fields of soil liquefaction and earth pressure. Dr. Kabeyasawa also joined us after Dr. Minami passed away in September, 1999.

Most researchers of this group have been involved in at least one of the subtopics shown above, and sometimes all three because the topics are closely correlated with each other in actuality, and because the researchers were urged to find the causes and effects of the Kobe earthquake from various points of view. Accordingly, individual papers arranged in the following part of this report are only the examples that they have studied in recent years under these topics.

4. RECENT SITUATION RELATED TO THIS TOPIC

Following the 1995 Hyogoken-Nanbu earthquake, several proposals were issued from engineering points of view in Japan. For example, Japan Society of Civil Engineering (JSCE 1996) issued twice the "Proposal on Earthquake Resistance for Civil Engineering Structures"[1]; the first in May, 1995 and the second in January, 1996. One of the requirements of the proposal is to consider two levels of input earthquake motion for seismic design of structures. Level 1 (L1) motion covers motions of moderately high intensity, while Level 2 (L2) addresses motions of extremely high intensity of the nature of the strong motion experienced in Kobe city during the 1995 earthquake.

In accordance with this kind of proposals, most seismic codes for civil engineering structures have been revised to take into consideration of L2 motion in near-field. The revised codes include those for highway bridges, railway structures, and port and harbor facilities. Each revision is not necessarily the same in detail, but seems to share basic concept of the JSCE proposal in common, at least for the input motion. For this reason, L2 motion in the JSCE proposal is summarized in the rest of this paper.

5. JSCE PROPOSAL ON LEVEL 2 EARTHQUAKE MOTIONS

5.1 Introduction

The selection of the L1 and L2 motions is implicitly based on the expectation that the L1 motion will be experienced once or twice during the lifetime of the structure while the L2 motion has a very low probability of being experienced by the structure. The underlying design assumption is that the intensity of the L1 motion is comparable to the seismic loadings traditionally used in Japanese seismic codes for which structures are to remain within their elastic limits; for the L2 motion, structures are allowed to undergo plastic deformations as long as collapse and loss of life are prevented. For most Japanese seismic codes for civil engineering structures, the L2 motion is a new type of input earthquake motion to be considered in design. For this reason, in the above mentioned proposals, a main focus is placed on the L2 motion.

In Japan, L2 motion can most likely be caused by two types of earthquakes: interplate earthquakes occurring under the ocean and intraplate earthquakes associated with inland active faults. Regardless of the earthquake type and the difficulties associated with implementation, the proposal requires the L2 motion to be determined from the rupture process of the relevant faults affecting the structure considered.

As a whole, the concept of L2 motion as described in the proposals appears to be too general to be applied directly in design. For practical applications, more detailed guidelines are required for the estimation of the L2 motion, such as how to select scenario earthquakes and how to deal with the uncertainty inherent in the fault rupturing mechanism of future events. To respond to this need, a task committee formed by the JSCE two years ago clarified a number of these points. The committee's recommendations have been summarized in a recent report (JSCE 1999)[2].

This paper is based on work done by the JSCE committee on Level 2 Earthquake Motion. Any opinions, findings and conclusions or recommendations expressed in this paper are those of the author and do not necessarily reflect the views of the JSCE and the committee.

5.2 Definitions and Features of the L2 Motion

In general, the concepts of intensity and probability of occurrence are not differentiated from one another when one refers to "level" in Level 2 Earthquake Motion. This tends to create some confusion considering the two types of earthquakes contributing to the L2 motion, i.e., interplate and intraplate events. These events have different return periods and different potential intensities. Intuitively one would expect long return period events to have higher intensities than shorter return period events. This is not necessarily the case for Japanese interplate and intraplate events. The interplate or subduction earthquakes of large magnitude have relatively short return periods (of the order of a few hundred years) while the intraplate earthquakes of moderate to large magnitude caused by active faults have very long return periods (of the order of thousand years). However, the more frequent interplate events are capable of more intense shaking than the longer return period intraplate events.

To eliminate this potential source of confusion, it is advised to refer to "level" as a measure of the intensity only and defines Level 2 Earthquake Motion as follows:

- The Level 2 Earthquake Motion to be used as an input motion for the seismic design of a specific civil engineering structure is the maximum intensity earthquake motion to be reasonably possible at the site for the structure considered.

  This definition for the L2 motion implies the following:

- L2 motion is dependent of the seismic environment and geology of the site, but is independent of social factors such as importance of the structure
- The L2 motion is a "so-called" source specific, site specific and structure specific motion.
- A preferred procedure to determine the L2 motion consists of selecting a set of scenario earthquakes based on the tectonic setting of the region, to evaluate the respective ground motions at the site taking into account the site soil characteristics and finally to select the most critical of these inputs based on the response of the structure considered.
- It is desirable to formulate the L2 motion from observed earthquake motions compatible with the points presented above by using a semi-empirical method
- A lower bound of L2 motion is given by moderate local earthquakes (about M_J 6.5) caused by blind faults, which are assumed to occur uniformly throughout Japan.

5.3 Selection of Scenario Earthquakes

The first step to estimate L2 motion consists of selecting a set of realistic earthquakes that provide the greatest seismic threat to the structure. Taking into account all information available, one or more scenario earthquakes are selected by comparing intensity of ground motion resulting from every seismic source affecting the site under investigation. In this comparison process, empirical attenuation relationships are often used to estimate ground motion intensity in terms of peak acceleration, peak velocity, JMA seismic intensity or response spectrum.

In general, candidates for the scenario events are repeats of devastating historical earthquakes and potential large earthquakes on active faults. Hence, a large database containing in-depth information about active faults and historical earthquakes facilitates the selection of the scenarios to be considered. It should be noted that scenario earthquakes for a given structure may not be applicable to nearby structures if the structures have significantly different response characteristics. Accordingly, the structure's natural period is one key factor entering into the selection of the scenario earthquakes.

5.4 Evaluation of L2 Motion from Scenario Earthquakes

Once a set of scenario earthquakes have been selected, the L2 motion can be estimated by various methods. These methods can roughly be classified into three groups: empirical, semi-empirical and theoretical. Since each of these methods have their own advantages and limitations, it is necessary to adapt them adequately. For example, at the present state, the empirical methods are applicable to a period range shorter than 1 or 2 sec, while the theoretical methods are applicable to the range longer than 1 or 2 sec. The semi-empirical methods [3], which use observed ground motion of small or medium size earthquakes are the most appropriate for the present purpose of L2 motion estimation. The main advantage of the semi-empirical methods (Irikura 1986) is twofold: if properly applied, they appropriately reflect, without much effort, the wave propagation path and the local site effects of the L2 motion and they are adaptable to both the short and long period ranges. These methods however require observed earthquake motion at the site. Hence, the availability of a recorded earthquake motion at the site prior to the planning and design process greatly facilitates the L2 motion estimation.

In the absence of recorded time histories at the site, empirical or theoretical approaches can be used. As long as a seismic source and the subsurface soil condition are given, the associated ground motion for different periods can be evaluated to a satisfactory level of accuracy by numerical simulation.

5.5 Lower Bound of L2 Motion

Uncertainty is inherent in the formulation of L2 motion. The uncertainty lies not only in the rupture process of future seismic faulting, but also in the location of active faults. As a matter of fact, present maps of active faults do not contain blind faults. However, inland earthquakes caused by blind faults have often affected various civil engineering structures.

Active faults are mapped mostly in the middle part of Japan (RGAFJ 1991)[4], while shallow crustal events have occurred in many instances outside known fault zones. It seems safe to say that inland earthquakes are likely to occur anywhere in Japan, no matter whether they are caused by known active faults or blind faults.

In addition, according to recent studies [5](Shimazaki 1986), inland earthquakes of magnitude M_J smaller than or equal to 6.5 are not likely to reveal their fault traces on the ground surface, even if the surface is not covered with sedimentary layers. On this basis an inland earthquakes of M_J 6.5 is thought to be a scenario earthquake that gives a lower bound for L2 motion. Trial calculations have shown that ground motion intensity produced by M_J 6.5 earthquakes is 6- on the JMA instrumental intensity scale for most part of Japan except for exposed hard rock sites.

5.6 Conclusive Remarks

Since the JSCE Proposal was issued, various efforts have been made to facilitate practical application of the L2 motion. The efforts include detailed description about definitions and features of the motion, and a trial evaluation of its lower bound. In a word, the L2 motion is evaluated as a source-specific and site-specific motion. However, in designing a structure of less importance, a simplified procedure may be needed for practical application. In such a case, the lower bound of the L2 motion evaluated on a site-specific basis can be a substitute. This is because the L2 motion is much associated with the so-called performance-based design where the importance is taken into account in the structural performance under input earthquake motions, but not in evaluation of the motions.

There still remains much room for full implementation of the Proposal as regards:

(1) The L2 motion should be described in terms of probability of occurrence in order to be widely used in the performance-based design.

(2) Similarly, the L1 motion should be defined in a similar context as the L2 motion.

(3) A subsurface ground structure extending to seismic bedrock should be explored throughout Japan as soon as possible by public sectors.

(4) Causes and effects of active faults should be studied from civil engineering points of view.

(5) Rupture process of seismic faults should be characterized in detail to reduce uncertainty in evaluation of the L2 motion.

REFERENCES

Japan Society of Civil Engineers. 1996. Proposal on Earthquake Resistance for Civil Engineering Structures.

JSCE Working Group on L2 Motion: Level 2 Earthquake Motions. 1999. (In Japanese).

Irikura, K. 1986. Prediction of strong acceleration motion using empirical Green's function. In *Proc. 7th Jpn Earthq. Eng. Symp.,* pp.151–56.

The Research Group on Active Faults of Japan. 1991. Active faults in Japan, rev. ed. Tokyo: University of Tokyo Press.

Shimazaki, K. Small and large earthquakes, effects of the thickness of seismogenic layer and the free surface. 1986. *Earthquake Source Mechanics,* Am. Geophys. Union, Geophys. Monogr. 37, Maurice Ewing 6, pp.209–16.

Keywords

Near-field, seismic design, input ground motion, liquefaction, seismic microzonation

CHARACTERIZATION OF NEAR-FAULT GROUND MOTIONS

Paul SOMERVILLE [1]

ABSTRACT

This paper describes the characteristics of near fault ground motions that need to be considered in seismic design, and examines the magnitude scaling of near fault ground motions implied by the strong motion data from recent earthquakes in Turkey and Taiwan.

1. INTRODUCTION

The distribution of ground motion amplitudes in the near-fault region is strongly influenced by the fault geometry. For vertical strike-slip faults, rupture directivity effects cause a strong spatial variation in ground motions for a given closest distance to the fault. For dipping faults, there are two prominent effects: the rupture directivity effect and the hanging wall effect. The hanging wall effect is due mainly to the proximity of much of the fault to hanging wall sites. It is most pronounced for periods shorter than about 1 second, and occurs away from the top edge of the fault on the hanging wall side. The rupture directivity effect is due to rupture propagation and radiation pattern effects. It is most pronounced at periods longer than 1 second, and is concentrated over the top edge of the fault. The relationship between the rupture directivity effect and the hanging wall effect is thus complementary both spatially and in period range, enhancing the degree of spatial variation of strong ground motion around dipping faults.

1.1 Hanging Wall Effects

Sites on the hanging wall of a dipping fault have closer proximity to the fault as a whole than do sites at the same closest distance on the foot wall, causing larger short period ground motions on the hanging wall than on the foot wall. The hanging wall effect augments the style of faulting factor for short period ground motions from reverse and thrust earthquakes, which are typically 1.3 to 1.4 times larger than those from strike-slip earthquakes. The empirical model of hanging wall effects developed by Abrahamson and Somerville (1996) distinguishes the ground motions for sites on the hanging wall from those on the foot wall and off the end of the fault rupture. The effect is greatest (a factor of 1.45) in the closest distance range of 8 to 18 km for periods of 0 to 0.6 seconds, and decreases to unity at 5 seconds (Abrahamson and Silva 1997).

1.2 Near-Fault Rupture Directivity Effects

The propagation of fault rupture toward a site at a velocity that is almost as large as the shear wave velocity causes most of the seismic energy from the rupture to arrive coherently in a single large

[1] *URS, 566 El Dorado Street, Pasadena, CA 91101 email: paul_somerville@urscorp.com*

long period pulse of motion which occurs at the beginning of the record. This pulse of motion represents the cumulative effect of most of the seismic radiation from the fault. The radiation pattern of the shear dislocation on the fault causes this large pulse of motion to be oriented in the direction perpendicular to the fault, causing the strike-normal peak velocity to be larger than the strike-parallel peak velocity. The enormous destructive potential of near-fault ground motions was manifested in the 1994 Northridge and 1995 Kobe earthquakes. In each of these earthquakes, peak ground velocities as high as 175 cm/sec were recorded, and the period of the near-fault pulse lies in the range of 1 to 2 seconds, comparable to the natural periods of structures such as bridges and mid-rise buildings, many of which were severely damaged.

Forward rupture directivity effects occur when two conditions are met: the rupture front propagates toward the site, and the direction of slip on the fault is aligned with the site. The conditions for generating forward rupture directivity effects are readily met in strike-slip faulting, where the rupture propagates horizontally along strike either unilaterally or bilaterally, and the fault slip direction is oriented horizontally in the direction along the strike of the fault. However, not all near-fault locations experience forward rupture directivity effects in a given event. Backward directivity effects, which occur when the rupture propagates away from the site, give rise to the opposite effect: long duration motions having low amplitudes at long periods.

The conditions required for forward directivity are also met in dip slip faulting, including both reverse and normal faults. The alignment of both the rupture direction and the slip direction updip on the fault plane produces rupture directivity effects that are most concentrated updip from the hypocenter near the surface exposure of the fault (or its updip projection if it does not break the surface).

The effect of forward rupture directivity on the response spectrum is to increase the level of the response spectrum of the horizontal component normal to the fault strike at periods longer than 0.5 seconds. This causes the peak response spectral acceleration of the strike-normal component to shift to longer periods. Near-fault effects is not adequately described by uniform scaling of a fixed response spectral shape; the spectrum becomes richer in long periods as the level of the spectrum increases.

The 1997 UBC contains the near-source factor N to account for the fact that recorded near-fault ground motions frequently exceed the 1994 and previous UBC codes, in which the effective peak acceleration has a value of 0.4g in Zone 4. The near-source factor N has separate components, N_A and N_V for the short period (acceleration) and intermediate period (velocity) ranges of the spectrum, to accommodate the fact that near-fault rupture directivity mainly enhances the intermediate period part of the response spectrum (Somerville et al., 1997). The shape and level of the near-fault response spectrum described by Somerville (1996) was used as the basis for the development of the near-source factor N. However, differences between the fault-normal and fault-parallel components of motion at intermediate periods were not incorporated into the code. The values of the near-source factors N_A and N_V depend on the distance from the fault and on the seismic potential of the fault as described by its slip rate and maximum magnitude.

Based on an empirical analysis of near-fault data, Somerville et al. (1997) developed modifications to empirical strong ground motion attenuation relations to account for the effects of rupture directivity on strong motion amplitudes and durations. In the near-fault rupture directivity model, amplitude variations due to rupture directivity depend on two geometrical parameters. First, the smaller the angle between the direction of rupture propagation and the direction of waves travelling from the fault to the site, the larger the amplitude. Second, the larger the fraction of the fault rupture surface that lies between the hypocenter and the site, the larger the amplitude. Attenuation relations modified to include directivity effects can be used directly in probabilistic seismic hazard analysis by incorporating variability in the location of the hypocenter for each fault rupture scenario considered.

Although the response spectrum provides the basis for the specification of design ground motions in all current design guidelines and code provisions, there is a growing recognition that the response spectrum is not capable of adequately describing the seismic demands presented by brief, impulsive near-fault ground motions. This indicates the need to augment the response spectrum with a time domain representation of near-fault ground motions, preferably in the form of simplified pulses whose parameters (such as period and peak velocity) can be related to earthquake magnitude, fault distance, rupture directivity condition (forward, backward, or neutral), and site conditions (Somerville, 1998). Since the strike of the controlling fault is usually known, the differences between ground motions in the directions normal to and parallel to the fault strike can be readily specified.

The design and evaluation of critical structures located near faults often uses time histories containing near-fault pulses whose response spectra are compatible with a design response spectrum. It is important to select time histories that appropriately include forward rupture directivity effects. This is true even if time histories are being matched to a design spectrum, and even if the design spectrum explicitly incorporates near-fault conditions, because the spectral matching process cannot build a forward rupture directivity pulse into a record where none is present to begin with. This indicates the need to identify the directivity conditions that control the design spectrum, and select appropriate time histories, because forward rupture directivity effects are present in some but not all near-fault strong motion recordings.

Many analysis procedures assume that the two horizontal components are uncorrelated, and prescribe interchanging the two horizontal components in structural analyses. This is clearly inappropriate for near-fault ground motions, in which there are systematic differences between the strike-normal and strike-parallel components. Interchanging the components can represent physically unrealizable scenarios given the known orientation and sense of slip on the fault. The Turkey and Taiwan earthquakes provided some of the first reliable strong motion recordings containing permanent ground displacements due to the static displacement field of the earthquake. In cases where permanent ground displacements may be significant for design, it is important to specify the magnitude and orientation of the static ground displacements.

2. MAGNITUDE SCALING OF NEAR-FAULT GROUND MOTIONS

The recent earthquakes in Turkey and Taiwan provided a ten-fold increase in the number of near-fault strong motion recordings from crustal earthquakes with magnitudes of about 7.5. We compare the response spectra of near-fault recordings of magnitude 7 and 7.5 earthquakes at distances less than 10 km from the fault to gain insight into the magnitude scaling of near-fault ground motions. All of the recordings used in the comparison have forward rupture directivity effects, i.e. rupture propagated from the earthquake hypocenter toward the recording station. The figures show separate response spectra for the strike-normal and strike-parallel components.

In Figures 1 through 3, we show the spectra of three smaller earthquakes on the left: Mw 7 Loma Prieta, Mw 6.9 Kobe and Mw 6.7 Northridge, and three larger earthquakes on the right: Mw 7.2 Landers, Mw 7.4 Turkey, and Mw 7.6 Taiwan. For the Taiwan earthquake, we have chosen one of the few records, Tsaotun (TCU075), that show clear forward rupture directivity effects. The fault normal component is much larger than the fault parallel component in the strong motion recordings, as expected from the radiation pattern. We compare the spectra with the 1994 UBC spectra before the 1997 UBC near-source factor was added. The 1994 UBC spectrum is used as a reference for judging the discrepancy between the actual recording and a standard model; the exceedance is a measure of the near-fault factor appropriate for that record.

The acceleration spectra on the right side of Figure 1 for the large earthquakes are compatible with the 1994 UBC code spectrum in the intermediate period range, between 0.5 and 2.5 seconds, but have a bump at a period of about 4 seconds where they significantly exceed the 1994 UBC code spectrum. The spectra of the smaller earthquakes, shown on the left, are very different from those of the larger earthquakes, and have opposite trends. Their spectra are much larger than the 1994 UBC code spectrum in the intermediate period range of 0.5 - 2.5 sec, but are similar to the 1994 UBC spectrum at longer periods. This is very different from all current models of earthquake source spectral scaling and ground motion spectral scaling with magnitude, in which the ground motions from larger earthquakes are stronger than those of smaller earthquakes at all periods.

The spectral velocities of the same data (Figure 2) show the difference between the larger and smaller earthquakes even more clearly. The velocity response spectra of the larger earthquakes peak at about 4 or 5 seconds, while the spectra of the smaller earthquakes peak between 0.5 and 2.5 seconds and are stronger than the larger earthquakes in this intermediate period range. The spectral displacements (Figure 3) also clearly show the differences in spectral shape between the larger and smaller earthquakes.

3. DISCUSSION

In the period range of 0.5 to 2.5 seconds, current strong motion data indicate that the near-fault ground motions of smaller earthquakes (Mw 6.7 to 7.0) are stronger than those from larger earthquakes (Mw 7.2 to 7.6). This raises important questions about the characterization of near-fault ground motions from large crustal earthquakes (magnitudes larger than 7) which frequently constitute the design basis in tectonically active regions such as California. The near-source factor N in the 1997 UBC is based on relatively abundant data, primarily from the 1989 Loma Prieta, 1994 Northridge and 1995 Kobe earthquakes, whose magnitude range of 6.7 to 7 corresponds to Seismic Source Type B (maximum magnitude 6.5 to 7, slip rate 2 to 5 mm/yr). The near-source factors for Seismic Source Type A (maximum magnitude > 7, slip rate > 5 mm/yr) are based on very few data. The new data from the 1999 Turkey and Taiwan earthquakes suggest that these factors are conservative for periods less than 2.5 seconds, but are appropriate for periods longer than 2.5 seconds.

A literal representation of the data described in Figures 1 through 3 would give lower N factors for Seismic Source Type A than for Seismic Source Type B for periods less than 2.5 seconds. However, if it were assumed that Seismic Source Type A faults are capable of generating Type B earthquakes in the magnitude range of 6.5 to 7, then the N factors for Type B would govern for periods less than 2.5 seconds. Clearly, the N factors would have to undergo extensive modification to represent the new near-fault data. The main change would consist of lowering the N_V factor (at periods shorter than 2.5 seconds) and the N_A factor for Source Type A.

The appearance of rupture directivity effects at periods longer than 3 seconds in recordings of the 1999 Turkey and Taiwan earthquakes confirms the indication provided in the Lucerne recording of the 1992 Landers earthquake (Somerville et al., 1997, Figure 4) that rupture directivity effects in large earthquakes may be confined to long periods. It also conforms to the expectation, based on studies of the magnitude scaling of earthquake source parameters (Somerville, 1998; Somerville et al., 1999), that the period of the pulse is magnitude dependent because it is related to the duration of slip at a point on the fault, which increases with magnitude.

All three large earthquakes shown in Figures 1 through 3 produced large surface rupture. Among the smaller earthquakes, the rupture of the Loma Prieta and Northridge ruptures stopped several km below the surface, and in the Kobe earthquake, it only reached the surface on Awaji Island, and the strong motion recordings in Kobe were almost unaffected by the Awaji Island segment of the fault. It is possible that some of the difference in Figures 1 through 3 is due to differences in ground motion characteristics between surface and buried faulting earthquakes, not just due to magnitude differences.

4. REFERENCES

Abrahamson, N.A., and W.J. Silva.1997. Empirical response spectral attenuation relations for shallow crustal earthquakes. *Seismological Research Letters* 68: 94–127.

Abrahamson, N.A., and P.G. Somerville. 1996. Effects of the hanging wall and foot wall on ground motions recorded during the Northridge earthquake. *Bull. Seism. Soc. Am.* 86: S93–S99.

Somerville, P. 1996. Forward rupture directivity in the Kobe and Northridge earthquakes, and implications for structural engineering. In *Proceedings of the Seventh U.S.-Japan Workshop on Improvement of Structural Design and Construction Practices, Lessons Learned from Kobe and Northridge,* January 18–20, Kobe, Japan.

Somerville, P.G., N. F. Smith, R. W. Graves, and N. A. Abrahamson. 1997. Modification of empirical strong ground motion attenuation relations to include the amplitude and duration effects of rupture directivity. *Seismological Research Letters* 68(1): 199–222.

Somerville, P.G. 1998. Development of an improved representation of near fault ground motions. In *Proceedings of the SMIP98 Seminar on Utilization of Strong Motion Data,* Oakland, September 15, 1998, pp. 1–20.

Somerville, P.G., K. Irikura, R. Graves, S. Sawada, D. Wald, N. Abrahamson, Y. Iwasaki, T. Kagawa, N. Smith, and A. Kowada. 1999. Characterizing crustal earthquake slip models for the prediction of strong ground motion. *Seismological Research Letters* 70(1): 59–80.

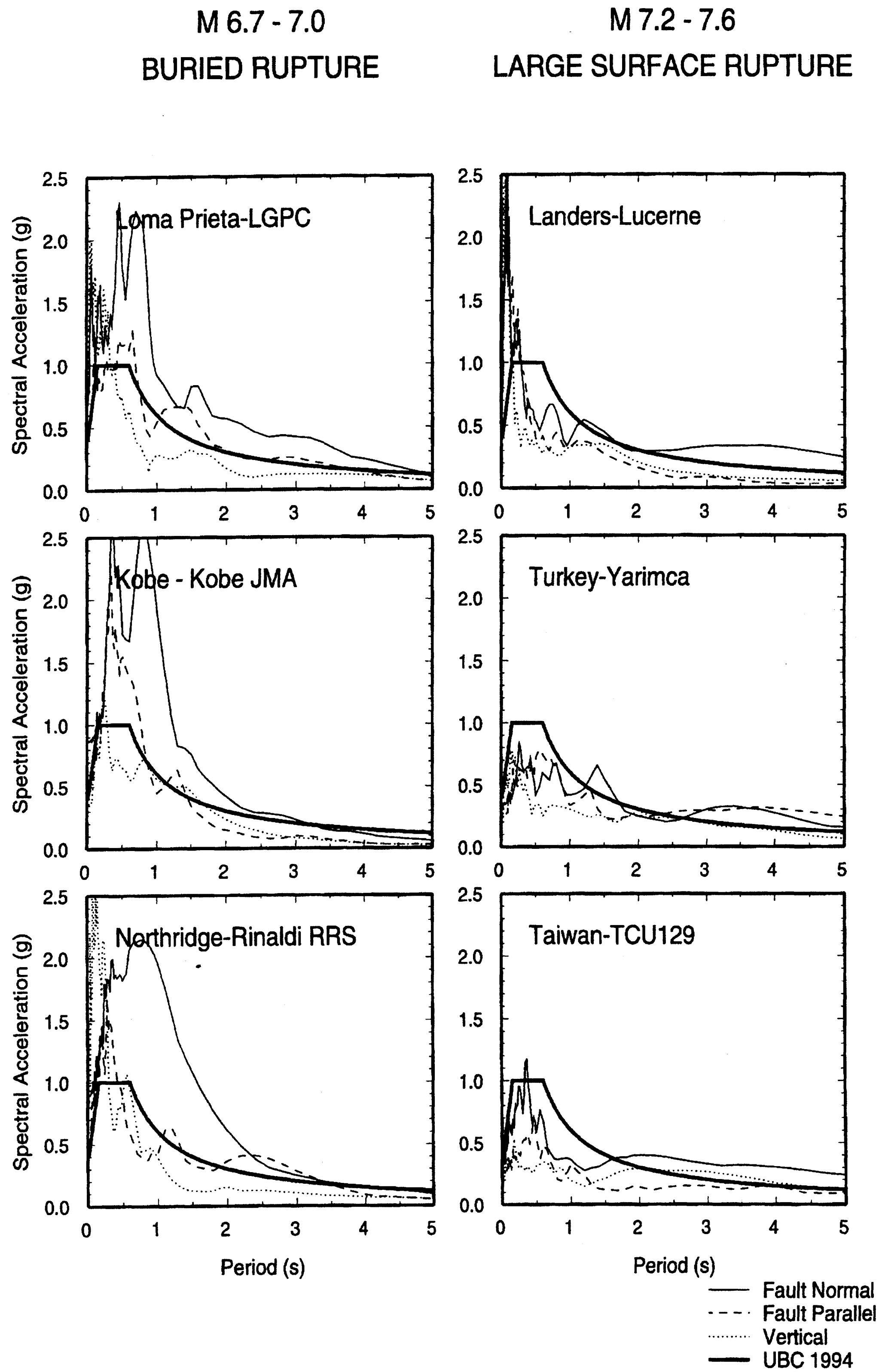

Figure 1. Comparison of acceleration response spectra of moderate (left) and large (right) earthquakes.

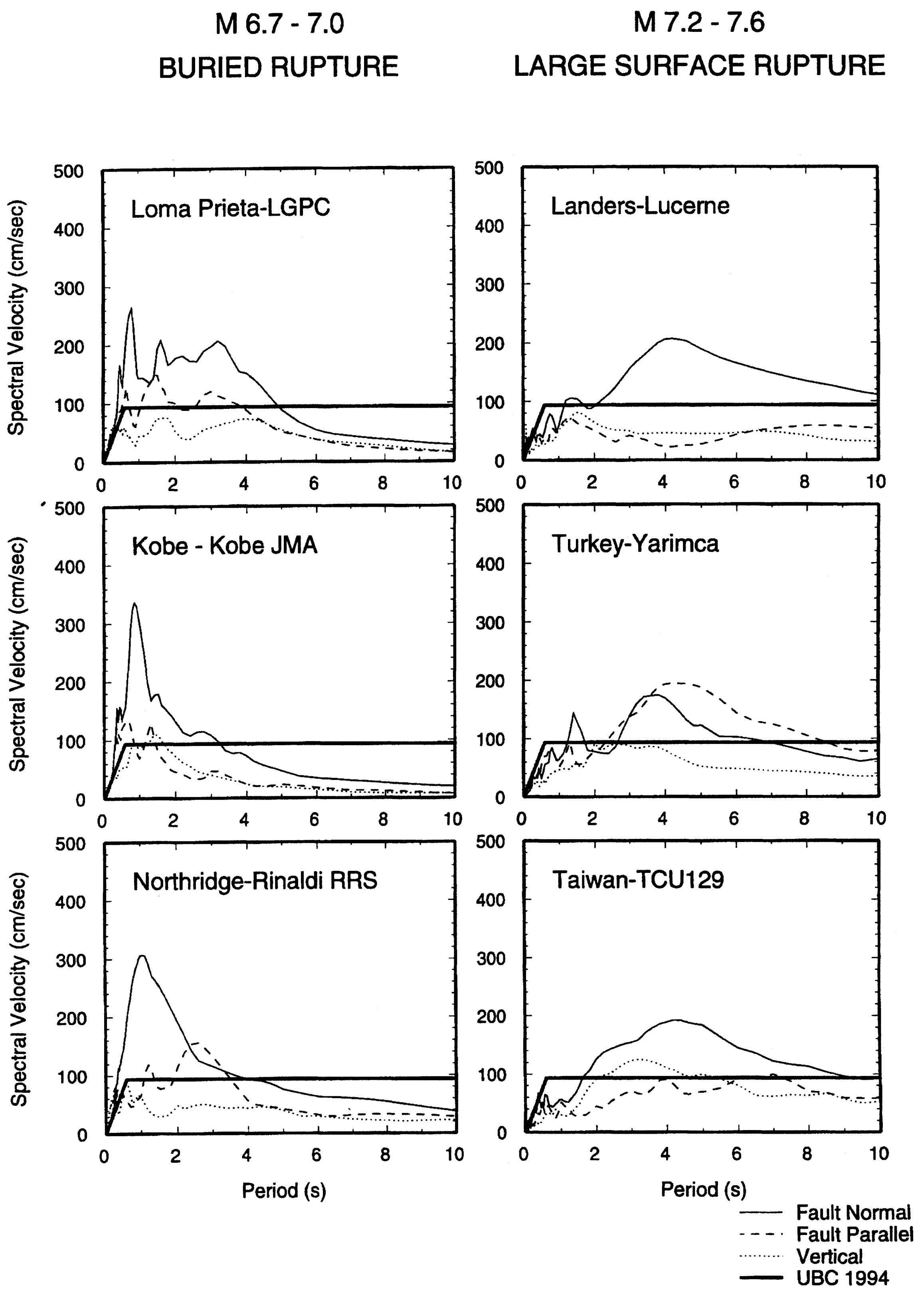

Figure 2. Comparison of velocity response spectra of moderate (left) and large (right) earthquakes.

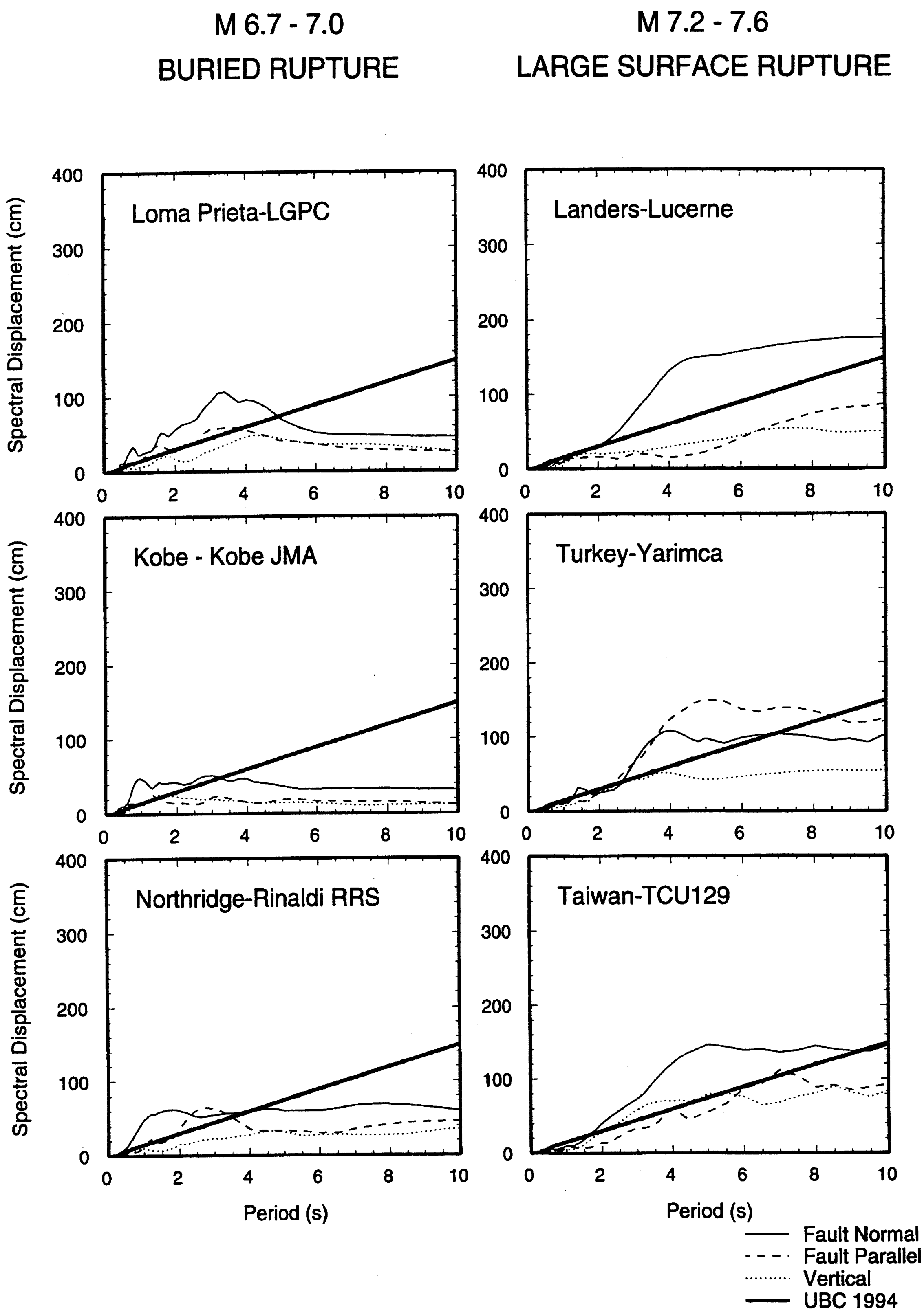

Figure 3. Comparison of displacement response spectra of moderate (left) and large (right) earthquakes.

MACRO-ZONATION OF POTENTIAL SEISMIC RISK IN URBAN CITIES

Suminao MURAKAMI[1], Tsuneo OKADA[2],
Masaya MURAKAMI[3], Yoshiaki NAKANO[4],
Yoshiteru MUROSAKI[5], Koichi OHAMI[6],
Satoru SADOHARA[7], Masanori NAGASHIMA[8],
Masakazu MORIYAMA[9], Hiroshi MIYAZAKI[10]

ABSTRACT

This study aims at evaluating factors related to potential seismic risk in a city or a group of cities based on the concept of "macro-zonation". These factors are associated with regional characteristics including natural features such as topography, climate and location of active faults, human features such as population and population density and artificial features such as buildings and roads . Countermeasures such as disaster measure of local government in Japan were uniform all over Japan, so we focused on "Regional characteristics" of each cities and necessity of index to compare each cities. The main objective of this study is to develop a countermeasure system utilizing macro information of urban cities to mitigate earthquake disaster, especially near-field earthquake, considering their regional characteristics. We defined four categories to evaluate cities considering times scale. Four categories are "Damage of Cities", " Potential of Mitigation of Cities", "Accessibility and Supportability from Other Cities", " Potential of Recovery of Cities". In order to evaluate cities relatively, we extract data by researching the Hanshin Awaji Great Earthquake (1995) and a field survey.

1. INTRODUCTION

Index of Macro is placed Fig1.1 as follows by considering times scale.

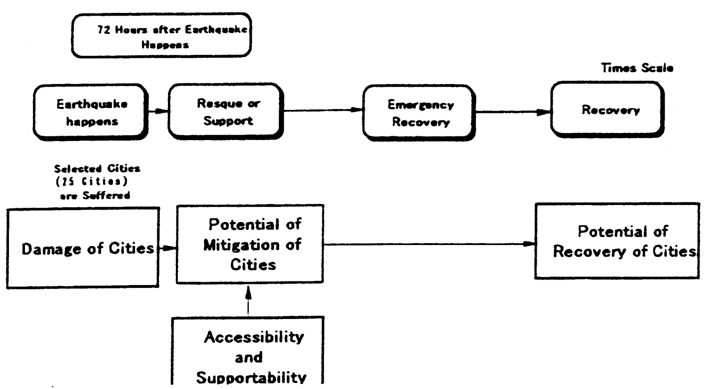

Fig.1.1 Category for Evaluation from Marco

[1] *Graduate School of Engineering, Built & Artificial Environments Systems, Yokohama National Univ, Yokohama, Japan*
[2] *Department of Architecture and Building Engineering, Shibaura Institute of Technology, Shibaura, Japan*
[3] *Department of Design and Architecture, Faculty of Engineering, Chiba University, Chiba, Japan*
[4] *Institute of Industrial Science, University of Tokyo, Tokyo, Japan*
[5] *Research Center for Urban Safety and Security, Kobe University, Kobe, Japan*
[6] *Department of Design and Architecture, Faculty of Engineering, Chiba University, Chiba, Japan*
[7] *Graduate School of Engineering, Built & Artificial Environments Systems, Yokohama National Univ, Yokohama, Japan*
[8] *Informatix Inc. Kitashinagawa, Japan*
[9] *Division of Construction, Kobe University, Kobe, Japan*

2. DAMAGE OF CITIES (Part.1)
- Potential Seismic Risk Assessment of Urban Cities in Japan Considering Their Regional Characteristics -

This study proposed a methodology to estimate potential seismic risk involved in urban cities based on their regional characteristics. Regional characteristics included topography, climate, background history of urban development, accessibility from neighboring cities, etc. that had not been fully considered in the conventional seismic risk assessment as well as soil conditions, buildings conditions, open-space, etc. taken into account in the conventional seismic risk assessment. Also typical urban cities in Japan are selected and their potential seismic risk based on the proposed methodology is estimated, and the relationships between the estimated potential seismic risk and the damage observed in Kobe districts damaged by 1995 Hyogoken-Nambu Earthquake are investigated. Fig2 is the result.

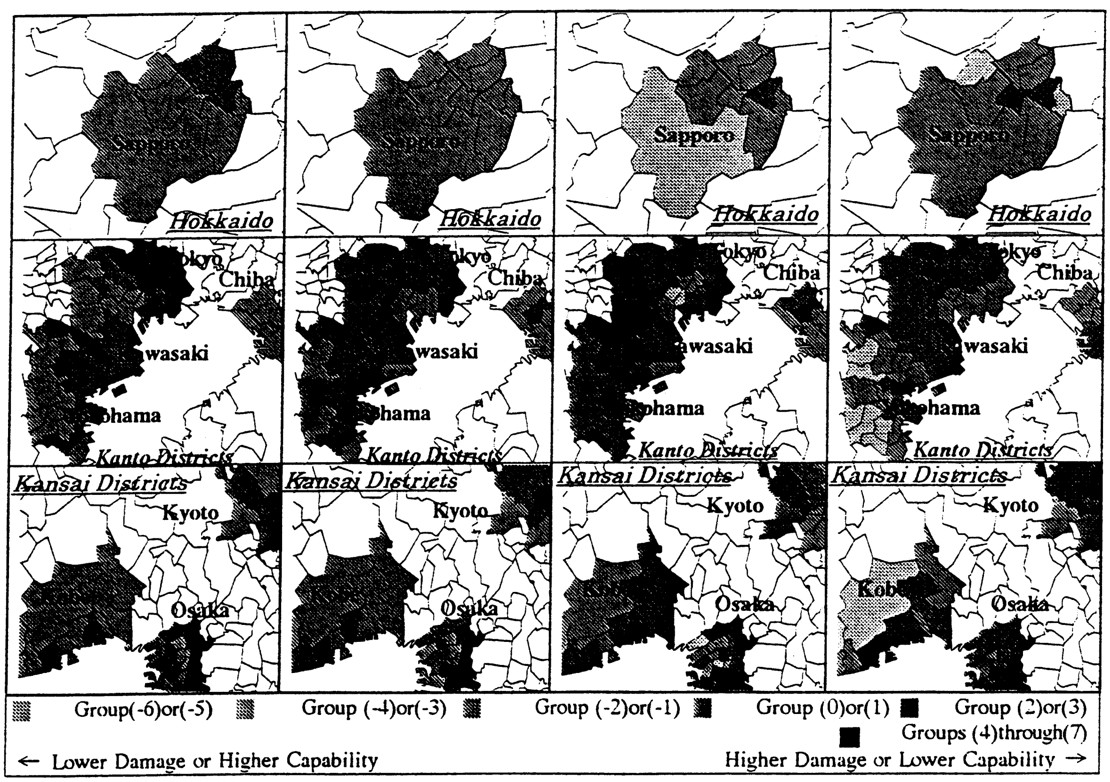

(a) *Risk of Bamage to Buildings (R_B)* (b) *Risk of Fire (R_F)* (c) *Capability of Rescue within Intra-City (C_{RES})* (d) *Capability of Building Reconstruction (C_R)*

Figure 2 Estimated potential seismic risk

3. DAMAGE OF CITIES (Part 2)
Seismic Performance of Existing Reinforced Concrete Buildings and Earthquake Damage in Japan

The relationship between the seismic performance and the degree of damage of the R/C buildings, which suffered six past damaging earthquakes, was discussed evaluating the seismic performance in terms of the Is-index of the Standard for Evaluation of Seismic Capacity of Existing Reinforced Concrete Buildings. In the same manner the current state of the seismic performance of R/C buildings constructed before 1982 was shown, because R/C buildings designed by BSL(1981) scarcely suffered severe damage under the Hyougoken-Nanbu earthquake. From a structural point of view, it is suggested though these results that evaluating the seismic performance of buildings and strengthening them as the need arises are essentially necessary as a pre-event countermeasure and also that the emergency assessment of damaged buildings is very important as a post-event countermeasure.

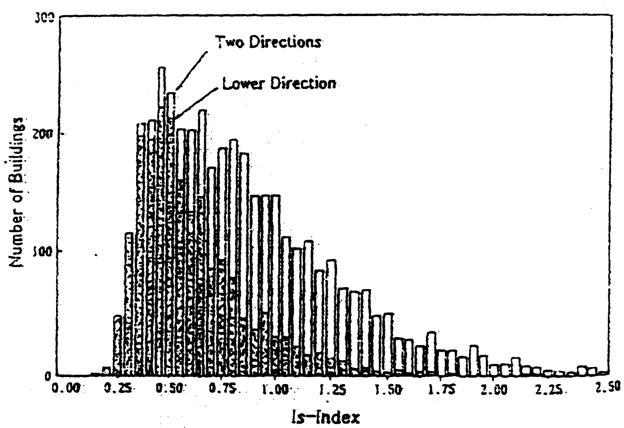

Figure 3.1 Distribution of Is-Index

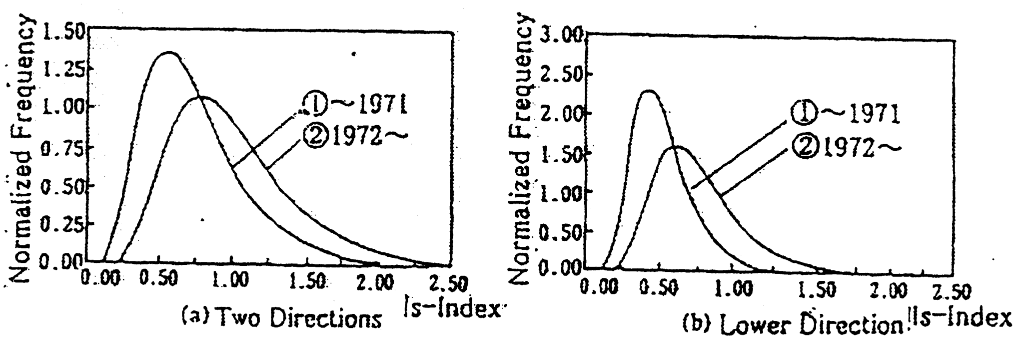

Figure 3.2 Times of Construction and Is-Index

4. DAMAGE OF CITIES (Part 3)

- Present State of Seismic Performance of Reinforced Concrete Buildings in Japan -

This chapter examines the present state of the seismic performance of reinforced concrete buildings in Japan, in order to obtain basic data for the assessment of the structural seismic risk of urban facilities. It consists of next two investigations; 1// The present state of the seismic performance in each region in Japan is examined based on past papers. 2// In order to examine the regional characteristics of the seismic performance in detail, a case study is carried out for two regions.

This research got the main results as follows. The proportion of low seismic performance buildings is considerably high. Although there was the regional difference in its characteristics in detail, the regional difference in the seismic performance could not be very much observed in used data in this paper. On the contrary, it was confirmed that differences by building attributions, such as the construction year and the number of stories, were large. This fact shows the possibility in which the composition ratio with respect to each building attribution in the cluster of buildings produces the regional difference. In order to verify these points exactly, more detailed and prudent examination is necessary by accumulating much data in many regions and carrying out the statistical analysis directly for these integrated data.

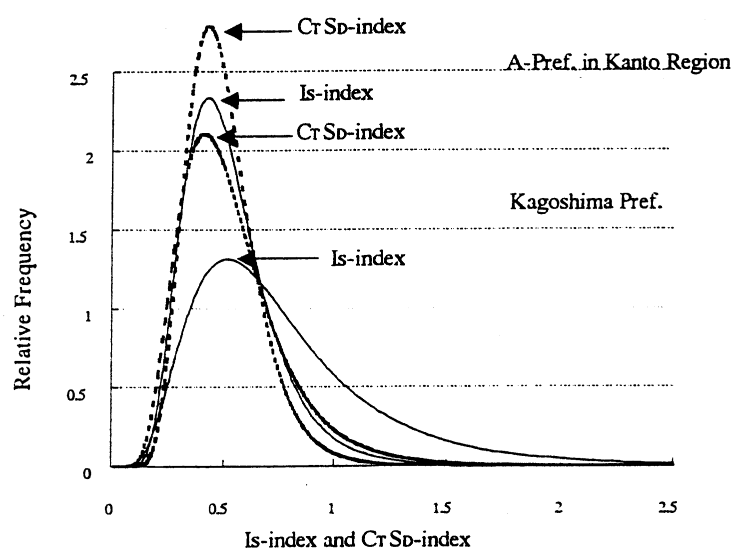

5 MACROZONING BY REMOTE SENSING

It pays attention to open space from the case in Kobe, and thinks that the evaluation of the open space in the city will be done by this research. But, it is difficult to take the open space that has various quantity and extent in the city quantitatively. So, before evaluating open space, it considers that macro point of view is necessary. First, the character of open space, which is available as repression of a disaster, is explained. Next the amount and distribution of open space in the city are led from remote sensing that has high treatment ability in the large area. On that the disaster repression ability of the city is examined by grasping it.

Each result of land covering classification is shown in the Fig 5.1 and the Fig5.2. Also Fig5.3 shows the result evaluating the open space around one person in three cities.

Figure5.1 Tokyo 23 ward

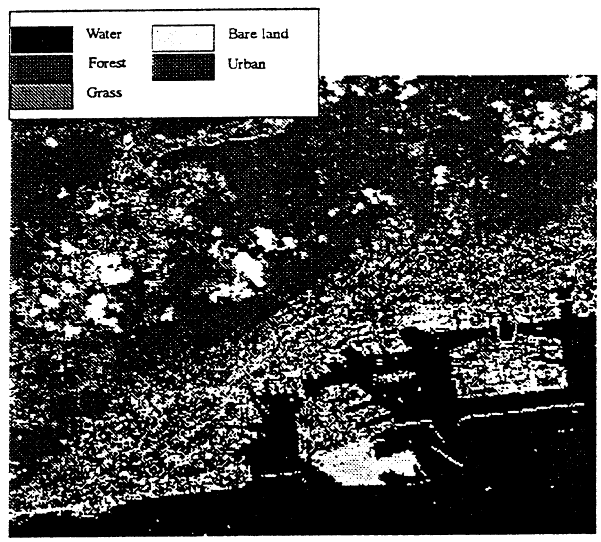

Figure5.2 Kobe city

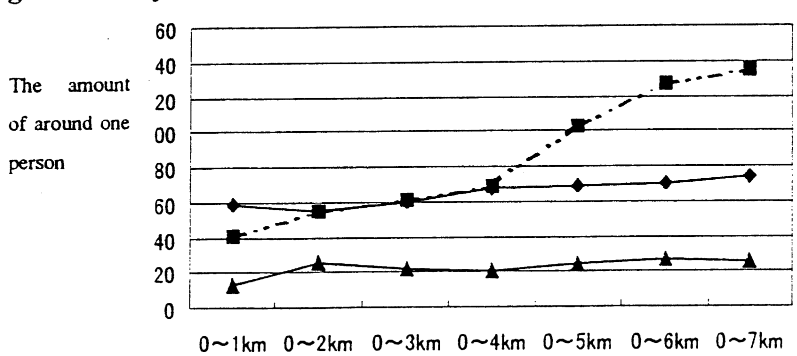

Figure.5.3

Yokohama Kobe Tokyo

6. POTENTIAL OF MITIGATION OF CITIES

In this research, we focus the potential capability that the damage of the casualties and the injured by near-field earthquake is decreased as much as possible. Specifically, it is the disaster-prevention consciousness to the earthquake disaster and the community of the local residents. Both factors have regionalism in the Japan whole country, so we did the questionnaire in 25 cities. Fig6.1 is the result of it and Fig6.2 shows the analyzed result.

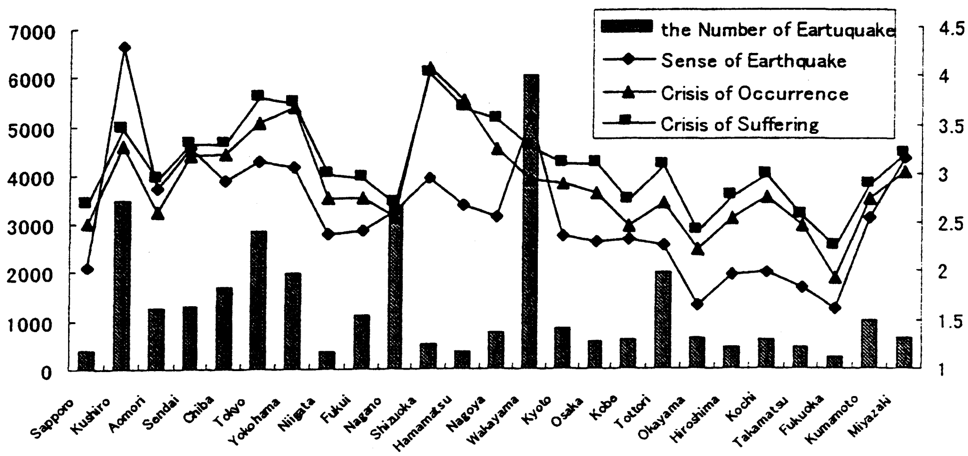

Fig.6.1 Number of Earthquake, Human Sense against

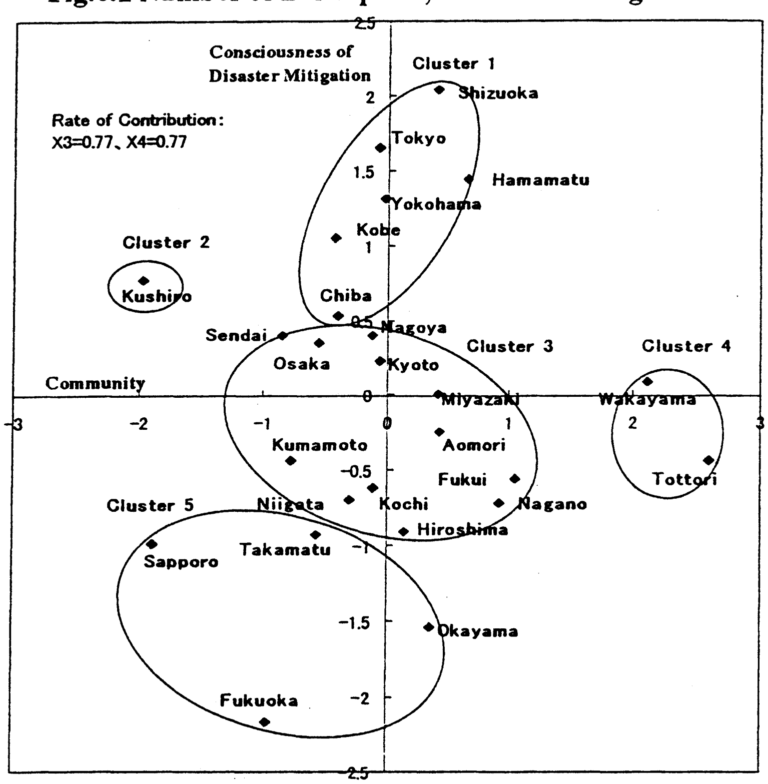

Fig.6.2 Classification of Urban Cities

7. ACCESSIBILITY AND SUPPORTABILITY FROM OTHER CITIES

In this study, "Accessibility and Supportability" means the possibility that the damaged city by earthquake can receive rescue and support from a circumference city by marine transportation and land transportation, or accept support from a circumference city in a short time (about 72 hours is assumed) when it is assumed that the city suffered by near-field earthquake. Using its measure, we compare and group cities and make clear a regional characteristic about support and rescue.

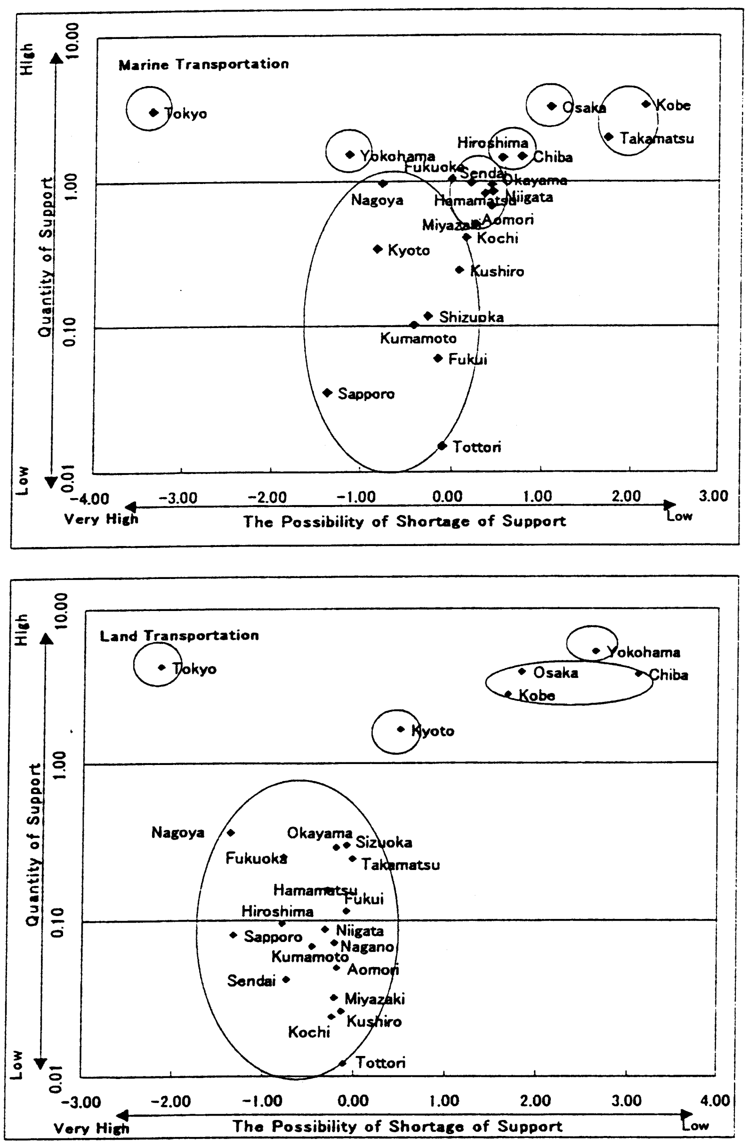

Fig.7 Quantity of Support and Shortage of support (Land and Marine)

8.POTENTIAL OF RECOVERY OF CITY

It aims at clearing the matter whether the character of the city gives the reconstruction and the restoration what kind of influence in the long-term process from the macro point of view. It suffers the damage of the city earthquake directly above its epicenter, a balance of the society and the economy collapses. As for the phenomenon such as a movement of the quantity which decreased due to the damage, it is difficult to prove conclusive evidence from the statistics materials being processed in each local government unit.

Relations between center city and the circumference municipalities were investigated based on the unique technique. (**Fig 8.**) An arrow in the figure and numerical value show the rate which flows out so that the working person who lives in the city of the starting point again may work in the terminal city. This rate showed a transfer after disaster and high correlation. And, the rate that it flowed out from Kobe City before Hanshin great earthquake disaster into Osaka City was 8.2%.

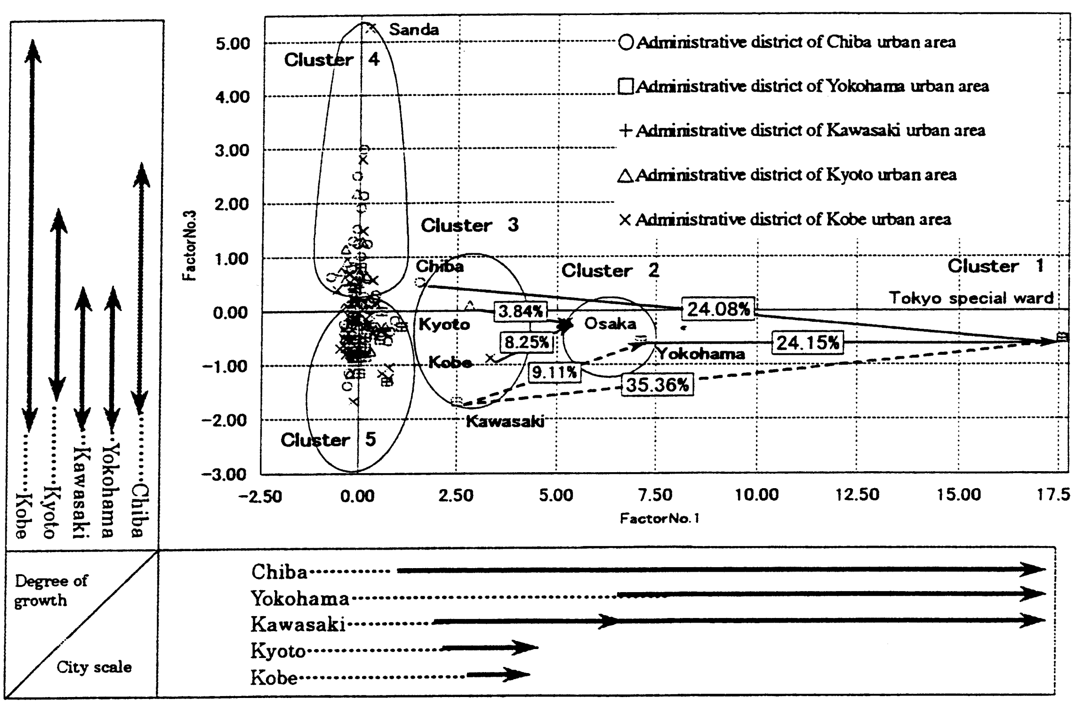

Fig 8 Human movement among circumference cities

NEAR-FAULT SEISMIC SITE EFFECTS

Jonathan D. BRAY and Adrian RODRIGUEZ-MAREK
University of California, Berkeley

INTRODUCTION

Significant damage and loss of life has been directly related to the effect of local site conditions in recent earthquakes. While there are potentially other factors contributing to damage (such as topographic and basin effects, liquefaction, ground failure, or structural deficiencies), the amplification of ground motion due to local site conditions plays an important part in increasing seismic damage. The correlation between site effects and building damage is dramatically illustrated in Figure 1 for the 1967 Caracas, Venezuela, Earthquake. Larger amounts of damage occurred when the natural period of the buildings and the site were closely matched. These observations suggest that a correct quantification of site effects is necessary for a complete assessment of seismic hazard.

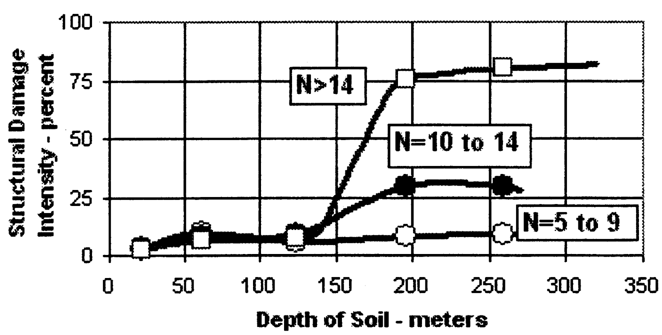

Figure 1. Relationship between structural damage intensity and soil depth in the Caracas Earthquake of 1967; N = # of stories (from Seed and Alonso 1974).

The importance of site effects in characterizing seismic ground motions has long been recognized. Recently, Borcherdt (1994) developed intensity-dependent, short and long period amplification factors based on the average shear wave velocity measured over the upper 30 m of a site. This work, along with work by Seed [Seed et al.,1991] and Dobry [Dobry et al., 1994] has been incorporated into the 1997 Uniform Building Code (UBC). Using the average shear wave velocity to classify a soil profile has the advantage of simplicity and uniformity. As shown in Figure 1, site response is also a function of profile depth, thus ignoring profile depth may have a detrimental effect in ground motion prediction. Moreover, the Borcherdt [1994] site amplification factors are based primarily on observations from the 1989 Loma Prieta earthquake, which shows significant nonlinear site response effects; whereas, observations from the 1994 Northridge earthquake indicate that site amplification factors should not decrease as significantly with increasing ground motion intensity.

A SITE CLASSIFICATION SCHEME THAT INCLUDES DEPTH OF SOIL

The amplification of ground motions at a nearly level site is significantly affected by the natural period of the site ($T_n = 4H/V_s$; where T_n = natural period, H = soil depth, and V_s = shear wave velocity). Both dynamic stiffness and depth are important. Other important seismic site response factors include the impedance ratio between the soil deposit and underlying bedrock, the material damping of the soil deposits, and the nonlinear response of soft and potentially liquefiable soil deposits. The effect of nonlinearity is largely a function of soil type (e.g., plasticity index in Vucetic and Dobry, 1991). Factors such as cementation and geologic age may also affect the nonlinear behavior of soils. To account partially for these factors, a site classification scheme should include a measure of the dynamic stiffness of the site and a measure of the depth of the deposit.

The site classification scheme proposed by Bray and Rodriguez-Marek (1997) is an attempt to account for the factors affecting seismic site response while minimizing the amount of data required for site characterization (see Table 1). The site classification scheme is based on two main parameters and two secondary ones. The primary parameters are:

- Type of deposit, i.e. hard rock, rock, weathered rock, stiff soil, soft soil, and potentially liquefiable sand. These general divisions introduce a measure of dynamic stiffness to the classification scheme. However, a generic description of a site is sufficient for classification, without the need for measuring shear wave velocity over the upper 30 m.
- Depth to bedrock or to a significant impedance contrast.

The secondary parameters are depositional age and soil type. The former divides soil sites into Holocene or Pleistocene groups, the latter into primarily cohesive or cohesionless soils. These subdivisions are introduced to capture the anticipated different nonlinear responses of these soils.

Table 1. Geotechnical Site Categories [Bray and Rodriguez-Marek, 1997]

Site	Description	Site Period	Comments
A	Hard Rock	≤ 0.1 s	Hard, strong, intact rock (Vs ≥ 1500 m/s).
B	Rock	≤ 0.2 s	Most "unweathered" California rock cases (Vs ≥ 760 m/s or < 6 m of soil).
C-1	Weathered/Soft Rock	≤ 0.4 s	Weathered zone > 6 m and < 30 m (Vs ≥ 360 m/s increasing to ≥ 700 m/s).
-2	Shallow Stiff Soil	≤ 0.5 s	Soil depth > 6 m and < 30 m
-3	Intermediate Depth Stiff Soil	≤ 0.8 s	Soil depth > 30 m and < 60 m
D-1	Deep Stiff Holocene Soil, either S (Sand) or C (Clay)	≤ 1.4 s	Soil depth > 60 m and < 210 m. Sand has low fines content (< 15%) or non-plastic fines (PI < 5). Clay has high fines content (> 15%) and plastic fines (PI > 5).
-2	Deep Stiff Pleistocene Soil, S (Sand) or C (Clay)	≤ 1.4 s	Soil depth > 60 m and < 210 m. See D1 for S or C sub-categorization.
-3	Very Deep Stiff Soil	≤ 2 s	Soil depth > 210 m.
E-1	Medium Depth Soft Clay	≤ 0.7 s	Thickness of soft clay layer 3 m to 12 m.
-2	Deep Soft Clay Layer	≤ 1.4 s	Thickness of soft clay layer > 12 m.
F	Special, e.g., Potentially Liquefiable Sand or Peat	≈ 1 s	Holocene loose sand with high water table ($z_w \leq 6$ m) or organic peats.

This site classification scheme was used to investigate the effects of local site conditions for the 1989 Loma Prieta and 1994 Northridge earthquakes. The primary findings from this study (Rodriguez-Marek et al. 1999) were

- There are significant differences between the seismic responses of "competent rock" sites, "soft rock/shallow stiff soil" sites, and "deep stiff soil" sites." Hence, a simple "rock" vs. "soil" classification scheme as is often employed in current attenuation relationships should not be used.
- Due to the significantly greater number of ground motion recordings at "soft rock/shallow stiff soil" sites compared to that at "competent rock" sites, current "rock" attenuation relationships that are largely based on both "soft rock/shallow stiff soil" and "competent rock" sites overestimate the actual response at "competent rock" sites. The spectral ordinates of acceleration response spectra (5% damping) are in general 30% lower for "competent rock" sites than that predicted using current "rock" attenuation relationships.
- The standard deviations resulting from the Bray and Rodiguez-Marek (1997) classification system are comparable with the standard deviations obtained using a more burdensome average shear wave velocity classification system. This illustrates that depth of the soil deposit is an important parameter for the estimation of seismic site response. A site classification scheme should account both for site stiffness and profile depth.

NEAR-FAULT ISSUES

A major limitation of the Rodriguez-Marek et al. (1999) empirically based evaluation of seismic site effects is the low number of recordings in the near-fault region. Hence, the findings of this study that were summarized above are limited to sites located at least 20 km from the fault rupture plane. The large number of near-fault recordings from the 1999 Chi-Chi, Taiwan, and 1999 Kocaeli, Turkey, earthquakes could potentially offer important insights regarding the effects of local site conditions in the near-fault region. Unfortunately, at this time, all necessary site classification data for examining these two data sets are not available. Even with these data sets, our understanding of near-fault seismic site effects will need to be augmented by insights gained from simulations. This paper reports the preliminary findings from using simulations to evaluate the effects of local site conditions in the near-fault region.

Near-fault motions are greatly different from ground motions away from the fault. Yet, our traditional understanding of site conditions is based on observations of site effects for ground motions away from the fault. In the near-fault region, it is useful to examine ground motions through velocity-time histories (Fig. 2). The key ground motion parameters are peak ground velocity (PGV), pulse period (T_V), and number of significant pulses (n_V). Because of forward-directivity, the fault-normal and fault parallel components of motion can differ significantly, so one should also examine these motions with the use of horizontal velocity traces as shown in Figure 3. A series of bi-directional seismic site response analyses were performed for a deep stiff soil site undergoing near-fault motions. Representative results are shown in Figure 4.

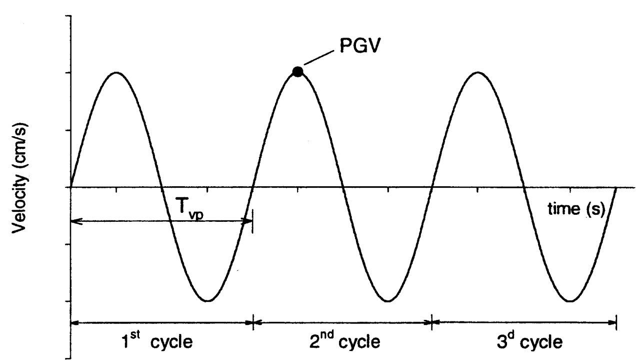

Figure 2. Simplified Velocity-Time History Showing Peak Ground Velocity (PGV), Period of the Velocity-Pulse (T_V), and number of significant cycles of motion

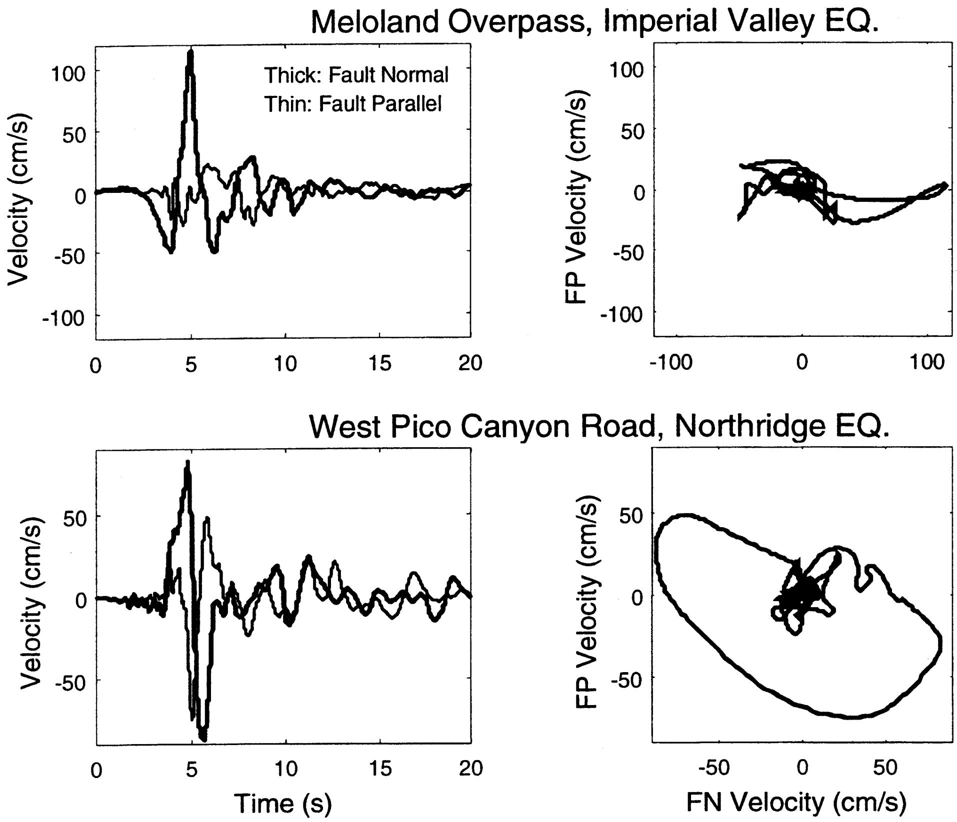

Figure 3. Fault normal (FN) and fault parallel (FP) velocity time-histories and horizontal velocity-trace plots for two near-fault recordings. Both recordings have significant fault normal velocities, but the Meloland Overpass recording from the Imperial Valley earthquake has much lower fault parallel velocities than the West Pico Canyon Road record from the Northridge earthquake.

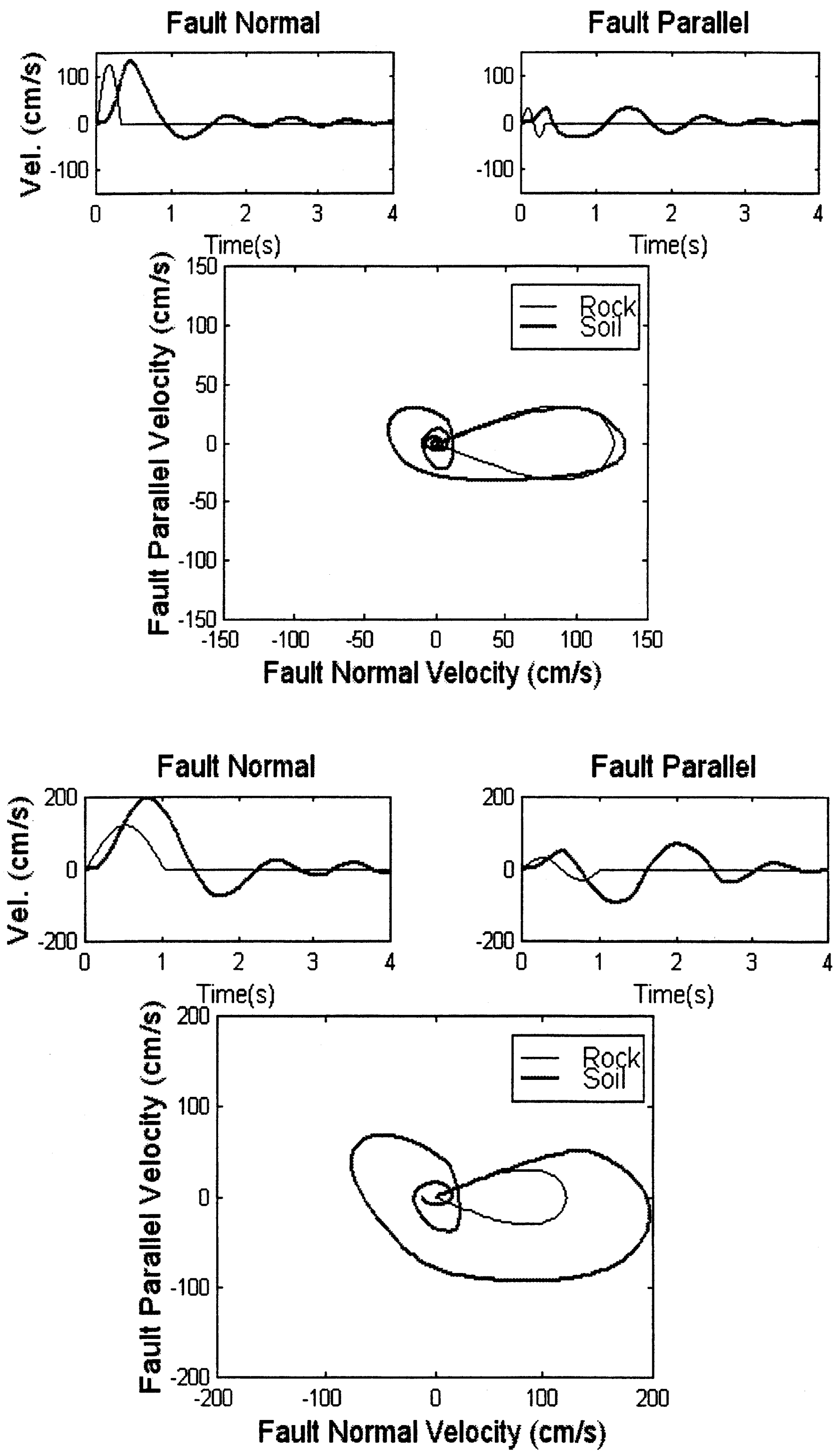

Figure 4. Response of deep, stiff soil site to half-pulse input rock motion with PGV = 120 cm/s. The top figures are for an input pulse period of 0.6 s, and the bottom figures are for an input pulse period of 2.0 s.

Results from these analyses are summarized in Figures 5 and 6. The results from these simulations indicate that site effects can be an important factor in the near-fault region, and hence, should be considered in developing ground motions in the near-fault region.

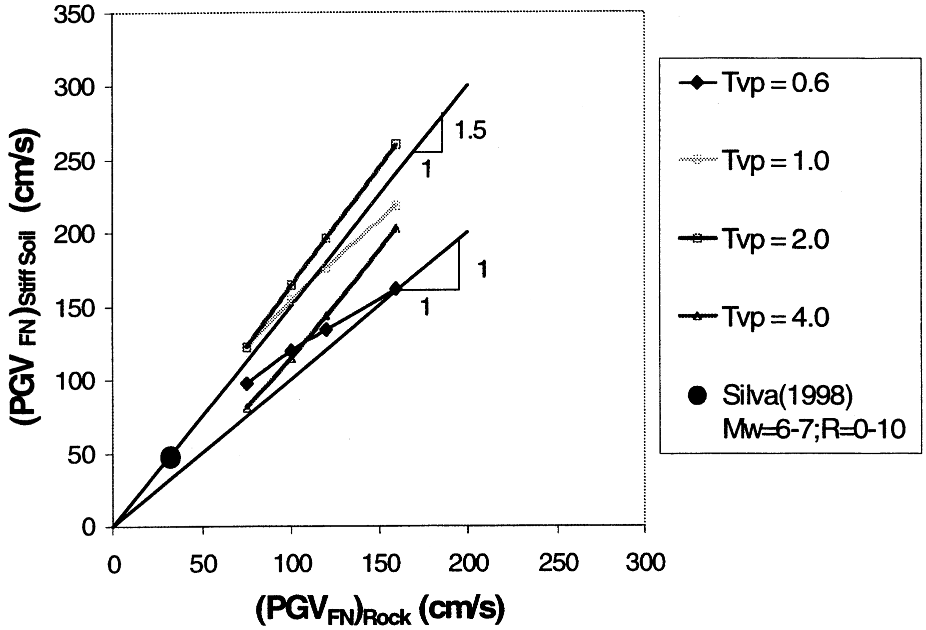

Figure 5. Amplification of PGV due to site conditions and the effect of pulse period of the input rock velocity-time history.

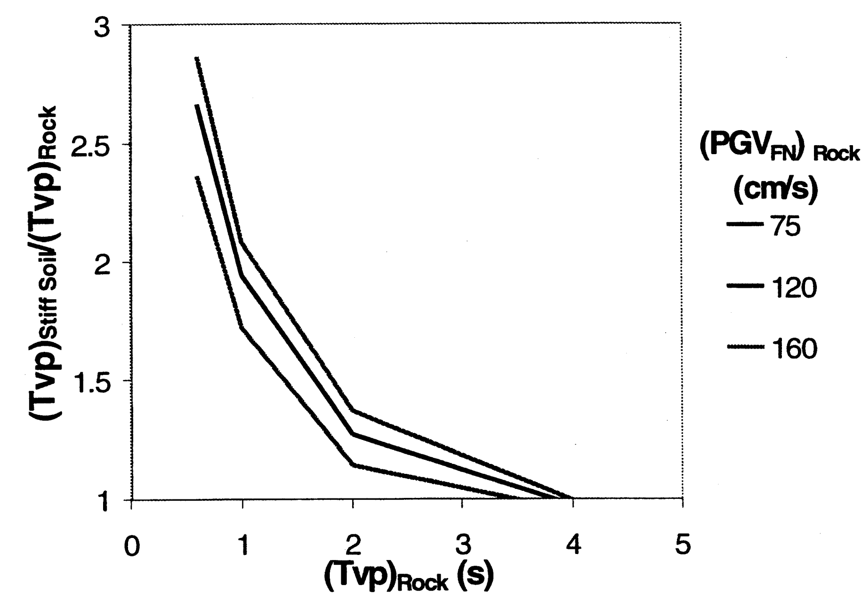

Figure 6. Lengthening of pulse period due to site conditions, especially for those input rock motions that have short pulse periods.

PRINCIPAL FINDINGS

- A bi-directional fully nonlinear soil column captures the combined effects of fault-normal and fault-parallel components of motion.
- Lengthening of pulse period occurs for rock velocity pulses less than the degraded site period.
- Significant amplification of PGV occurs when the pulse period "matches" the degraded site period.

ACKNOWLEDGMENTS

The authors wish to thank Dr. Walter Silva of Pacific Engineering and Analysis for his assistance in providing the ground motion database used in this study; Dr. Paul Somerville for providing event-specific attenuation relationships for the Northridge and Loma Prieta earthquakes; Dr. François E. Heuze, Dr. Mladen Vucetic, Dr. Sandy Figuers, and Dr. David Rogers for providing essential geotechnical data for ground motion sites; Dr. Jon Stewart for the information on the Oakland Bart Station site and numerous sites in Southern California; and Dr. Susan Chang for her willingness to share knowledge and information on ground motion site classification. Financial support was provided by the Pacific Gas and Electric Company through the Pacific Earthquake Engineering Research Center, and the David and Lucile Packard Foundation.

REFERENCES

Borcherdt, R. D. (1994). "Estimates of Site-Dependent Response Spectra for Design (Methodology and Justification)." *Earthquake Spectra*, Vol. 10(4), pp. 617-653.

Bray, J. D., and Rodriguez-Marek, A. (1997). "Geotechnical Site Categories." *Proceedings. First PEER-PG&E Workshop on Seismic Reliability of Utility Lifelines*, San Francisco, CA, 1997.

Dobry, R., Martin, G. M., Parra, E., and Bhattacharyya, A. (1994). "Development of Site-Dependent Ratios of Elastic Response Spectra (RRS) and Site Categories for Building Seismic Codes." Proceedings of the NCEER/SEAOC/BSSC Workshop on Site Response during Earthquakes and Seismic Code Provisions, University of Southern California, Los Angeles, November 18-20, edited by G. M. Martin.

Rodriguez-Marek, A., Bray, J. D., and Abrahamson, N. (1999). "Task 3: Characterization of Site Response: General Site Categories," PEER Report 1999/03. Pacific Earthquake Engineering Research Center, Univ. of California, Berkeley, CA.

Seed, H. B. and Alonso, J. L. (1974). "Soil-structure interaction effects in the Caracas Earthquake of 1967," Report No. 73023, Earthquake Engineering Research Center, Engineering Department, University of California, Berkeley, CA.

Seed, R. B., Dickenson, S. E., and Mok, C. M. (1991). "Seismic Response Analysis of Soft and Deep Cohesive Sites: A Brief Summary of Recent Findings." *Proceedings, CALTRANS First Annual Seismic Response Workshop, Sacramento*, California, December 3-4.

Vucetic, M. and Dobry, R. (1991). "Effect of Soil Plasticity on Cyclic Response." *Journal of Geotechnical Eng.*, ASCE, Vol. 117(1).

STRUCTURAL LESSONS FROM 1995 KOBE EARTHQUAKE DISASTER

Shunsuke OTANI

ABSTRACT

This paper discusses the 1995 Kobe disaster from structural engineering point of view. The structural damage investigation revealed much less damage with the application of current building code requirements. It is important retrofit old buildings for the reduction of an urban earthquake disaster. The damage pointed out the desirability of the performance-based design.

INTRODUCTION

The Hyogo-ken Nanbu earthquake occurred at 5:46 am on January 17, 1995. The earthquake killed nearly 6,432 people (including direct and indirect causes by the earthquake), injured more than 40 thousands people, destroyed nearly 94,000 buildings and heavily damaged approximately 107,000 buildings. More than 7,500 buildings were burnt by fire after the earthquake. The highway viaducts and Shin-Kansen overpasses collapsed. Had the earthquake occurred at even slightly later hours, the collapses must have lead to much larger disaster.

CAUSES OF DEATH

Approximately 5,500 people were killed immediately after the earthquake or 6,432 including indirect causes. The Ministry of Health and Welfare investigated the cause of death in 5,479 direct cases on the basis of individual death and medical reports. The investigation (Table 1) revealed that 4,816 people (88 %) were killed by pressure and suffocation under collapsed buildings; 570 (10 %) were killed by fire and burn under fire; and 65 (1.2 %) were killed by the overturned furniture and equipment.

Medical inspectors studied 3,651 direct death cases in Kobe City, and reported that 3,540 (97 %) were killed on the same day of the earthquake; 2,940 deaths (80.5%) within 15 minutes.

Major death occurred under the collapse of old traditional timber houses. This was related to their construction; i.e., heavy mud and tiles were used in the roof in these timber houses. The heavy materials were necessary on the roof, in the old days, for the heat insulation in hot and humid summer days and for the protection of the roof against blow-up failure from a few annual typhoon attacks. Naturally the heavy roofs attracted inertia forces during the earthquake. It should be noted that the last major earthquake in this region occurred in 1592; i.e., more than 400 years ago. People chose the amenity during hot summer and and safety from annual typhoons over the safety from very rare earthquake events.

Department of Architecture, University of Tokyo, Tokyo 113--8656, Japan
email: otani@sake.t.u-tokyo.ac.jp

Figure 1 shows damage statistics of timber houses near the epicenter in Awaji Island (Timber Construction Committee 1995). The construction age was classified as new if constructed within 5 years, normal within 5 to 20 years, old within 20 to 50 years, and very old more than 50 years. Note that heavy damage decreased with construction age. The collapse took place more in old houses partially attributable to the old design and construction technology, and partially attributable to the deterioration in structures and materials with age. The roofs of new construction are much lighter; the houses are well insulated and air-conditioned for comfortable summer life, and the roofs are tightly fixed to the structure. Therefore, the recent construction has less problem from heat or from typhoons, and also from earthquakes.

The elderly people lived in these old houses. After retirement without any additional income, they could not afford to retrofit these houses. Furthermore, the evaluation of properties in Japanese taxation system will not recognize the improvement of the properties by additional investment and improvement. Therefore, even if they had an extra income their priority was not to spend it on strengthening their properties.

It is difficult to guide people to invest their money toward earthquake safety. The engineering profession, however, should inform the citizen of the earthquake hazard and associated risk. If people could spend more money to improve the structures of their houses partially by maintenance work on decayed materials and partially by strengthening old construction, the damage and accompanying casualties could have been reduced. The advancement in earthquake engineering becomes meaningful only when people utilize the technology in real construction.

DAMAGE OF REINFORCED CONCRETE BUILDINGS

Many reinforced concrete buildings collapsed during the earthquake by brittle failure of columns; i.e., the failure mode commonly known as "shear failure." The same failure mode was observed in school buildings after the 1968 Tokachi-oki earthquake; the Building Standard Law Enforcement Order was revised in 1971 to require 100-mm tie spacing in the end regions of a column. The Building Standard Law Enforcement Order was further revised in 1981 to require higher lateral resistance from a building irregular in plan or along height in addition to the examination of lateral load resisting capacity at the formation of the yielding mechanism under earthquake loading.

The Architectural Institute of Japan investigated the damage level of all buildings in a heavily damaged area of Nada and Higashi-Nada districts in Kobe City; 3,911 buildings in total (Reinforced Concrete Committee 1996). The damage level was classified as operational damage (no, light and minor damages), heavy damage (intermediate and major damages), and collapse (including those already removed at the time of investigation). Buildings with operational damage could be occupied immediately after the earthquake. Buildings with heavy damage needed some or major repair work for the occupancy. The investigation (Fig. 2) shows that eighty-nine percent suffered operational damage, 5.9 percent suffered heavy damage and 5.7 percent collapsed. Among those 2,035 buildings constructed before 1981, 7.4 percent suffered heavy damage and 8.3 percent collapsed. Among those 1,859 buildings constructed after 1981, 3.9 percent suffered heavy damage and 2.6 percent collapsed. The 1981 revision of the Building Standard Law enhanced significantly the performance of reinforced concrete buildings against the earthquake attack.

Figure 3 compares the damage of pre-1971 buildings with number of stories. Note the increase of the ratio of buildings suffering heavy damage and collapse with height. A structural designer should pay more attention to earthquake resistant design of taller buildings. Figure 4 shows a similar diagram for those constructed after 1981. A significant improvement may be observed in the protection of buildings using current Building Standard Law.

One characteristic failure of reinforced concrete buildings in Kobe was the collapse in the first story. This type of failure was observed in many apartment and condominium buildings, where residential units were separated by reinforced concrete structural walls. The ground floor was normally used for garage or shops, and no partition walls were placed in the ground floor. In other words, the upper stories are generally strong with ample structural walls whereas the ground floor is bare against the earthquake attack. This type of the structure is called "soft first-story buildings." The collapse took place in the ground floor.

Figure 5 compares the damage of soft first-story buildings with construction age. Note a significant improvement in the safety of the soft first-story buildings with the revisions of the Building Standard Law. Almost one half of those soft first-story buildings constructed before 1971 suffered severe damage or collapse.

IS SAFETY AGAINST EARTHQUAKE ENOUGH?

Since the 1923 Kanto (Tokyo) earthquake, the methodology of structural design and construction has been studied extensively in Japan toward the protection of human life from earthquakes. The damage survey in Fig. 2 shows that 93.5 % of buildings constructed after 1981 could be used without repair work after the earthquake, while 3.9 percent suffered heavy damage and 2.6 percent collapsed. The current state of the art has achieved the goal although further efforts are needed to improve the design of the soft first-story building.

Let us discuss the damage of an apartment building shown in Fig. 6. Only minor cracks were observed in structural elements such as columns and girders; i.e., the damage level was minor from a structural viewpoint. Damage was observed only in non-structural elements such as partitions, doors and windows. Without these non-structural elements, the building could not function as a residential unit.

The main objective of a structure is to provide space for the intended function of a building. Even though a structure survives an earthquake with minor damage, if the building loses its function, the design may not be said successful. It seems that structural engineers are only concerned about their own profession; i.e., the design of a structure for the sake of the structure rather than the design of a structure for building function. If the owner of a building is informed of a possible consequence about the function of his building after an earthquake, he might be willing to pay additional expenses toward higher performance. There should have been closer communication between the owner and engineers about the performance of a structure.

CONCLUDING REMARKS

The state of the art and practice in earthquake resistant building design and construction allows us to construct safe buildings against earthquakes. Such technology is meaningful only when it is utilized in real construction by the choice of people. Structural engineers should continue to inform citizens of the hazards and risk from earthquakes. Close communication between the owner and structural engineers is necessary to achieve desired performance of a building.

REFERENCES

Timber Construction Committee. September 1995. Damage of timber construction, the 1995 Hyogo-ken Nanbu earthquake. (In Japanese), Architectural Institute of Japan, Kinki Branch.

Reinforced Concrete Committee. July 1996. Damage investigation report on concrete buildings, the 1995 Hyogo-ken Nanbu earthquake. (In Japanese), Architectural Institute of Japan, Kinki Branch.

Table 1: Causes of death by the 1995 Hyogo-ken Nanbu earthquake

Causes	Number	%
Collapse of Buildings	4,816	87.9
Fire	570	10.4
Highways	17	0.3
Land Slides	11	0.2
Overturned Furniture	65	1.2
Total	5,479	100.0

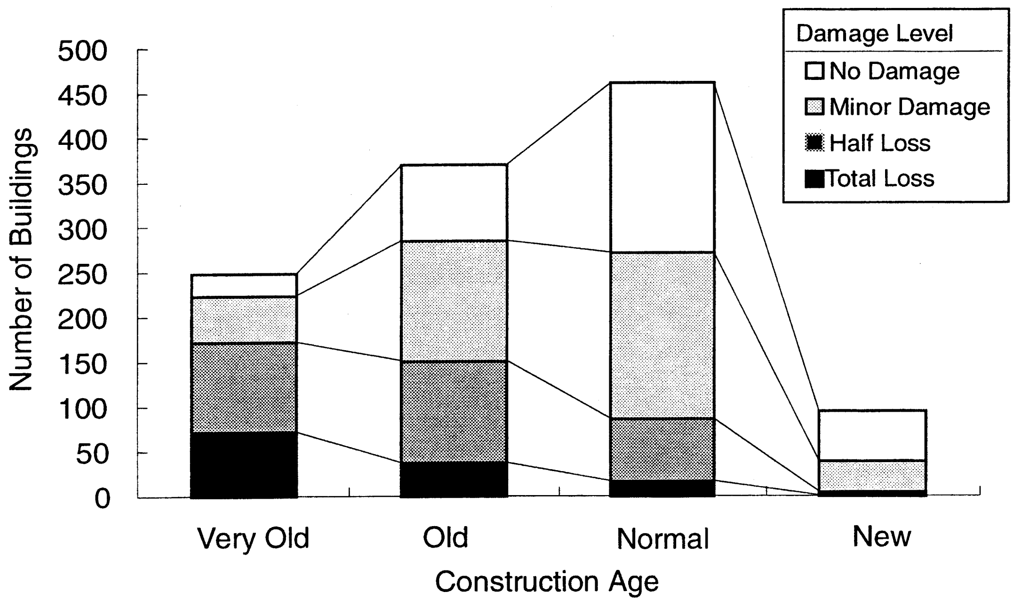

Fig. 1. Damage statistics of timber houses

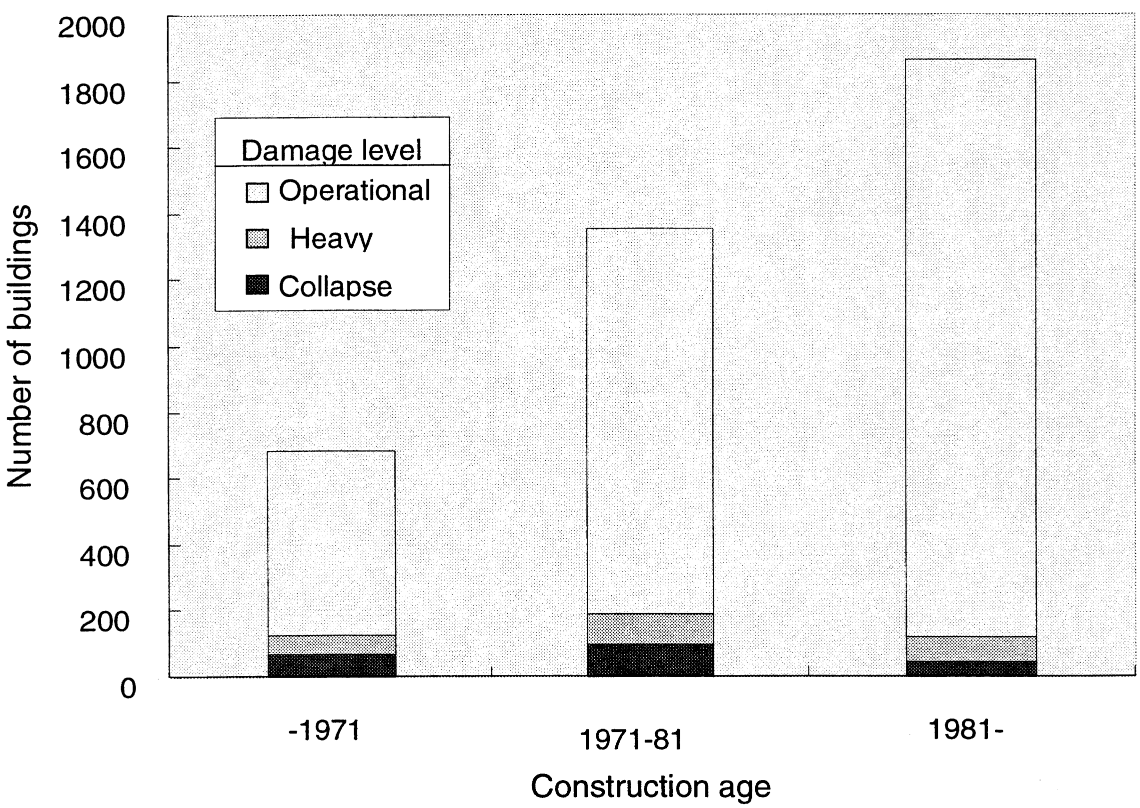

Fig. 2: Damage of reinforced concrete buildings with construction age

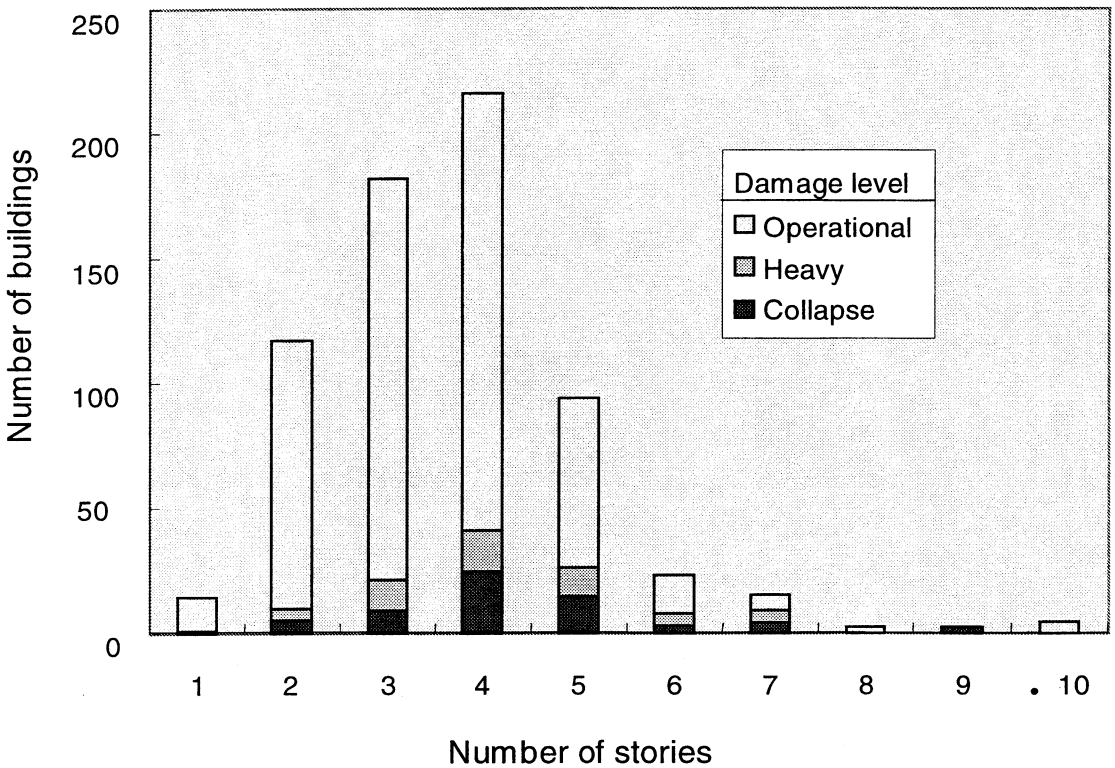

Fig. 3: Damage of pre-1971 reinforced concrete buildings with story height

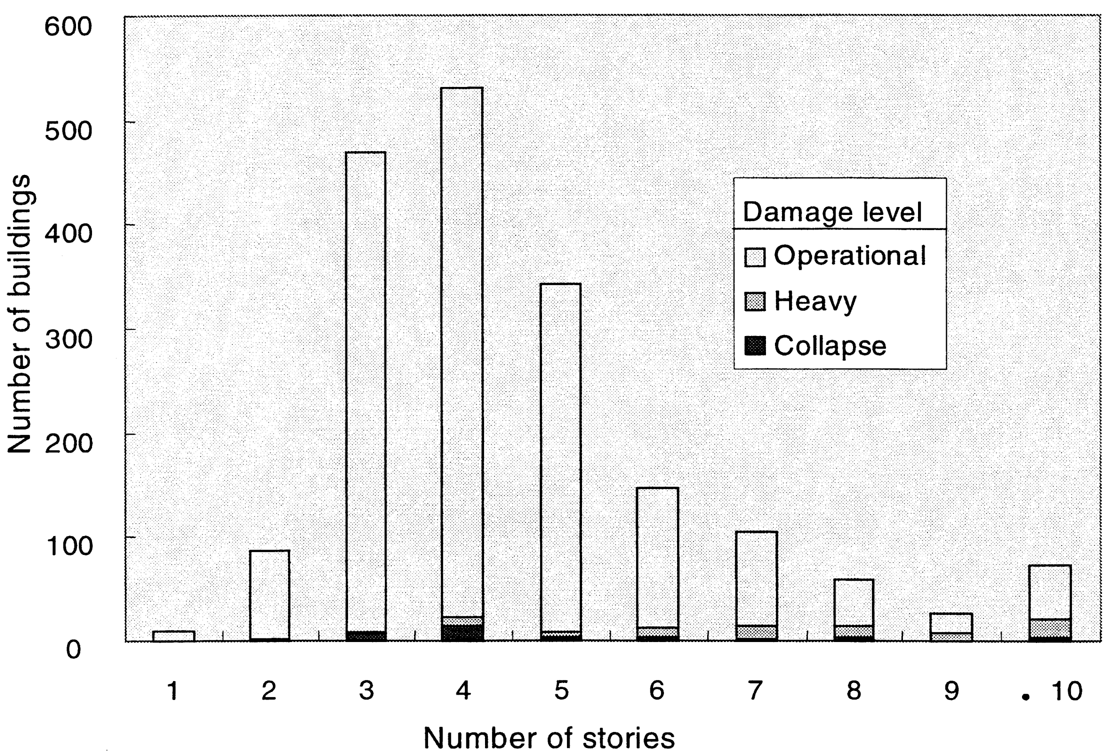

Fig. 4: Damage of post-1981 reinforced concrete buildings with story height

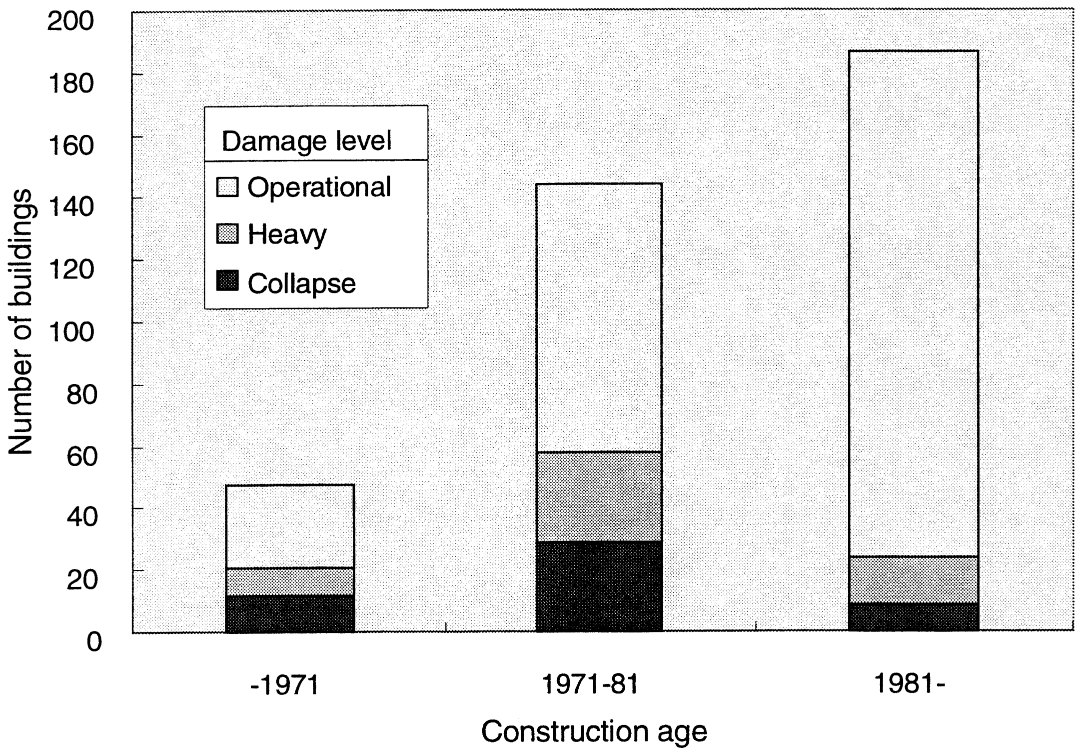

Fig. 5: Damage of soft first-story buildings with construction age

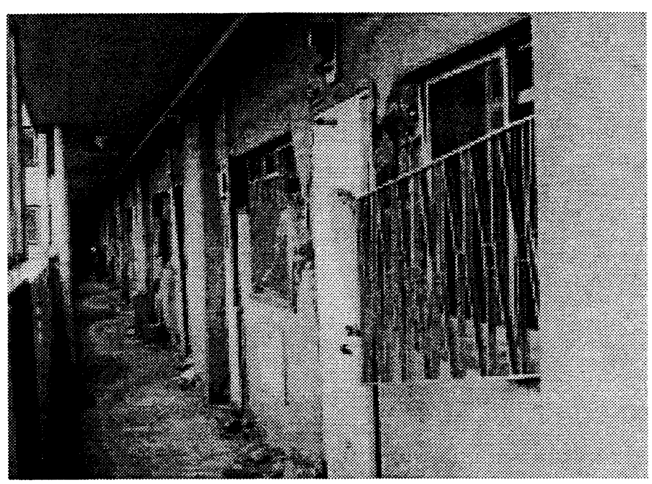

Fig. 6: Damage of non-structural elements

DESIGN CONSIDERATIONS FOR NEAR-FAULT GROUND MOTIONS

Babak ALAVI and Helmut KRAWINKLER [1]

ABSTRACT

Near-fault ground motions with forward directivity impose very large seismic demands on frame structures designed to present code requirements. Simple pulses may be utilized to represent near-fault ground motions and to quantify seismic demands for frame structures. The employment of shear walls in conjunction with frames is investigated to provide more protection for structures against near-fault ground motions. It is shown that shear walls with a hinged base are more effective than walls with a fixed base in reducing drift demands.

1. INTRODUCTION

Recordings from recent earthquakes have provided much evidence that ground shaking near a fault rupture is characterized by a pulse with very high energy input. Velocity spectra of the fault-normal and fault-parallel components of a typical near-fault record are shown in Fig. 1. The figure shows a large difference between the two components, and indicates in the velocity spectrum of the fault-normal component a dominant peak at a well-defined period, which is the period of the pulse contained in the record. The large intensity and impulsive nature of the fault-normal component deserves much attention in the design of structures located near seismic sources. This paper summarizes a few of the findings of a study that is concerned with the effects of near-fault ground motions on frame structures and with the effectiveness of various strengthening techniques. The findings are based on analytical studies of structural models subjected to a set of fault-normal components of near-fault records and to simple pulses that represent the effects of these records.

2. DUCTILITY DEMANDS FOR RECORDED NEAR-FAULT GROUND MOTIONS

The velocity spectra of several records (see Table 1) are shown in Fig. 2. Superimposed is the mean spectrum from a set of reference ground motions (15-D*) that are scaled to match the 1997 UBC soil profile S_D ground motion spectrum disregarding near-fault effects.

The ductility demands imposed by these ground motions on frames with a fundamental period of 2.0 sec. and of two different strengths are shown in Fig. 3. The base shear strength of the frame structures is defined by the seismic coefficient $\gamma = V_y/W$, and the distribution of shear strength over the height follows an SRSS pattern . For the strong structure ($\gamma = 0.4$, Fig. 3(a)), the ductility demands are relatively high in the upper stories, but for the weak structure ($\gamma = 0.15$, Fig. 3(b)), the ductility demand is high in the lower stories. This migration of maximum story ductility demands from the upper to the lower portion of structures, with a decrease in strength, is a fundamental characteristic of the response of long period frame structures to near-fault records. So are the very

[1] *Dept. of Civil & Environmental Engineering, Stanford University, Stanford, CA 94305-4020*
E-mail: hk@ce.stanford.edu

large demands imposed by these records compared to the demands imposed by "ordinary" ground motions (see curves for 15-D*).

3. REPRESENTATION OF NEAR-FAULT RECORDS BY EQUIVALENT PULSES

Studies by the authors (Alavi and Krawinkler 1999) have shown that the effects of near-fault records with forward directivity can be represented by those of equivalent pulses. Figure 4 shows one of the basic pulses investigated (pulse P2). The pulse is defined by a pulse period T_p and a maximum ground acceleration $a_{g,max}$. A comparison of Figs. 3 and 5(b) indicates that for long period structures ($T/T_p > 1.0$) the response of frame structures to this pulse shows similar characteristics as the response to near-fault records. For strong structures (defined by large η values, where $\eta = V_y/(m.a_{g,max})$) the story ductility demands are highest in the upper stories, whereas for weak structures (or very severe ground motions) the high demands migrate towards the bottom stories. A comparison of Figs. 5(a) and 5(b) shows that the response characteristics of short period structures ($T/T_p < 1.0$) is different, with the highest demands in the bottom stories regardless of strength.

Elastic and inelastic SDOF strength demand spectra for pulse P2 are shown in Fig. 6. If MDOF effects are explicitly accounted for, the relationships between the maximum story ductility demand over the height of the structure and the base shear strength shown in Fig. 7 are obtained (Alavi and Krawinkler 1999). If the pulse period T_p and effective ground acceleration $a_{g,max}$ of the pulse that represents the near-fault ground motion are known, this figure can be used directly for design (i.e., required base shear strength to limit the maximum story ductility demand to a prescribed value).

4. DESIGN IMPLICATIONS

The authors have proposed the following *preliminary* model to relate period and effective velocity ($v_{eff} = v_{g,max} = a_{g,max}T_p/4$) of the equivalent pulse to earthquake magnitude (M_w) and distance (R), using regression analysis with recorded and simulated records (Alavi and Krawinkler 1999):

$$\log_{10}T_p = -1.76 + 0.31\, M_w \quad (1)$$

$$\log_{10} v_{eff} = -2.03 + 0.65\, M_w - 0.47 \log_{10} R \quad (2)$$

Results from this model are tabulated in Table 2 for several M_w and R values. Design implications can be investigated by using this model and the strength demand spectra in Fig. 7.

For instance, for a magnitude 7.0 event, the base shear strength demands shown in Fig. 8 are obtained for frame structures located 3 and 10 km from a seismic source. Also shown are estimates of the strength of structures designed according to the 1997 UBC, without and with the appropriate near-fault factor. An R-factor of 8 and an overstrength of 2 are assumed, thus, the UBC spectral values are divided by 4. As can be seen, in certain period ranges the ductility demands for code-designed structures are very large, especially for R = 3 km.

5. STRENGTHENING OF FRAMES WITH WALLS

The results presented here show that the maximum story ductility demands are very high and that the distribution of ductility demands over the height is very non-uniform and depends strongly on the T/T_p ratio. Attempts were made to strengthen the frame selectively (by increasing the base shear and changing the story shear strength distribution over the height) to decrease the maximum story ductility demand and make the ductility distribution more uniform (Somerville et al. 1999). No single strengthening scheme was found that will provide consistent improved protection at all performance levels and for frames with different periods.

As an alternative to the strengthening of the frame, a shear wall can be added to form a dual system. The effects of pulse-type ground motions on two types of dual systems are investigated here. Frames whose base shear strength is defined by the parameter $\eta = V_y/(m.a_{g,max})$ are strengthened by adding shear walls that are either fixed or hinged at the base. At this time the shear walls are assumed to have sufficient strength to behave elastic (studies with inelastic shear walls are in progress). The wall stiffness is defined using the parameter $\lambda = (E_w I_w/H^3)/K_f$, where E_w, I_w, and H are the elastic modulus, moment of inertia, and height of the wall, respectively. K_f is the frame stiffness, defined as the frame base shear associated with a unit roof displacement for the SRSS load pattern (frame stiffness for a point load at the roof level is $0.6K_f$). If the wall base is fixed, the ratio of wall to frame stiffness, K_w/K_f, is equal to 5.0λ.

Figures 9 to 11 illustrate the effects of the addition of <u>elastic</u> walls with various stiffnesses on the distribution of drift angle demands, θ_ι, (story drift normalized by story height) for strengthened systems subjected to pulse P2. Results for the unstrengthened system ($\lambda = 0$) are shown in heavy solid lines, on which also the maximum story ductility demand is indicated. To put these results in perspective it should be noted that $\gamma = \eta(a_{g,max}/g)$, and that representative values of $a_{g,max}$ and T_p are listed in Table 2. Cases with the wall fixed or hinged at the base are illustrated. Since the first mode shape of the frame is close to a straight line, linking a wall that can rotate freely about its base will not affect the fundamental period, whereas adding a fixed-base wall shortens the period of the system considerably. The figures show the drift demands for systems with $T/T_p = 0.5$ and 2.0, where T is the period of the frame alone. Shear force demands for the wall are shown in Figs. 12 and 13, and wall moment demands are shown in Fig. 14. From Figs. 9 to 14, and other graphs not shown here, the following observations are made:

- Fixed-base walls are very effective in reducing drift demands for structures with $T/T_p < 1.0$, but become much less effective in reducing the demands for $T/T_p > 1.0$. The reason for the latter is higher mode effects.
- For stiff fixed-base <u>elastic</u> walls ($\lambda > 0.1$) the shear strength demands become very large in the bottom stories, regardless of T/T_p and strength of the frame (η).
- Stiff hinged-base walls ($\lambda > 0.1$) are about equally effective in reducing the drift demands

for structure with T/T_p smaller and larger than 1.0. These walls result in a close to uniform distribution of drift demands over the height.

- The relative wall stiffness (relative to the frame stiffness) needed for effective drift control increases with the ratio T/T_p, i.e., with the first mode period of the frame.
- The shear strength demands for the elastic walls are much larger for the fixed-base case than for the hinged-base case, particularly in the bottom stories. This is in part because of the period shift that occurs by adding a fixed shear wall to the system. Since wall shear strength is a critical parameter (see example below), these preliminary results indicate that hinged-base walls are a more effective strengthening scheme.
- The wall moment demands for the hinged-base cases are a small fraction of those for the fixed-base cases.

The following example serves to illustrate strengthening by means of a hinged-base R/C wall in an actual design. The SAC 9-story LA steel frame structure (Gupta and Krawinkler 1999) is used for this purpose. This frame structure has a base shear strength coefficient $\gamma = V_y/W = 0.21$. In order to provide sufficient stiffness for the wall and achieve a roughly uniform drift distribution, $\lambda = 0.3$ is chosen. From the definition of λ, the wall moment of inertia is estimated as follows (assuming an R/C wall made of 4,000 psi concrete):

$$I_w = \frac{\lambda H^3 K_f}{E_w} = \frac{\lambda H^3 K_f}{57\sqrt{f_c'}} = \frac{(0.3)(1464\ \text{in})^3(120\ \text{k/in})}{57\sqrt{4{,}000}} = 3.1*10^7\ \text{in}^4$$

If the width of the wall is chosen to be equal to the length of one bay of the frame (360 in), the required wall thickness $t_w = 12(3.1*10^7)/(360)^3 = 8.0$ in. To estimate the shear strength demand the wall is expected to experience (provided that it behaves elastically), a scenario event with $M_w = 7$ and $R = 3$ km is considered, which corresponds to $a_{g,max} = 0.31g$ and $T_p = 2.6$ sec. (Table 2). The maximum normalized elastic shear strength demand for $T/T_p = 2.2/2.6 = 0.85$ and $\eta = 0.21/0.31 = 0.68$ is about $V/(m.a_{g,max}) = 0.5$. Thus, the strength demand V can be estimated as:

$V = 0.5\ m.a_{g,max} = 0.5\ W.a_{g,max}/g = 0.5(9{,}931\ k)(0.31) = 1{,}540$ k. The average shear stress for the wall is then 1,540,000/(360)(8) = 535 psi. This large stress indicates that it is hardly feasible to design the R/C wall to remain essentially elastic.

Thus, the strengthening scheme investigated so far, which is based on elastic wall behavior, needs to be modified to incorporate inelastic shear behavior (recognizing that the ductility capacity of R/C walls in shear is limited). Work on this modification is in progress. The use of steel plate shear walls may provide an attractive alternative, considering that the moment demands for hinged-base walls are very small.

6. CONCLUSIONS

Recordings from recent earthquakes lead to the realization that forward directivity ground motions near the fault rupture can be very severe and have pulse-like characteristics. The demands these ground motions impose on frame structures is not adequately represented in present code design procedures. The pulse representations summarized in this paper provide a means to assess these demands as a function of the magnitude and distance dependent period and effective acceleration of an equivalent pulse. Increased protection can be achieved by increasing the strength and stiffness of the frames, but this increase would have to be very large. Alternatively, shear walls can be added to the frame structures. Walls with fixed and hinged base conditions have been investigated. The elastic shear strength demands for fixed-base walls are very large. The elastic strength demands for hinged walls are much smaller, but still relatively large. A study of the effectiveness of walls that can undergo inelastic behavior is in progress.

ACKNOWLEDGMENTS

This manuscript contains selected results of an ongoing study on the effects of near-fault ground motions on frame structures. This study has been supported by a grant from the CUREe/Kajima research program, by the California Department of Conservation as a SMIP 1997 Data Interpretation Project, and more recently by the NSF Grant CMS-9812478. This support is greatly appreciated.

REFERENCES

Alavi, B., and H. Krawinkler. 1999. *Structural design implications of near-fault ground motion.* Kajima-CUREe Research Report 1999.12.

Gupta, A., and H. Krawinkler. 1999. *Seismic demands for performance evaluation of steel moment resisting frame structures.* John A. Blume Earthquake Engineering Center Report No. 132. Palo Alto, Calif.: Department of Civil Engineering, Stanford University.

Somerville, P.G., H. Krawinkler, and B. Alavi. 1999. *Development of improved ground motion representation and design procedures for near-fault ground motions.* CSMIP Data Utilization Program. Report CSMIP/99-xx.

Table 1. Near-fault ground motions whose characteristics are illustrated in Figs. 2 and 3.

Designation	Earthquake	Station	Magnitude	Distance
LP89lgpc	Loma Prieta, 1989	Los Gatos	7.0	3.5
LP89lex	Loma Prieta, 1989	Lexington	7.0	6.3
EZ92erzi	Erzincan, 1992	Erzincan	6.7	2.0
LN92lucr	Landers, 1992	Lucerne	7.3	1.1
NR94rrs	Nothridge, 1994	Rinaldi	6.7	7.5
NR94sylm	Nothridge, 1994	Olive View	6.7	6.4
KB95kobj	Kobe, 1995	JMA	6.9	3.4
KB95tato	Kobe, 1995	Takatori	6.9	4.3

Table 2. Predictions of pulse properties from regression models.

M_w	T_p (sec)	R = 3 km		R = 5 km		R = 10 km	
		$v_{g,max}$ (cm/sec)	$a_{g,max}$ (g)	$v_{g,max}$ (cm/sec)	$a_{g,max}$ (g)	$v_{g,max}$ (cm/sec)	$a_{g,max}$ (g)
6.0	1.3	44	0.14	35	0.11	25	0.08
6.5	1.8	93	0.21	74	0.17	53	0.12
7.0	2.6	198	0.31	155	0.25	112	0.18

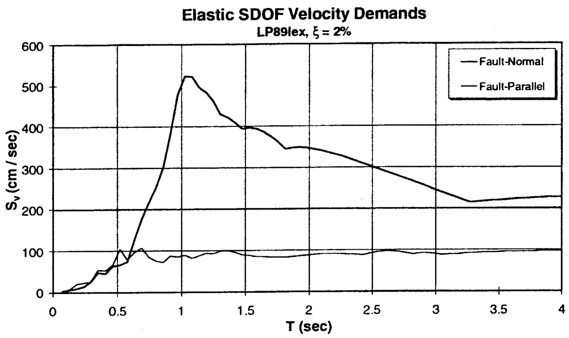

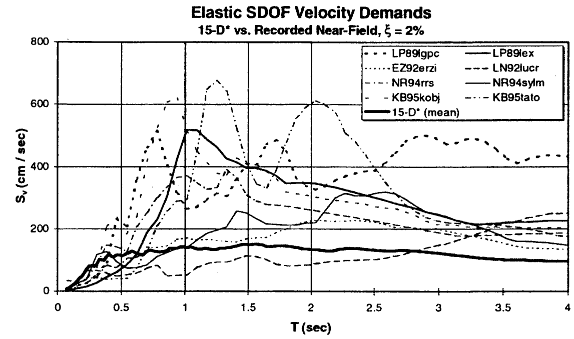

Fig. 1. Velocity spectra of a near-fault record, fault-normal and fault-parallel comp.

Fig. 2. Velocity spectra of near-fault records, and reference ground motions

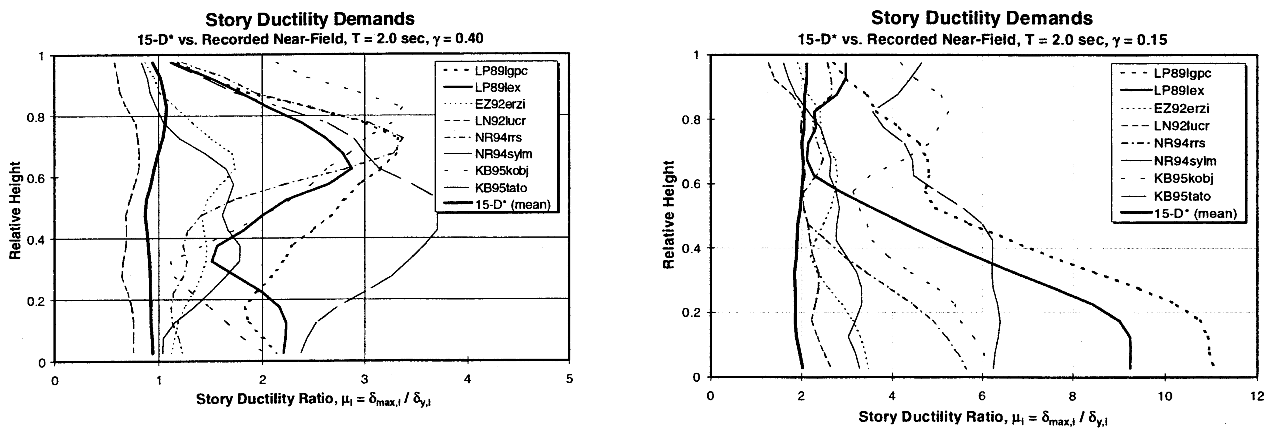

(a) $\gamma = 0.40$ (b) $\gamma = 0.15$

Fig. 3. Story ductility demands for several near-fault records, T= 2.0 sec

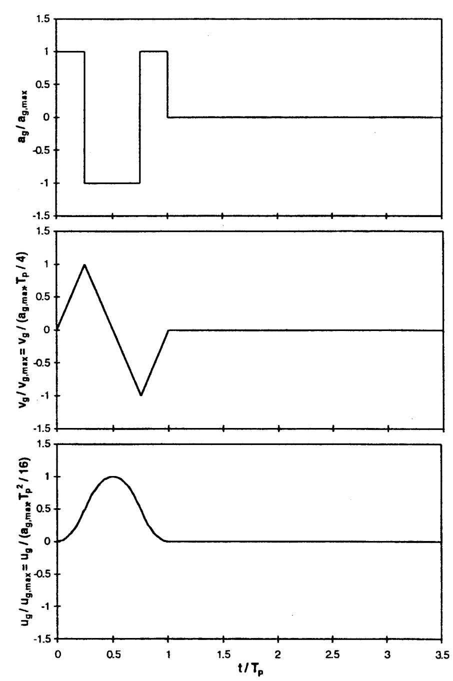

Figure 4. Acceleration, velocity, and displacement time histories of pulse P2

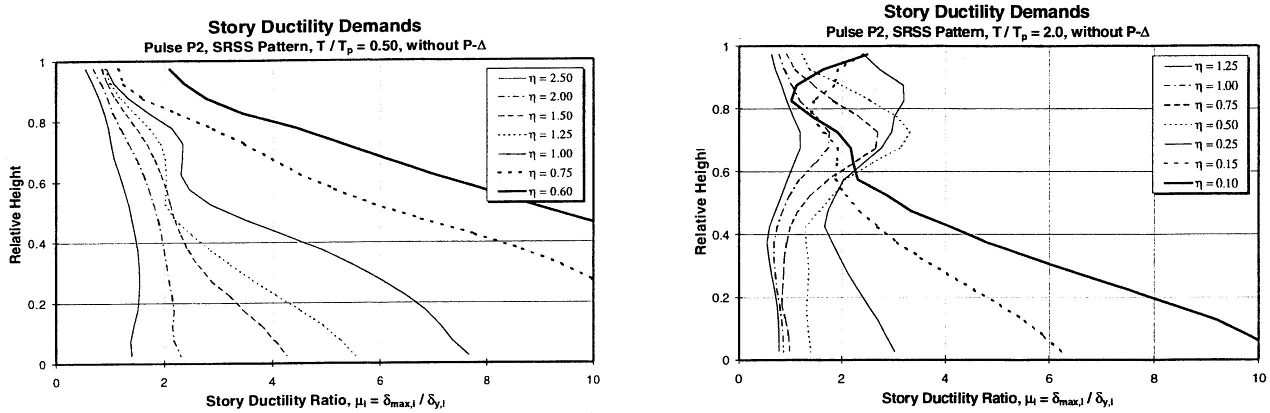

(a) $T/T_p = 0.5$ (b) $T/T_p = 2.0$

Fig. 5. Story ductility demands for pulse P2, various values of η

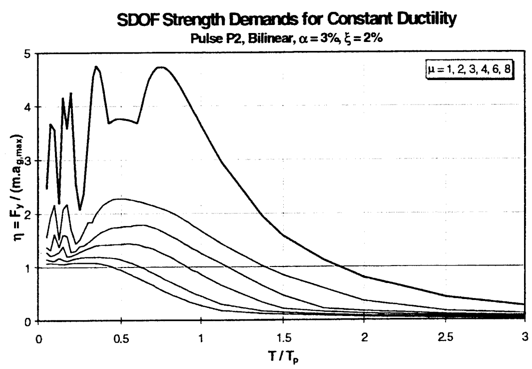

Fig. 6. Elastic and inelastic strength demand spectra for pulse P2

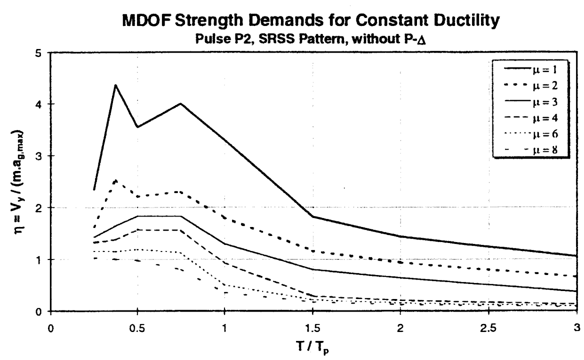

Fig. 7. MDOF base shear strength demands for target max. story ductilities

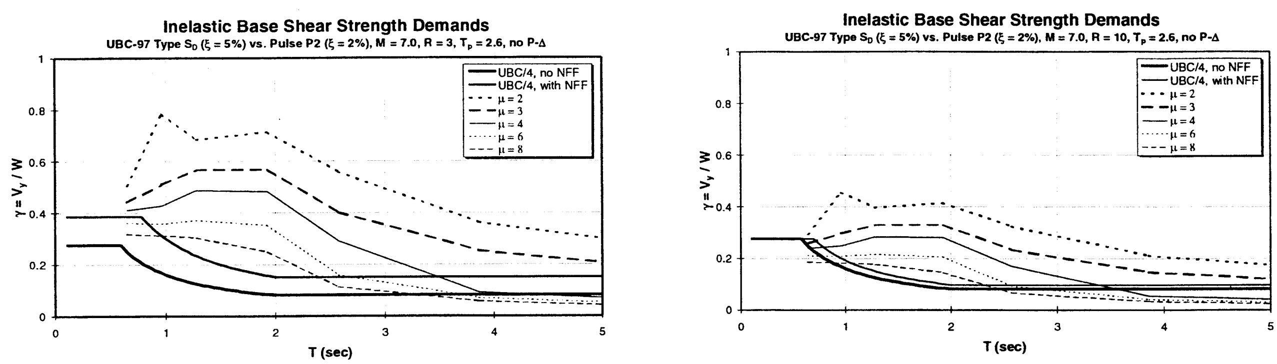

(a) R = 3 km (b) R = 10 km

Fig. 8. MDOF base shear strength demands for equivalent pulse P2 and M_w = 7.0

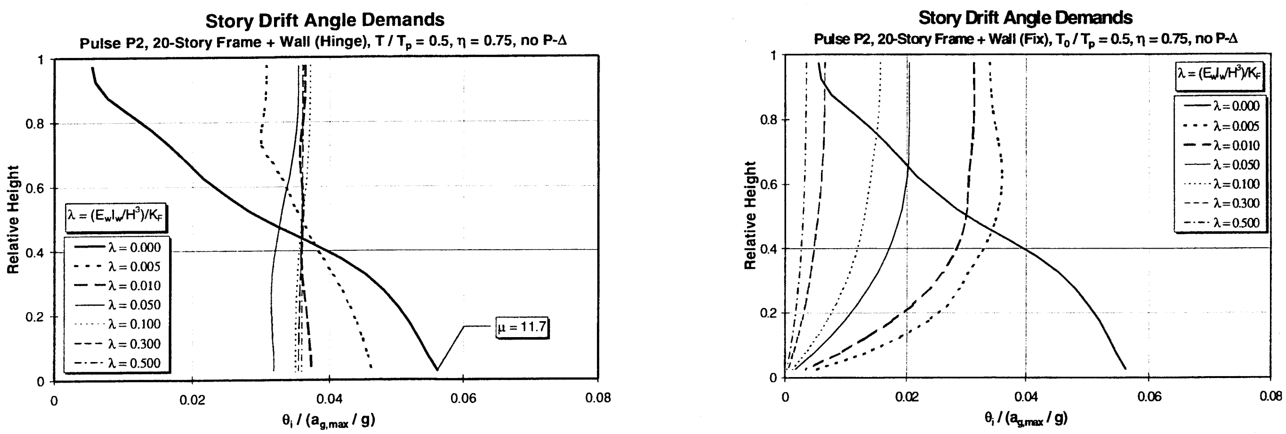

(a) Hinged-base wall (b) Fixed-base wall

Fig. 9. Distribution of story drift angle demands for dual system, $T/T_p = 0.5$, $\eta = 0.75$

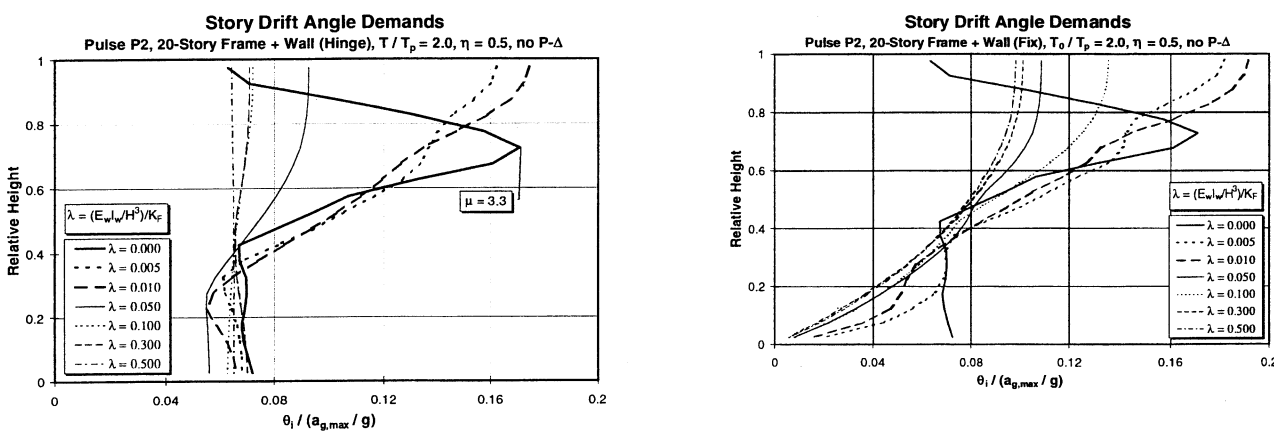

(a) Hinged-base wall (b) Fixed-base wall

Fig. 10. Distribution of story drift angle demands for dual system, $T/T_p = 2.0$, $\eta = 0.5$

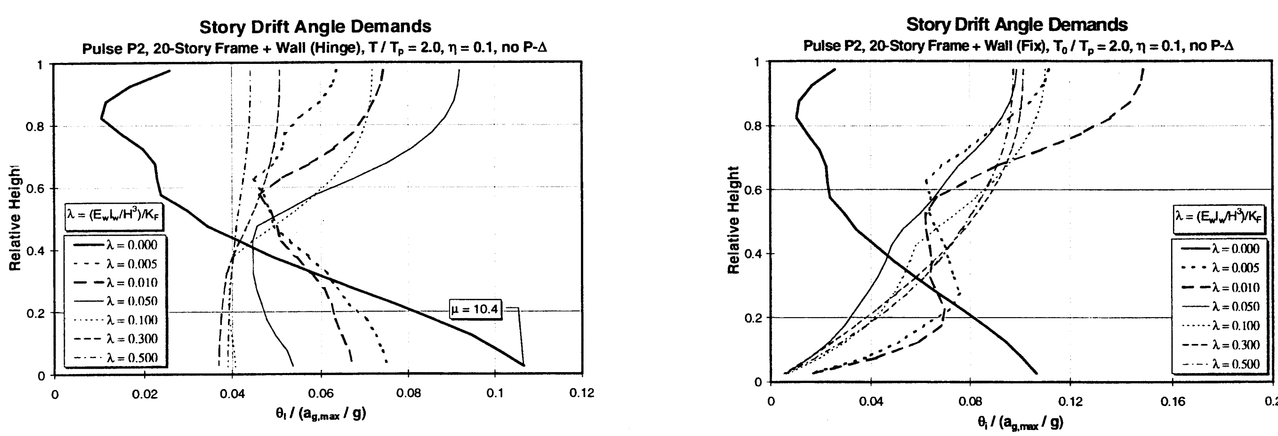

(a) Hinged-base wall (b) Fixed-base wall

Fig. 11. Distribution of story drift angle demands for dual system, $T/T_p = 2.0$, $\eta = 0.1$

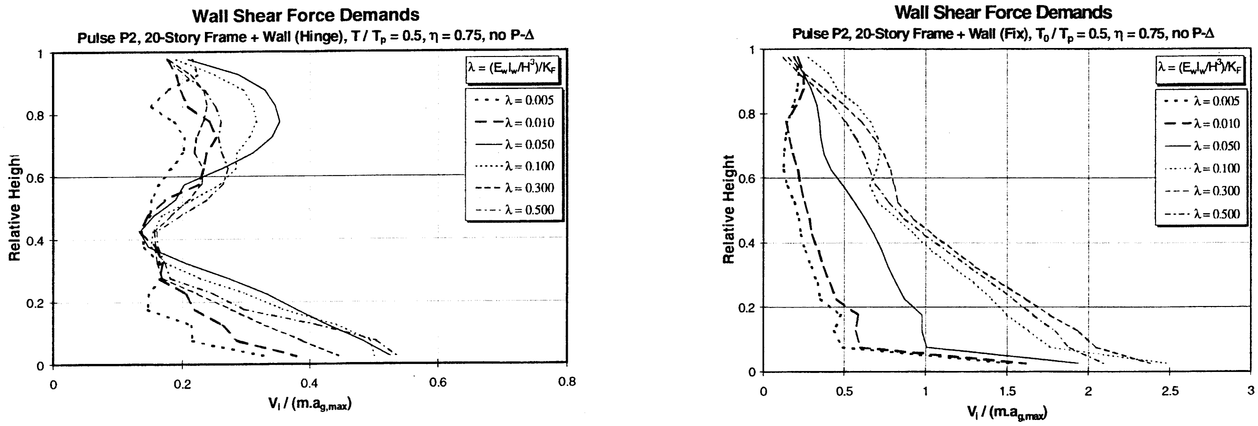

(a) Hinged-base wall

(b) Fixed-base wall

Fig. 12. Distribution of wall shear strength demands for dual system, $T/T_p = 0.5$, $\eta = 0.75$

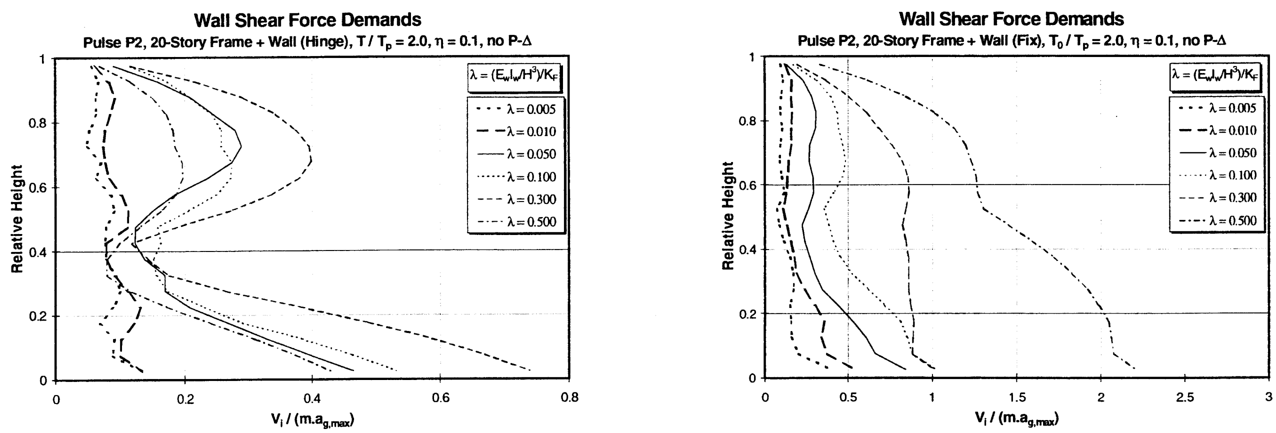

(a) Hinged-base wall

(b) Fixed-base wall

Fig. 13. Distribution of wall shear strength demands for dual system, $T/T_p = 2.0$, $\eta = 0.1$

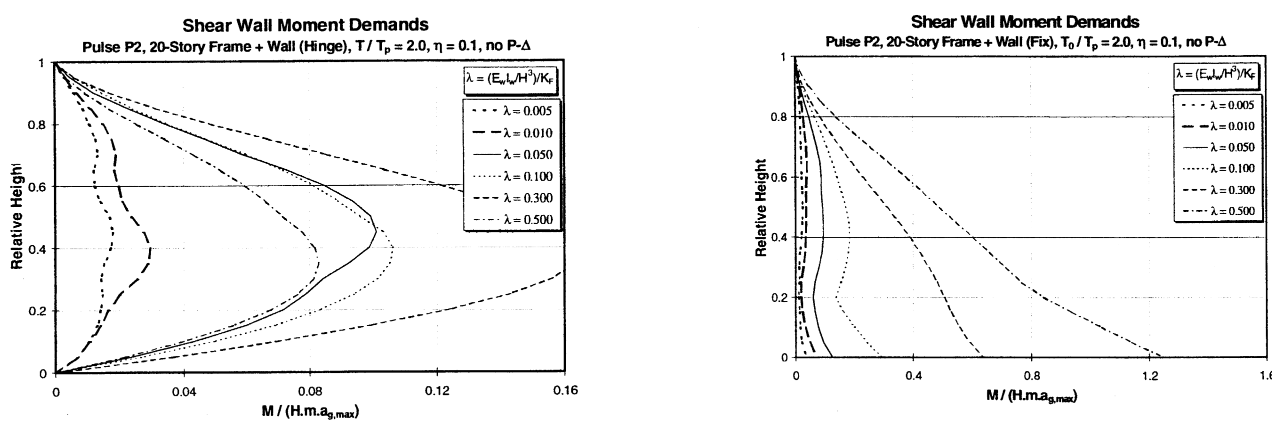

(a) Hinged-base wall

(b) Fixed-base wall

Fig. 14. Distribution of wall moment demands for dual system, $T/T_p = 2.0$, $\eta = 0.1$

HUMAN RESPONSE TO EARTHQUAKES IN DENSELY POPULATED AREAS

Osamu HIROI and Yoshiaki HASHIMOTO [*1]
Atsushi TANAKA [*2]
Toshihiro TSUGANEZAWA and Shigeo TATSUKI [*3]
Shunji MIKAMI [*4]

ABSTRACT

In order to mitigate damages of earthquakes in urban area, we need to conduct intensive researches from the social and human science perspectives, in addition to the seismological and technological approach to urban earthquake. In this paper, we present some of our four-year studies of social and human dimensions of the urban earthquake disasters in Japan. Especially the findings of three studies are discussed here. First, we studied on the anxiety about earthquakes in densely populated spaces in Tokyo. Second, we discuss on the factors generating the vulnerable people in earthquake disasters. The third study focuses on two aspects of individual post disaster adaptation on preparedness and on life recovery, valued information during restoration and the life concerns and living condition among different types of social support providers and elderly earthquake victims.

1. OBJECTIVES

The Great Hanshin-Awaji Earthquake raised several serious questions about Japan's emergency information and transportation systems. A point raised by many observers, for example, was the slowness with which national and local governments initiated search, rescue, and fire-fighting activities after the earthquake, resulting in greater damage and loss of life than would have been the case with a timely response. This criticism reflects the fact that emergency information systems almost ceased functioning as a result of the tremble, and it was impossible to collect immediate information on the extent and location of damage or on the fact that expressways and other transportation trunk lines had been severed, paralyzing traffic and preventing emergency relief teams from arriving on the scene.

The above-mentioned facts strongly suggest that in addition to the seismological and technological approach to urban earthquake, we also need the intensive research from the social and human science perspectives. We must investigate, for example, the effective systems to minimize the extent of the damage even though earthquakes give some damage to urban areas, and to make the restoration of the areas as soon as possible.

In emergency periods immediately after the earthquake, we also need to study some countermeasures for mass panics among passengers in urban areas during earthquake, and disaster

*1 *The Institute of Socio-Information and Communication Studies , University of Tokyo, Tokyo, Japan Email: hiroi@isics.u-tokyo.ac.jp*
*2 *Faculty of Informatics, Bunkyo University, Kanagawa, Japan. Email: tanaka@bunkyo.shonan.ac.jp*
*3 *School of Sociology, Kwansei Gakuin University, Hyogo, Japan*
*4 *Faculty of Sociology, Toyo University, Tokyo, Japan. E-mail: mikami@toyonet.toyo.ac.jp*

syndromes of refugees, and distribution of foods and water to victims. In restoration periods that last for a long time after earthquakes, we need to establish supply and management systems of temporary housing, medical and psychological management systems and information dissemination systems to refugees. In the following sections, we will present some of our research results in detail.

2. ANXIETY ABOUT EARTHQUAKES IN DENSELY POPULATED SPACES IN TOKYO

It was generally believed that underground spaces are relatively safe during seismic disaster. However in the 1995 Hanshin-Awaji Earthquake, underground shopping centers in Kobe were damaged by the quake. People feel uneasy especially in an emergency under the ground. The feeling of uneasiness is apt to cause a panic. An outbreak of panic would disturb smooth evacuation in emergencies.

To analyze anxiety about earthquakes or hypothetic behavior during the earthquake, Yoshiaki Hashimoto and his associates conducted four survey researches. In this paper we will report about two surveys. One was carried out toward about 1,800 passers-by in 17 overcrowded spaces such as underground passageways or high-rise buildings and so on in August 1997 to analyze the anxiety about earthquakes. The other was conducted toward 406 residents in 4 wards of Tokyo in November 1998 to examine the attitudes toward the earthquake or the knowledge about shelters.

We found that females are much more likely to feel anxious than males and that the reliance on the instruction system of evacuation have significant negative correlation with the anxiety to a high degree . As for the survey of Tokyoites 85% of the residents have anxiety about large-scale earthquake (Figure 1) and 35% of residents didn't know the designated shelters in their community.

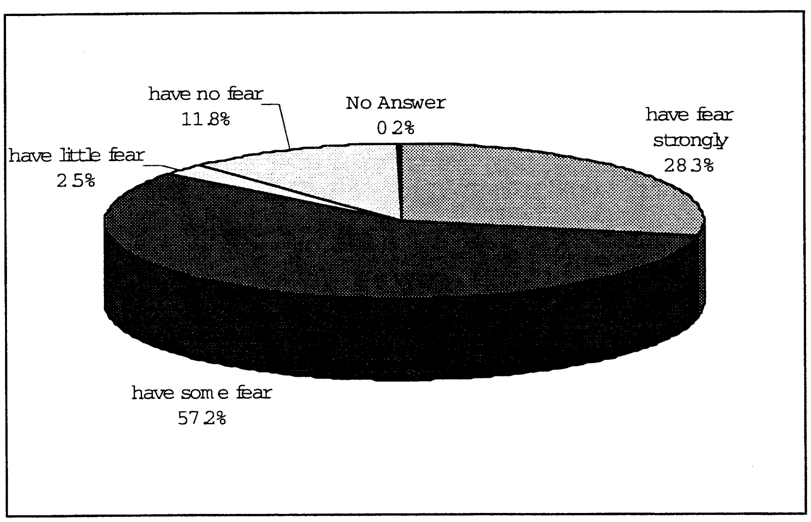

Fig.1. Anxiety about Earthquakes ("Do you think this place safe?")

In the questionnaire we also asked the respondents "Suppose that an big earthquake has occurred, then what do you do first of all?" The dispersion of the answer is shown in Table 1.

Table 1 Assumed Behavior in the Earthquake	
Will go to the exit looking around surroundings	37.8(%)
Will stay here	23.7
Will wait for the instruction of police	15.0
Will rush into the exit and try to go out	**13.6**
Will follow the people around me	7.8

As shown in Table 1 the largest percentage of respondents answered that they would go to the exit looking around the surroundings. It should be noted that the percentage of the answer that they would rush into the exit and try to go out was not negligible (13.6%). If a lot of people rush into the exit, a kind of panic will be caused. The percentage of that answer was greater among men (15.4%) than women (11.9%) and among old generation especially fifties (22.9%). And those who feel anxious about earthquakes were apt to answer that they would rush into the exit .

According to the basic plan of Tokyo for the mitigating disasters , 172 large shelters are designated currently. We asked the respondents where their designated shelters are. Those who knew about their shelters were 65.3%, while 25.6% did not know about their shelters and 8.9% mistakenly understood them. The percentage is small among younger people than aged people. More over 60.6% of the respondents thought their wide area shelters were not situated in appropriate place.

In conclusion, most residents in Tokyo have great fear about earthquake but they do not know their shelters or evacuation routes correctly. Much more publicity about the protection against disasters is needed in the future.

3. FACTORS GENERATING THE VULNERABLE PEOPLE IN DISASTERS

The second study, conducted by Atsushi Tanaka, aims to discuss what factors generate the vulnerable people in a disaster processes and what measures should be called for according to a model of disaster processes.

From the past researches, it is known that some people, especially the aged, the disabled, the infant, or the foreigners, are more vulnerable to disaster than others. In the Hanshin-Awaji Earthquake of 1995, more than 50% of the dead in this disaster were aged people. Also in the nuclear accident in Tokai village (1999), many hearing impairments failed to realize the alarm which had warned them to stay at home in order not to be contaminated with radioactivity.

A disaster causes many kinds of damage to social systems and some form of emergency social system develops in such situation. Although such emergency systems could save victims' lives and make a quick recovery from a disaster damages by restricting a variety of private activities, this restrictions often cause a great deal of troubles for some victims and generate vulnerable people.

It makes the chronic invalids difficult to receive the medical treatment by traffic regulations or by the priority shifting of treatments in the hospital. However it is important to catch information on changes of the allocation rules, sensory impairments may fail to get such information. And even the rule of mutual aid may make the weak people feel constraint, because they have nothing to offer in return to the others' favors. For example, in the Great Hanshin-Awaji Earthquake, many aged and the disabled had a hard time under the emergency systems, especially in public shelter. Countermeasures were so insufficient for some aged or the disabled that they faced threat to life under ordinary measures.

After the disaster, the local governments started to reconsider their planning for measures against earthquake disaster from various points of view. One of them is the improvement of measures for vulnerable people. Indeed, many cities made the measures for the vulnerable people, as shown Figure 2. But, when we examine them closely, there are several problems in these measures.

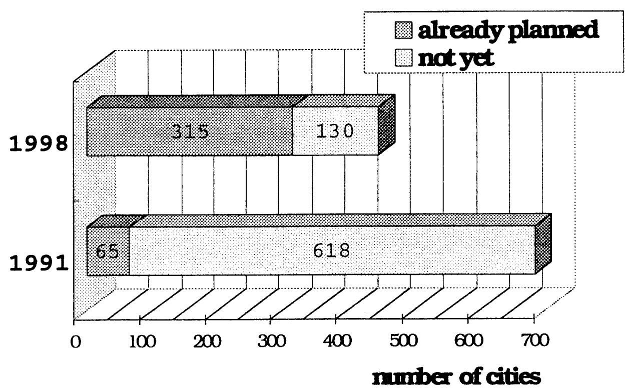

Fig. 2 The rate of the cities which made the measures for the vulnerable people

Only 27% of cities established the division or team which will work full-time for the vulnerable people. In the Great Hanshin-Awaji Earthquake, many staffs who ought to be in charge of the aged or the disabled were totally occupied by other work, and consequently they could not cope with the troubles which such victims were faced.

Many aged and the disabled could not live in public shelters. In order to improve the life in shelters, 35% of cities prepared the foods which are fit to the aged or babies. And 27% of cities planned to set up exclusive shelters for the aged and the disabled who can not live in the ordinary shelters. But only a few made the ordinary shelters barrier-free(12%). And also only a few cities planned to provide the temporary lavatories for the disabled(20%), to put out the bulletins on important information in the shelters(9%), and to send guide-helpers for the visually impaired or sign-language interpreters(15%).

In order to improve these conditions, the model of emergency social system will be useful, because it teaches us that there are many kinds of problems and that the measures for the vulnerable people must be planned to resolve the essential presuppositions which make some people vulnerable.

4. POST DISASTER STUDIES OF INDIVIDUAL PREPAREDNESS AND LIFE RECOVERY: TWO PERSPECTIVES

Disaster causes an imbalance in interactions among society, built and natural environment (Mileti, 1999). In order to adjust to this imbalance, measures are taken to both the built and natural environment. These measures tend to be specific and short-term-based (White & Haas, 1975). Disruption of everyday life, at the same time, leads to a more general and long-term adaptation in order to cope with the new reality that has emerged in the post-disaster society (Burton et al., 1978). This societal adaptation can be identified by changes in values, worldviews, attitudes and behaviors among individuals.

This study, done by T. Tsuganezawa and his associates, focused on two aspects of individual post disaster adaptation on preparedness and on life recovery. It was assumed that individual preparedness is a matter of valuation and could be detected by attitudinal survey method. On the other hand, an examination of the use of various types of social support can describe the structure of differential needs and matching services in a recovery setting.

Questionnaire surveys on 1) post-disaster attitudinal differences in preparedness among college students in impacted and un-impacted regions and on 2) life recovery of elderly earthquake victims who moved from temporary to permanent housing were conducted. A total of 492 college students from two regions, Kyoto-Osaka-Kobe (N=261) and Shizuoka-Kanagawa (N=231), responded to a questionnaire designed to examine attitudinal differences in preparedness.

In both regions, the three most valuated information were in regards to 1) supply of food and relief material, 2) safety of family members and 3) secondary disaster and aftershock. Different preference patterns emerged with regard to the remaining informational categories, suggesting that respondents in an impacted region valuated information that was necessary for the maintenance of post-disaster everyday life, and that those in an un-impacted region valuated information concerning governmental assistance programs.

The life recovery study examined the current life concerns and living condition, and frequencies of contact with different types of social support providers among 61 elderly earthquake victims (22 male and 39 female) who were settled in permanent public housing units specifically designed for the elderly.

The provision of "Silver Housing", the special public housing units in order to meet the needs of lower income, single or married couple elderly earthquake victims is an innovation in Japan (Nigg, 2000). The purpose of "Silver Housing" was to let these older victims to live as independently as they had before the earthquake. At the same time, they had been relocated from their regular social networks and thus need some additional assistance in order to regain a sense of

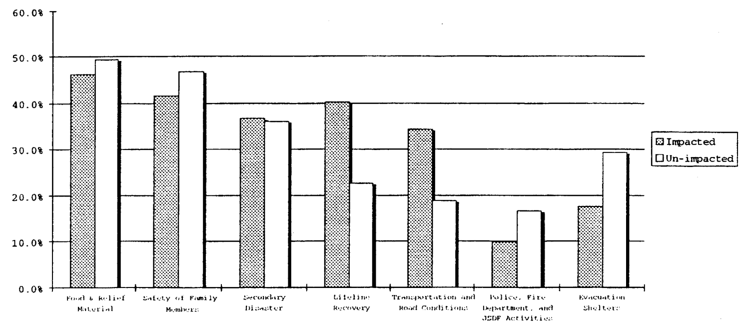

Fig. 3. Important Information at the Time of Disaster by Region

life reconstruction and recovery. These elderly victims were forced to relocate at least three times since the earthquake; evacuation to a neighborhood shelter, a move to temporary housing, and final settlement at a public housing unit. At each time, formal and informal help was offered to prevent social isolation from family and friends. Provision of Silver Housing was one governmental response to this concern, and was based on a model of social support network.

One unique feature of Silver Housing is the provision of Life Support Advisor (LSA). One LSA is assigned to every thirty residential units in Silver Housing. LSAs offer on-site emergency health care, assist elderly residents with other medical and health care needs, and facilitate social support network by collaborating *minsei-iin* or a government appointed welfare volunteer, resident association representatives, public health nurse, nursing home stuff members, district welfare office caseworkers, and friendly visit volunteers.

Three quarters of the elderly evaluated life of Silver Housing to be "Very, Fairly, or Somewhat Satisfactory". The general characteristics of the respondents indicate that only half of the respondents feel "Good" or "Somewhat Good" about their health condition (50.8%), and that the top most worrisome concerns were physical (Ill Health, 16.4%), social (Loneliness, 13.1%) and psychological matters (Future, 13.1%). In order to cope with these physical, social and psychological concerns, Silver Housing residents seem to be utilizing social support from their neighbors, resident association, Life Support Advisors (LSAs), and friendly visit volunteers.

REFERENCES

Mileti, D. S.1999. *Disaster by design: A reassessment of natural hazards in the United States.* Washington, D.C.: Joseph Henry Press.

White, G.F., & Haas, E. 1975. *Assessment of research on natural hazards.* Cambridge, Mass: MIT Press.

Burton, I., R. W. Kates, and G. F. White. 1978. *The environment as hazard.* NY: Oxford University Press.

Hayashi, H. & S Tatsuki. 1999. *Determinants of the changes of residence and life reconstruction among the 1995 Kobe earthquake victims.* (A Research Report). Kyoto: Kyoto University, Disaster Prevention Research Institute.

Nigg, J. M. January 2000. Measures to restore victims' independence following the Great Hanshin-Awaji earthquake. Paper presented at the "Global Assessment of Earthquake Countermeasures," Kobe, Japan.

SEISMIC RISK MODEL FOR A DESIGNATED HIGHWAY SYSTEM: OAKLAND / SAN FRANCISCO BAY AREA

James E. Moore, II [1]
Anne Kiremidjian[2]
Samuel Chiu[3]

PROJECT OBJECTIVE

Functionality evaluation and economic loss assessment are key components in the performance based decision process. The objectives of this project are to develop appropriate analytical and computational methods for evaluating the impact of a major earthquake (M>6.5 event) on the transportation system of an urban area and to illustrate the utility of these methods through an application to a region. More specifically, these should include:

- methods for identifying damaged links and critical paths, and providing near-real time resources for allocation decisions important in emergency response;
- models for direct and indirect economic impact assessment; and
- aggregate pertinent information needed for transportation systems risk assessment.

In general, risk analysis of highway transportation systems is performed with the objective to provide:

- appropriate information in the retrofit and disaster mitigation decision process (in the pre-event and post-event period, it is necessary to determine which bridges are to be retrofitted/ repaired/replaced, in what order and to what design level); and
- models and tools for estimating the socio-economic impact of transportation systems that have been damaged by an earthquake.

WORK TO DATE

During year one of the demonstration project several modeling efforts were initiated. These include the development of a direct damage and loss assessment method, an optimal post-earthquake emergency resource deployment model for highway networks, and a highway network impact model to a major port facility. The general framework for direct damage/loss estimation and for optimal post-earthquake emergency resource deployment has been developed and preliminary models for

---

[1] *Associate Professor, University of Southern California, Los Angeles, CA 90089-2531, E-Mail: jmoore@usc.edu*
[2] *Professor, Leland Stanford Junior University, Palo Alto, CA 94305, E-Mail: ask@cive.stanford.edu*
[3] *Professor, Leland Stanford Junior University, Palo Alto, CA 94305, E-Mail: samchiu@leland.stanford.edu*

these are currently being formulated. The San Francisco Bay region has been selected as the application area for the demonstration project and appropriate data are currently being collected. A significant portion of the seismological, geological and geotechnical data have already been gathered. In addition a database on bridges and the physical properties of the highway network has been obtained and are in the process of being combined. Additional information on the functional characteristics of the highway system and local street networks are being sought at the present time.

A highway transportation network analysis model is being developed for evaluating the availability of routes, identification of detours, and assessment of trip time delays due to a significant earthquake. A scenario event approach is considered for these analyses. At the recommendation of members of the Transportation Risk Analysis workshop held in July, 1998, the model will be applied to the highway transportation system in the San Francisco Bay Area. A dynamic transportation model is being developed to provide information before and after an event. This model includes a network representation of the Bay Area network of freeways, highways, major arterials, and bridges. Primary data sources include Caltrans District 4 and the Metropolitan Transportation Commission (MTC). The model will identify endogenous transportation link costs associated with pre and post-event traffic flows. The basic formulation is static, i.e., steady state, but extensions needed to treat dynamic, i.e., transient flow conditions likely to exist in the first days following a major event will be investigated and incorporated to the extent possible. Both static and dynamic flow scenarios will be considered leading to comparisons of long-term traffic flow patterns before and after an earthquake, and to analysis of traffic flow conditions few days after a major event.

One of the central aspects of the research focuses on integrating bridge and highway data, and developing an economic model of the Bay Area economy. We have available:

- The Metropolitan Transportation Commission (MTC) transportation network,
- MTC traffic analysis zones (TAZ) and origin-destination (OD) matrices, and
- the Caltrans District 4 bridge data base.

We have built-up a baseline network bank (same as database) based on MINUTP data files describing the Bay Area highway and transit networks provided by the Metropolitan Transportation Commission., We transferred these data into a GIS version of the same network. MTC's network data included O/D data files that were divided into several matrixes according to different travel modes. Combining these matrixes together mapping these networks are currently in progress. See Figures 1 through 4 following.

Thus, we have the means to compute user-equilibrium flows in the Bay Area network. This is complex because links congest and paths overlap. The cost of using any path depends on the flows present on overlapping paths between other origin-destination pairs. We use EMME/2 to compute these flows. EMME/2 is a well implemented version of the Frank-Wolfe algorithm for solving nonlinear programming problems (NLP).

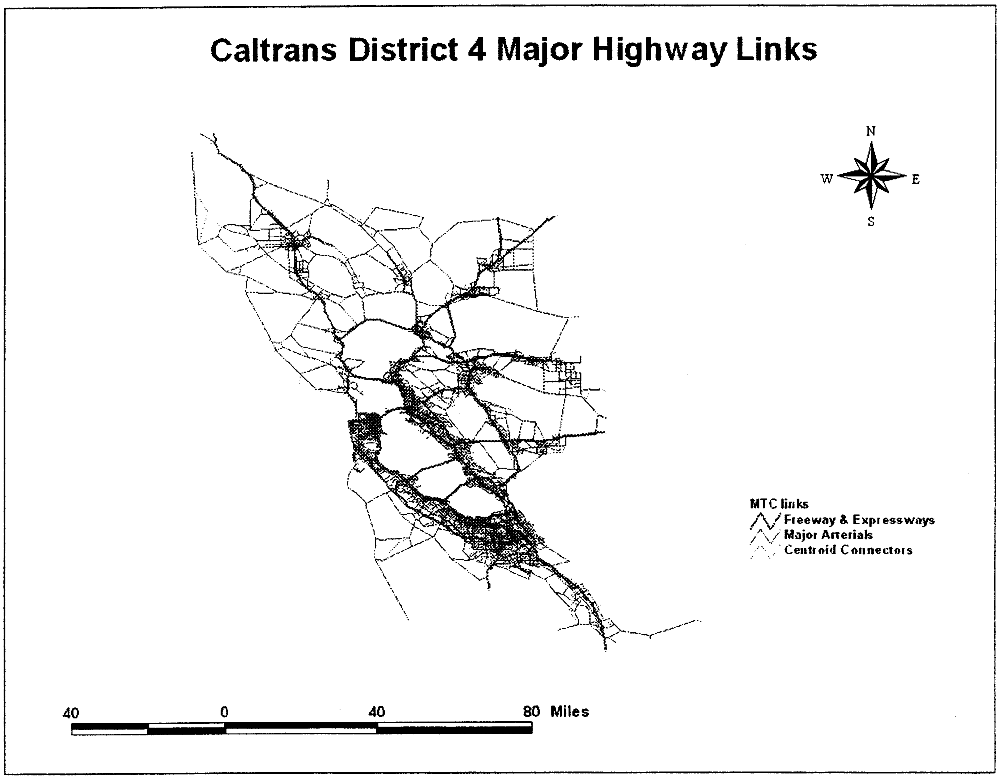

Fig. 1. Caltrans District 4 Major Highway Links

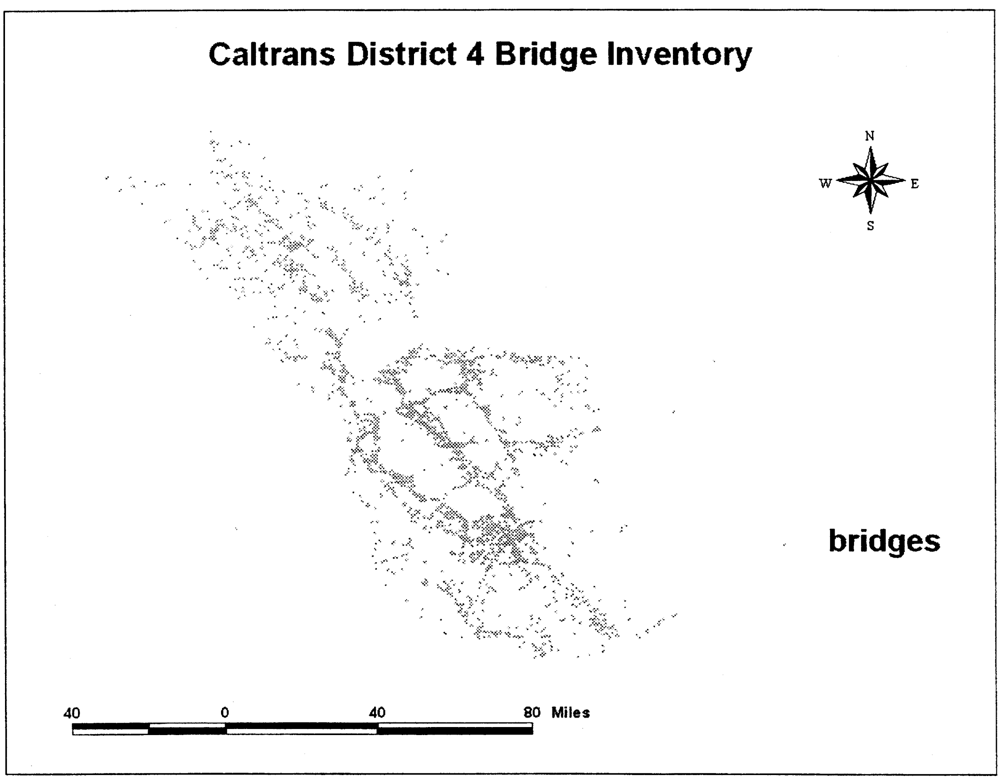

Fig. 2. Caltrans District 4 Bridge Inventory

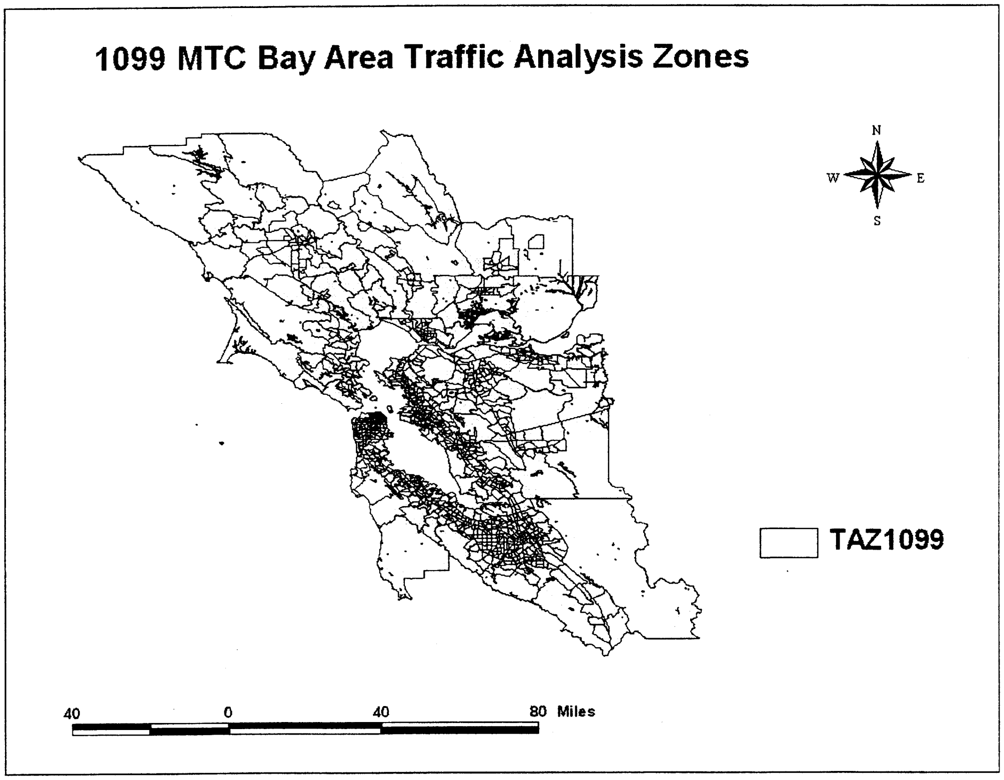

Fig. 3. MTC Traffic Analysis Zones (TAZ)

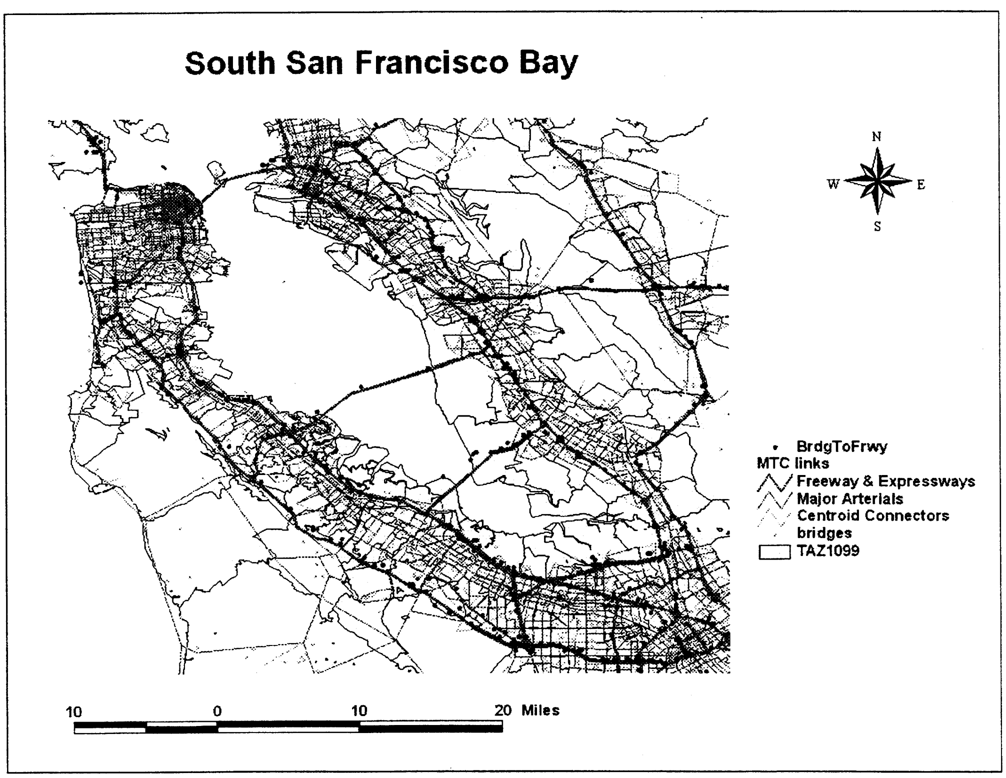

Fig. 4. South San Franciso Bay

The models developed under the proposed project will be general and will be applicable to other facilities with some modification. The application of the model to the San Francisco Bay Region transportation system, the Port of Oakland and to specific businesses in the Silicon Valley area will serve as the demonstration project. Significant components of the demonstration will be achieved during the year of this proposal. The demonstration, however, will be completed following this two-year model development stage of the project.

Treatment of data is an important component of this project. A strong recommendation from the Transportation Risk Analysis Workshop was the gathering of pertinent data and unifying these data in a format that can be widely used. As part of this project, sample data will be gathered for the demonstration project to illustrate how these data can be organized, cleaned, and unified.

The MTC network is a modeling network. It is not geo-coded. The Caltrans bridges are geo-coded. We have succeeded in reconciling MTC's network to State Plane coordinates, but a geo-coded network offered by Caltrans Headquarters remains vaporware. Consequently we are associating bridges with network links in an approximate fashion. Given a reasonable definition of proximity, bridge data sets are merged with geographically closest highway links. This auto-merge was done as programming step in ARC/INFO*TM*. Highway links and highway bridges together make the baseline highway network. It is important that we obtain a geo-coded network from Caltrans Headquarters. This resource will permit us to better translate bridge and highway data into the MTC planning network.

The merged set of links and bridges will be transferred into EMME2 format for transportation flow modeling. Baseline travel demand modeling is still in process. Baseline origin destination matrices are available, but relevant social-economic data for project area are not yet ready. These economic data are needed to predict how demand for transportation will change following an earthquake.

It is unclear that the region input/output data needed for a full evaluation of economics impacts will be available. We are searching for other alternatives for modeling the Bay Area activity system and associated demand for transportation. We have made some progress, and remain hopeful. There are many benefits associated with this approach, not the least of which is that computability has been demonstrated in the Southern California case.

ACKNOWLEDGMENTS

We are grateful to the Pacific Earthquake Engineering Research Center (PEER) for the Center's support of our research relating to performance based earthquake engineering for transportation systems.

EFFECTS OF NEAR-FAULT SHAKING ON STRUCTURES IN THE CHI-CHI (TAIWAN) EARTHQUAKE

J.-F. CHAI[1], W.-I LIAO[1] and C.-H. LOH[1]

ABSTRACT

This paper is to study the effects of near-fault shaking on structures in the Chi-Chi (Taiwan) earthquake. Firstly, the general observations of structural damages and the lessons learned from the Chi-Chi earthquake are described briefly. The dynamic behaviors of structures subjected to both near-fault and far-field ground motions are compared. Based on the concept of UBC97, the near-fault design response spectrum is proposed in this paper. Furthermore, the spectrum compatible near-fault ground motion is simulated based on the modeling of phase spectrum at near-fault sites.

1. INTRODUCTION

The Chi-Chi earthquake that occurred in Taiwan at 1:47 a.m. on September 21,1999 directly struck the central part of Taiwan. The epicenter of the earthquake is at 23.85°N and 120.78°E with focal depth of 7.5 km and magnitude 7.3 (M_L=7.3). This earthquake has caused heavy casualties and structure damages, 2469 lives were lost, more than 700 people were severely injured and over ten thousand buildings suffered moderate-to-collapsed damages. In recent years, people have learned that the near-fault earthquakes perform many different characteristics from the far-field earthquakes, and cause much more damages. In fact, the associated high PGA and the pulse-like velocity waveform of the near-fault ground motion will destroy severely the structures with short and long structural periods, respectively.

In this paper, the general observations of structural damages and the lessons learned from the Chi-Chi earthquake are described briefly. Next, the near-fault earthquake performance, especially the ductility demand and the base shear are studied. Furthermore, the near-fault design response spectrum and the compatible design ground motion are proposed.

2. OVERVIEW OF HIGHWAY BRIDGE DAMAGES

There are approximately 1000 highway bridges spread on the main provincial and county routes in central Taiwan. About 20% of these bridges suffered minor-to-major damage in the Chi-Chi earthquake while others escaped from serious damage. Most of the major damaged highway bridges are located on or very close to the Chelungpu fault or are in the vicinity of the epicenter in Chichi, where high PGAs in the range of 400 to 980 gals are measured. Most of the damaged highway bridges have simply-supported, rein-forced or prestressed concrete slab-and-girder superstructures, although continuous steel plate-girder and long-span cable-stayed girders are also included. The major damage modes include collapse of superstructures, displaced bearings,

[1] *National Center for Research on Earthquake Engineering, Taipei, Taiwan*
Fax:(886)-2-2732-2223

unseated girders from bearing supports, shear failure in columns and pier walls, abutment back-wall failure, settlement of approach slab, foundation failures due to slope instabilities, joint failures in column-to-girder connections, and cable fractures.

Fault rupture under or across bridge foundations is catastrophic to the structure and usually leads to collapse of spans. Therefore, it is necessary to conduct site-specific hazard analyses to have thorough comprehension on the near-fault effect, and 'easy to repair or reconstruct' should be a priority in the bridge design and construction. Furthermore, engineering shear keys are required to prevent span falling transversely from pier caps. Generous seat widths are excellent insurance against unintended actions such as ground failure and rotation in skewed spans. Also, column-to-girder joints should be accurately designed and constructed such that the seismic force can be translated by the expected load path, and further, sufficient and well-constructed hoop bars or confinements should be provided to prevent from shear failure in piers. In addition, application of innovative technology, such as structural control, can be considered in the design of bridges. Finally, capacity design procedures and ductile details are necessary to prevent collapse during large earthquake. Multi-level performance criteria and corresponding design strategies are necessary for important bridges.

3. OVERVIEW OF BUILDING DAMAGES

The Chi-Chi earthquake caused approximately 3000 buildings totally collapsed, with more than 6000 others partially collapsed and countless others damaged to various degrees. A large percentage of the collapsed buildings are old un-reinforced clay block masonry cottages and non-engineered RC frame structures (one-to-three stories) constructed with brick in-fill partitions and exterior walls. Also, more than two dozen modern high-rise apartment buildings with reinforced concrete moment resisting frames overturned or collapsed.

Some collapsed buildings near the Chelungpu fault were caused directly by the surface rupture or severe ground shakings. Many other collapsed buildings have a pedestrian corridor and open front with little interior walls at the ground floor, it translates into a lower structural stiffness and strength and hence leading to 'soft-story' effects. The damage of shear failure caused by short-column effect is rather common in many school buildings because the in-filled windows above half-height shortened the effective length of almost all the columns. In addition, some buildings are damaged by the liquefaction-induced settlement. Although those collapsed high-rise buildings were designed and constructed based on the current design code to consider the ductility effect, none exhibited evidence of ductile detailing, particularly at the end of beam-to-column joint. Reinforced concrete frame construction in Taiwan is commonly taken to include both pure frame construction and combined frame-wall construction. Wall constructions should be included in design in order to prevent the use of non-structural partitions as frame-wall systems.

Based on the observations of building damage in Chi-Chi earthquake, it is essential to ensure that should only ductile details be used in all new construction and in the repair of damaged structures, and building having 'soft-story' characteristics should not be allowable in new constructions. Furthermore, the near-fault ground motion characteristics (pulse-like velocity waveforms) should be implemented in our seismic design code.

4. NEAR-FAULT EARTHQUAKE PERFORMANCE OF STRUCTURES

Based on the recorded near-fault ground motions in the Chi-Chi earthquake, the dynamic responses of structures under near-fault earthquakes can be understood more clearly. Four near-fault ground motions with typical velocity pulses recorded in the Chi-Chi earthquake were selected in this study as listed in Table 1. In contrast, the far-field earthquake data recorded at the same sites (three data for each one site) ere selected to demonstrate the different earthquake performances.

Table 1: Properties of selected near-fault ground motion record

Station	PGA (cm/s^2)	PGV (cm/s)	Distance (km)	PGV/PGA	Pulse duration (sec)	Mean PGV/PGA (far-field)
TCU052	348.7	181.8	2.34	0.521	5.54	0.109
TCU068	501.6	280.2	0.49	0.559	3.85	0.114
TCU075	325.3	116.5	0.43	0.358	3.08	0.031
TCU102	298.4	86.5	0.81	0.290	7.69	0.106

The modified version of computer program DRAIN-2DX (Pakash and Powell 1993) is used in this study to analyze the dynamic response of RC structures. The reinforced concrete beam or column is represented by a line element with fiber model, so the interaction between axial force and bending moment can be calculated automatically. Each element is divided into slices along the axis of the member, and the slices are further separated into concrete and steel fibers. The strains in these fibers are calculated by the centroidal strain and section curvature with the assumption of that plane section remains plane. The concrete stress-strain curve adopted here is the model suggested by Kent and Park (1971). For the steel fiber, the stress-strain curve was modeled by bilinear model with 2% strain hardening ratio.

Figure 1(a) shows a five-span highway bridge, which is designed based on the current seismic design code in Taiwan. The continuous girder is modeled as a linear elastic element, and is supported by the piers with hinge or roller in the longitudinal direction and fixed connections in the transverse direction. Furthermore, the soil-structure interaction is simulated by using the equivalent linear elastic soil springs. The capacity curves of nonlinear responses can be obtained through pushover analysis. The distribution of imposed force in the bridge is according to the modal shape of the fundamental mode. The capacity in the longitudinal and transverse direction are shown in Figure 1(b), where the displacement is defined at the middle point of girder, and base shear is the summation of all pier shears. The yield base shear (V_y) and corresponding displacement (d_y) in the longitudinal direction are V_y = 1296 ton and d_y = 13.2 cm, and V_y = 2352 ton and d_y = 6.8 cm in the transverse direction.

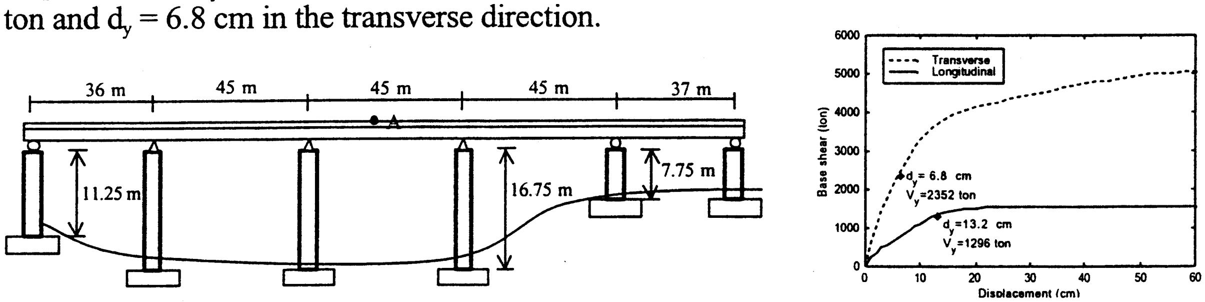

Figure 1: (a) Five-span continuous girder bridge and (b) the capacity curves

The response of the bridge was analyzed in longitudinal and transverse direction independently, and the vertical response of the bridge is ignored. The mean values of maximum base shears for near-fault and far-field ground motions at different PGA levels are compared in Figure 2(a). It is noted that the base shear is not proportional to the PGA value because of the nonlinear behavior. For the design stage of preventing collapse, a structure should possess a certain amount of ductility. The ductility demand is defined by $\mu = d_{max}/d_y$, where d_{max} and d_y are the maximum displacement and significant yield displacement in the specified point, respectively. Figure 2(b) shows the mean value of ductility demand under the selected near-fault and far-field ground motions. It can be observed that both the maximum base shears and ductility demands induced by near-fault ground motions are higher than those induced by far-field ground motions. Furthermore, it is observed that the system ductility demand in the longitudinal direction is higher than that in the transverse direction, especially for the near-fault ground motion input. It is because the impact of near-fault earthquake upon long period structures (longitudinal direction) is much higher than that upon short period ones (transverse direction).

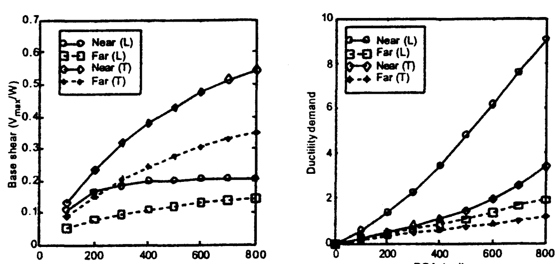

Figure 2: (a) Base shears and (b) ductility demand curves of the sample bridge

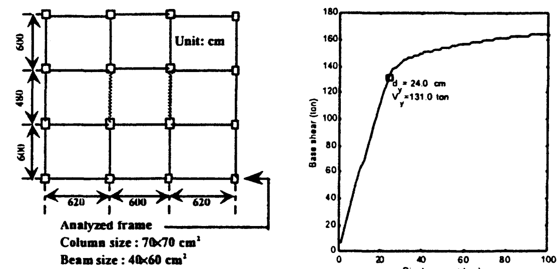

Figure 3: (a) 12F RC building and (b) the capacity curve

Also, a twelve-story RC building with moment resisting frame (fixed base) is designed based on the current Taiwan building code. The height of every floor is 3.0 m, and the top view and the analyzed frame are shown in Figure 3(a). The capacity curve is shown in Figure 3(b), the yield base shear and corresponding displacement are V_y=131.0 ton and d_y=24 cm, respectively. The mean values of maximum base shears and the ductility demand under near-fault and far-field ground motions are compared in Figure 4. Again, the larger values can be observed for near-fault ground motions than the far-field ones. Furthermore, the maximum story drift at each floor for different ground motion inputs with PGA=300 and 500 gals are compared in Figures 5(a), and the mean values of the maximum story drift of whole building for different PGA levels are shown in Figure 5(b).

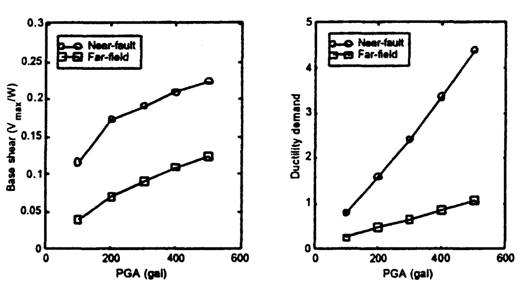

Figure 4: (a) Base shears and (b) ductility demand curves of the 12F building

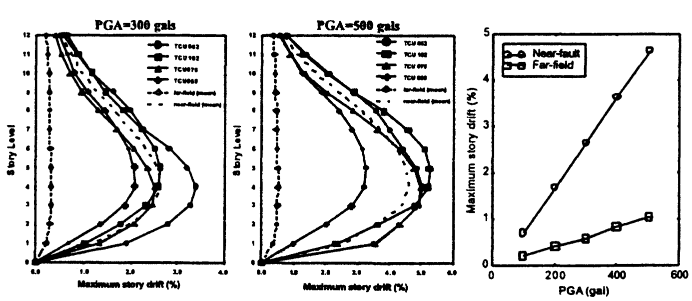

Figure 5: (a) Distribution of story drift and (b) maximum story drift of the 12F building

5. NEAR-FAULT DESIGN RESPONSE SPECTRUM

Based on the current Taiwan building code (from 1997), the elastic seismic demand is defined by the spectral acceleration as S_A=ZIC, in which Z is the zoning factor presenting the seismic design level, I denotes the important factor, and C is the normalized spectrum coefficients. Based on the concept of UBC97, the near-source factors are incorporated to modify the design response spectrum for the sites near the Chelungpu fault. It is noted that these sites are almost under rock site conditions (Type 1 soil profile) and within the seismic zone 1A with Z=0.33g. The current normalized response spectrum coefficients, $C(T)$, for rock site are specified in Table 2.

Table 2: Current code specified $C(T)$ for rock site in Taiwan

Period Range(sec)	Extremely Short	Very Short	Short	Moderate	Long
	$T\leq 0.03$	$0.03\leq T\leq 0.15$	$0.15\leq T\leq 0.333$	$0.333\leq T\leq 1.315$	$T\geq 1.315$
$C(T)$	1.0	12.5T+ 0.625	2.5	$1.2/T^{2/3}$	1.0

Firstly, the recorded ground motions at sites near the Chelungpu fault in Chi-Chi earthquake are adopted to determine the near-fault attenuation functions for PGA and 5%-damped spectral acceleration demand at 0.3 and 1.0 period (denoted as $S_{A0.3}$ and $S_{A,1.0}$). The determined results are shown in Figure 6, where the rupture distance means the closest distance between the site and the surface trace of Chelungpu fault. By comparing with the seismic demands specified by the current design code (Soil profile type 1, Z=0.33g, I=1.0), the required elastic seismic demand and the associated amplification factors for a site near the Chelungpu fault can be defined as

$$
\begin{array}{lcl}
PGA(r) = \max\left(PGA(r)\big|_{Fig.6}, Z = 0.33g\right) & & N_g(r) = PGA(r)/Z \\
S_{A,0.3}(r) = \max\left(S_{A,0.3}(r)\big|_{Fig.6}, 2.5Z\right) & \Rightarrow & N_a(r) = S_{A,0.3}(r)/2.5Z \\
S_{A,1.0}(r) = \max\left(S_{A,1.0}(r)\big|_{Fig.6}, 1.2Z\right) & & N_v(r) = S_{A,1.0}(r)/1.2Z
\end{array}
\qquad (1)
$$

The resulted curves are shown in Figure 7. It is observed that the factors N_g and N_a perform the similar attenuation trend with almost the same magnitude. Then, by piecewise linearizing the curves of amplification factors, the code-specified near-source factors N_A (averaged from N_g and N_a) and N_V can be defined as shown in Figure7, and listed in Table 3. The near-source factor may be based on the linear interpolation of values for distance other than those shown in the table. Finally, based on N_A and N_V, the near-fault spectrum coefficients $C_{NF}(T)$ at rock sites near the Chelungpu fault can be modified as shown in Table 4. The shapes of $C_{NF}(T)$ for some specific distances from the Chelungpu fault are illustrated in Figure 8.

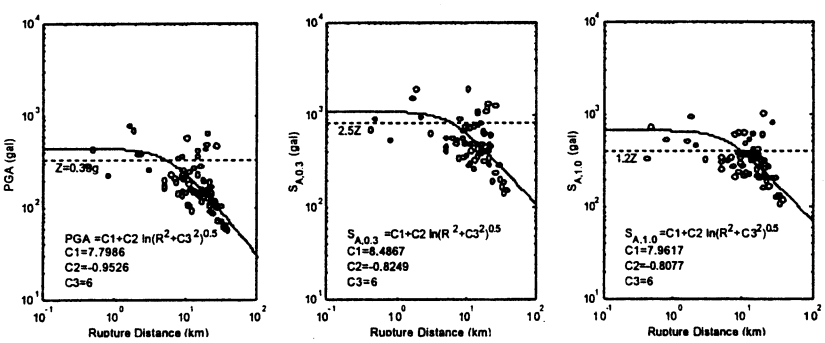

Figure 6: Attenuation relationship of PGA, $S_{A.0.3}$ and $S_{A.1.0}$

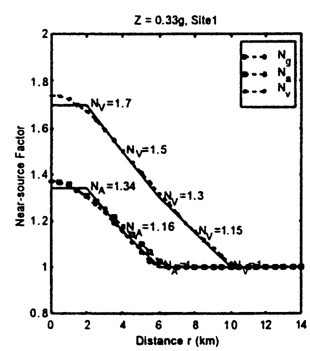

Figure 7: Near-source factors N_A and N_V

Table 3: Near-source factors N_A and N_V at sites near the Chelungpu fault

Distance	$r\leq 2$ km	$r=4$ km	$r\geq 6$ km
N_A	1.34	1.16	1.0

Distance	$r\leq 2$ km	$r=6$ km	$r\geq 10$ km
N_V	1.70	1.30	1.0

Table 4: Near-fault design spectrum for rock sites near the Chelungpu fault

Period Range(sec)	Extremely Short	Very Short	Short	Moderate	Long
	$T\leq 0.03$	$0.03\leq T\leq 0.15$	$0.15\leq T\leq T_1$	$T_1\leq T\leq 1.315$	$T\geq 1.315$
$C_{NF}(T)$	N_A	$N_A(12.5\text{T}+0.625)$	$2.5\,N_A$	$1.2\,N_V/\text{T}^{2/3}$	N_V
$T_1=[1.2N_V/2.5N_A]^{3/2}$					

In general, the code-specified inelastic base shear coefficient (BSC) C/F_u is constrained at short period range by $(C/F_u)_m\leq 1$ with subscript m noting the modification, and F_u means the reduction factor owing to the ductility of the structural system. When near-fault effect is considered, the BSC should be modified by the near-source factor N_A, it yields $(C_{NF}/F_u)_m\leq N_A$. Finally, based on the EPP model, the inelastic demand spectra of the BSC at distance less than 2.0 km from the Chelungpu fault are determined from the recorded earthquake data in the Chi-Chi earthquake. The mean and plus one standard deviation for ductility ratio $\mu=2$ are shown in Figure 9. The code-values of $(C/F_u)_m$ and $(C_{NF}/F_u)_m$ are compared. It can be found that the modification of the design response spectrum is indeed helpful to increase the resistance capacity for buildings against the near-fault earthquakes.

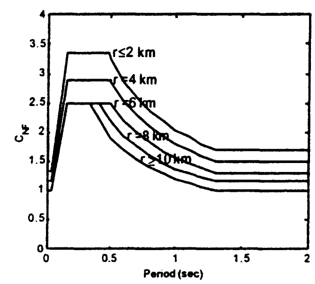

Figure 8: Near-fault spectrum coefficients C_{NF} at different rupture distance

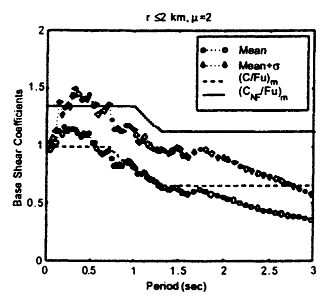

Figure 9: Near-fault inelastic demand spectrum of BSC

6. NEAR-FAULT DESIGN GROUND MOTION

Consider two earthquake data recorded at different sites, it is observed that if we permute the amplitude and phase pairs with each other, the recovered time histories are very similar to the ones providing the phase spectrum. It suggests that if we can simulate the phase spectrum at an interesting site and use the available design response spectrum to determine the amplitude, we can simulate the ground motion which will be compatible with the design response spectrum and also have the same characteristics as the real earthquake data at that site.

In this study, the phase spectrum will be simulated for the separated frequency support one by one rather than once for the whole frequency range. It is implemented by the Meyer wavelet decomposition (Sato and Murono, 1999), and the associated bandwidth of the j-th compact support is $2^j/3\leq f\leq 2^{j+2}/3$. It is noted that the adjacent compact supports are overlapped with each other in the frequency domain.

Take the earthquake data observed at TCU052 station in the Chi-Chi earthquake as an example, it is a typical near-fault ground motion and the PGA has been scaled to become 1g. The orthogonal components can be decomposed by means of the Meyer wavelet, the components with j= -1 and 2 are shown in Figure 10. It is found that the lower frequency component will form a group, while higher frequency component forming many groups with different arrival times. It may be due to the start and stop process of the fault rupture, or may be caused by the sub-events. The Fourier amplitude at the central frequency range on each compact support is coincident with the one determined from the total ground motion, but not true on the edges. Therefore, only the data within the central frequency range $2^{j-1} \leq f \leq 2^j$ are analyzed.

The so-called group delay time of the j-th component can be defined as the partial derivative of the phase respected to the circular frequency. Then, the mean value and standard deviation of the group delay time for j-th component can be determined. It is noted that the group delay time will satisfy the normal distribution on each compact support. Therefore, once we have the mean value and the standard deviation of the group delay time on each compact support, the group delay time can be generate randomly based on the normal distribution, and then integral to obtain the recovered phase spectrum within the un-overlapped frequency range $2^{j-1} \leq f \leq 2^j$.

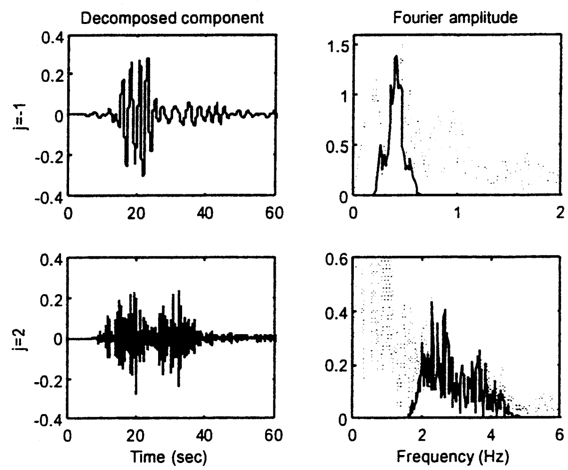

Figure 10: The decomposed time histories and the associated Fourier amplitude

Based on the simulated near-fault phase spectrum and a trial amplitude $A_n(\omega)$, we can recover the total ground motion, and then determine the associated spectral acceleration $S_A(T)$ for any structural period T. Because the response is dominated by the wave with resonant frequency, the modification factor for the Fourier amplitude at a circular frequency of $\omega = 2\pi/T$ can be defined as

$$MF_n(\omega)\big|_{\omega=2\pi/T} = C_{NF}(T)/S_A(T) \tag{3}$$

Then the amplitude on next iteration process can be defined as $A_{n+1}(\omega) = MF_n(\omega) \times A_n(\omega)$. Repeat this iteration process until $MF_n(\omega)$ for all frequency is equal to 1.0. The simulated design ground motion for a site with rupture distance less than 2.0 km are shown in Figure 11, the PGA is equal to the associated near-source factor N_A(=1.34) and the near-fault characteristic of velocity pulse can also be simulated.

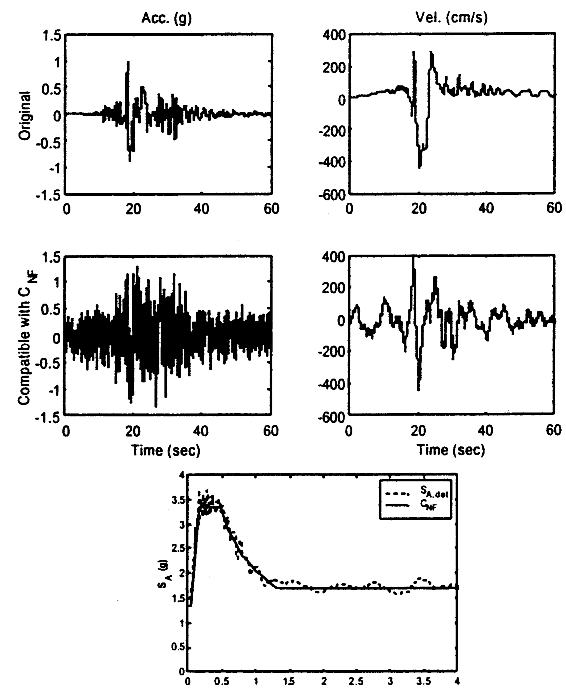

Figure 11: The design ground motion compatible with C_{NF}

However, how to predict the mean value and the standard deviation at the interesting site is still a problem. It may be solved by defining the mean and deviation of group delay time as functions of the earthquake magnitude and the rupture distance, and based on earthquake data to determine the coefficients by statistics. Also, it may be determined by the earthquake data observed at the nearby sites, such as the conditional simulation by Kalman filtering technique (Sato and Murono, 1999), or solved by other methods not been developed yet.

7. CONCLUSIONS

Based on the observations of the structural damages, some valuable lessons were learned from the Chi-Chi earthquake to review and improve the current seismic design code. Some design details, such as the near-fault effect and the ductile details should be comprehended thoroughly. A particular attention should be paid to buildings with soft stories and open front. When a structure subjected to the near-fault ground motion, the induced base shear and ductility demand are larger than those for far-field ground motions and should be highly respected. Based on the concept of UBC97, the modification of the design response spectrum in current Taiwan seismic design code is proposed by defining the so-called near-source factors to increase the seismic capacity for buildings against the near-fault earthquakes. Furthermore, the spectrum compatible near-fault ground motion is simulated based on the modeling of phase spectrum at interesting near-fault sites.

8. ACKNOWLEDGEMENTS

The authors gratefully thank the Central Weather Bureau for their kindness to provide the strong ground motion data recorded in the 921 Taiwan Chi-Chi earthquake.

9. REFERENCES

Chang, K.-C., D.-W. Chang, M.-H. Tsai and Y.-C. Sung (2000). Seismic performance of highway bridges. *Earthquake Engineering and Engineering Seismology* 2(1):55-77.

Kent, D. C. and R. Park (1971). Flexural members with confined concrete', *J. Struct. Div.*, ASCE **97**(ST7): 1969-1990.

Prakash, V. and G. H. Powell (1993). *DRAIN-2DX: Base program user guide, Version 1.10*, a computer program distributed by NISEE/Computer applications, Department of Civil Engineering, University of California, Berkeley, CA.

Sato, T. and Y. Murono (1999). Interpolation of observed earthquake motions using spatially correlated group delay time. *Proceedings of the International Workshop on Chi-Chi, Taiwan Earthquake of September 21, 1999*:6.1-6.18.

Tsai, K.-C., C.-P. Hsiao and M. Bruneau (2000). Overview of building damages in 921 Chi-Chi earthquake. *Earthquake Engineering and Engineering Seismology* 2(1):93-108.

Uniform Building Code (1997). International Conference of Building Officials, Whittier, CA.

Keywords: near-fault earthquake, structural damage, soft story, ductility demand, base shear coefficient, design response spectrum, phase spectrum, and design ground motion

FRAGILITY CURVES FOR BUILDINGS IN JAPAN BASED ON EXPERIENCE FROM THE 1995 KOBE EARTHQUAKE

Fumio YAMAZAKI and Osamu MURAO[1]

ABSTRACT

The number of recorded ground motion in the 1995 Hyogoken-Nanbu (Kobe) Earthquake was not large enough to estimate the detailed spatial distribution of ground motion. Yamaguchi and Yamazaki (1999) estimated the PGV distribution using the BRI's building damage data and the recorded strong motion indices. However the estimated PGV might be affected by the inventory characteristics of buildings in each district. Hence in this paper, the PGV distribution was re-evaluated using the building damage data surveyed by Kobe City for the purpose of property tax reduction. Using the re-evaluated PGV distribution and the building damage data, fragility curves in terms of the structural type and construction period were constructed. It was also demonstrated that the number of damaged buildings in Nada Ward estimated by the fragility curves fits the actual damage by the earthquake. The fragility curves thus obtained may be useful for damage assessments of buildings in Japan.

1. INTRODUCTION

More than one hundred thousand buildings were severely damaged and about one hundred and fifty thousand buildings were moderately damaged due to the Hyogoken-Nanbu (Kobe) Earthquake on January 17, 1995 (National Land Agency 1997). A large amount of data obtained in this earthquake should properly be analyzed for estimating and mitigating damage due to future seismic events. In order to evaluate the building damage in the affected area by the Kobe Earthquake, the strong motion distribution is required. However, since the number of recorded motions was not large enough to estimate the detailed spatial distribution of ground motion (JMA 1997), the strong motion distribution is necessary to be estimated using other data sources.

To estimate the strong motion distribution, the results of the building damage survey by the group of the Architectural Institute of Japan (AIJ), the City Planning Institute of Japan (CPIJ) and Hyogo Prefectural Government (AIJ & CPIJ 1995) may be most useful since the survey was conducted for the entire affected area using the unified damage classification. The data obtained by this survey were digitized on a geographic information system (GIS) by the Building Research Institute, Ministry of Construction (BRI 1996). Miyakoshi et al. (1998) estimated the distribution of the peak ground velocity (PGV) by comparing the BRI data and the PGV obtained from a two-dimensional response analysis. More recently, Yamaguchi and Yamazaki (1999) also estimated the distribution of the peak ground acceleration (PGA), PGV, spectrum intensity (SI), and the instrumental JMA intensity (Shabestari and Yamazaki 1998) using the BRI's building damage data and the strong motion indices calculated from the records.

[1] *Institute of Industrial Science, University of Tokyo, Tokyo, Japan*
Email: yamazaki@iis.u-tokyo.ac.jp

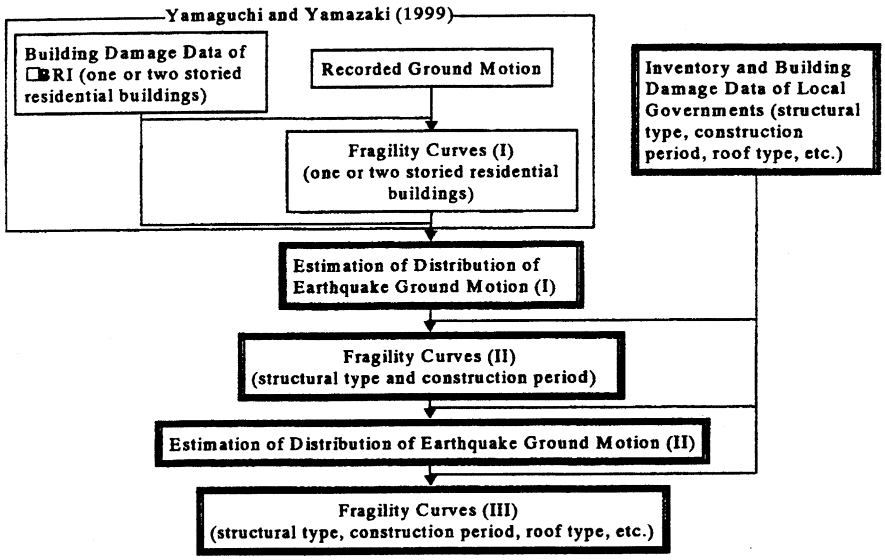

Figure 1: Flowchart for the development of fragility curves based on the damage data from the Kobe Earthquake

Note that, although the BRI data are very useful, the inventory of buildings (type of structure, construction period, etc.) was not associated with the data. Only the use of buildings (residential, commercial/office, or industrial) and story classification (one or two-storied, or higher than that) were given since the survey by the AIJ & CPIJ group was conducted visually from the outside of buildings. To construct the building fragility curves to be used for damage assessments, however, building damage data associated by inventory are necessary. In this view point, the results of building damage survey conducted by local governments are highly useful although the damage classification was different from that of the AIJ & CPIJ and it was even not the same among the local governments in the affected area (Murao and Yamazaki 1999).

The present authors have collected the building damage data surveyed by local governments and performed basic analyses on damage (Murao and Yamazaki 1997; Yamaguchi et al. 1998; Sugiura and Yamazaki 1998). Combining the damage survey data by Kobe City with the estimated ground motion distribution by Yamaguchi and Yamazaki (1999), this paper aims to construct the fragility curves (vulnerability functions) for Japanese buildings.

Figure 1 shows the flowchart for the development of the (empirical) fragility curves. First, fragility curves (I) were created by using the 17 recorded ground motion indices and the BRI damage data for one or two-storied residential buildings. Employing these fragility curves (I) to all the district blocks (corresponding to the postal address) in the stricken area, the distributions of PGA, PGV, SI and JMA intensity (I) were estimated (Yamaguchi and Yamazaki 1999). Using these estimated ground motion distributions and the building damage data for Nada Ward surveyed by Kobe City, the fragility curves (II) considering structural type and construction period are developed in this paper. Employing the fragility curves (II) to each district block of Nada Ward, the distribution of PGV is further refined. Using the updated strong motion distribution (II), further refined fragility curves (III) are finally obtained.

2. OVERVIEW OF BUILDING DAMAGE IN NADA WARD

Nada Ward is one of the nine wards in Kobe City having population of approximately 125,000 in 1994. While the northern part of the ward suffered only slight damage, a large number of buildings were seriously damaged or collapsed in the southern part due to strong shaking. Some buildings were burnt down due to fires and some buildings near the coast were suffered from displacements associated with liquefaction. As a whole, about thirteen thousand buildings were heavily damaged, about six thousand buildings were moderately damaged, and 924 people were killed in Nada Ward by the earthquake (Kobe City 1996).

Table 1 shows the number of buildings in Nada Ward with respect to the structural type and the period of construction for three damage levels: heavy (H), moderate (M), and slight/no damage (N). This damage classification was used for the purpose of property tax reduction for the damaged buildings in the fiscal year of 1995. Note that the damage classification is different from that of the BRI data (Murao and Yamazaki 1999). The following information such as "district block", "structural type", "construction period", "roof type", and "use" is associated with each building as well as the damage classification.

The type of structures is classified into four categories: wood-frame (W), reinforced concrete (RC), steel-frame (S), and light-gauge steel-frame (LS). In Nada Ward, wood-frame buildings were about three-quarters of all buildings. Since the number of buildings was large enough for wood-frame buildings, they were further classified into five construction periods. Figures 2 and 3 show

Table 1: Summary of building damage in Nada Ward due to the Kobe Earthquake

Type of Buildings		Heavy	Moderate	No/Slight	Total
Wood-frame (W)	-1951	5,032	1,636	1,138	7,806
	1952-61	2,897	936	992	4,825
	1962-71	2,588	928	1,126	4,642
	1972-81	1,006	764	1,218	2,988
	1982-94	384	542	1,523	2,449
	Subtotal	11,907	4,806	5,997	22,710
Rainforced Concrete (RC)		354	532	2,928	3,814
Steel (S)		532	462	1,179	2,173
Light Gauge Steel (LS)		272	164	865	1,301
Others		133	89	324	546
Total		13,198	6,053	11,293	30,544

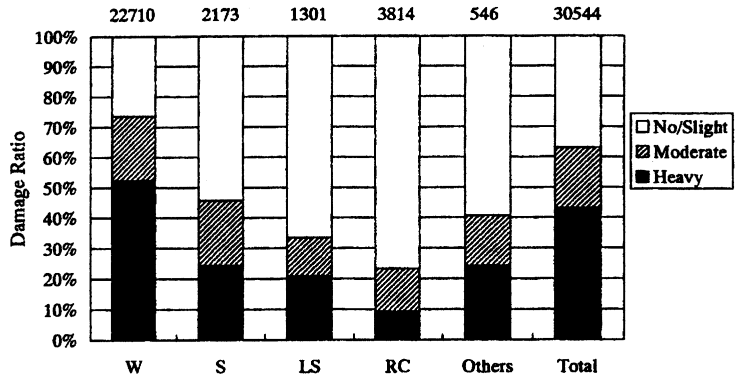

Figure 2: Damage ratio of buildings in Nada Ward for different structural types

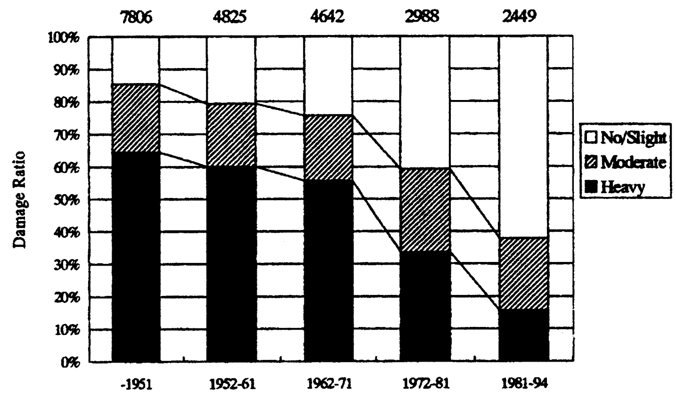

Figure 3: Damage ratio of wood-frame buildings classified by construction period

the damage ratio of buildings in Nada Ward with respect to the structural type and construction period (for wood-frame). The figures indicate that: 1) the damage ratio for wood-frame buildings is largest among all the structural types; 2) the damage ratio for old buildings is larger than that for new buildings for the most structural types.

3. RE-ESTIMATION OF PGV DISTRIBUTION

The distribution of PGV in Nada Ward estimated by Yamaguchi and Yamazaki (1999) is shown in Fig. 4 (a). The seaside area where liquefaction occurred and the mountain area with small number of buildings were excluded from the area to study since, for these areas, the estimation of strong motion indices was difficult from the building damage. In some blocks in Fig. 4 (a), PGV was not determined because a block consists of a large park with almost no residential buildings or blocks were outside of the investigation by the AIJ & CPIJ group.

Since the building damage data used for the development of Fig. 4 (a) do not include the detailed building information, such as the construction year, the estimated PGV may be affected by the characteristics of buildings in each block. Hence, it is desirable to correct this bias using another

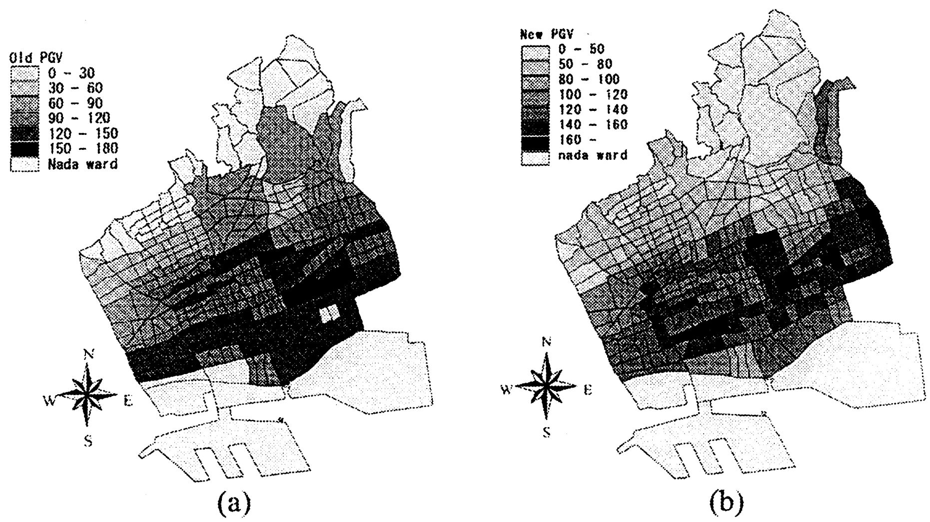

Figure 4: Comparison of (a) estimated PGV and (b) re-estimated PGV from the interim fragility curves (II) in Nada Ward due to the 1995 Kobe Earthquake

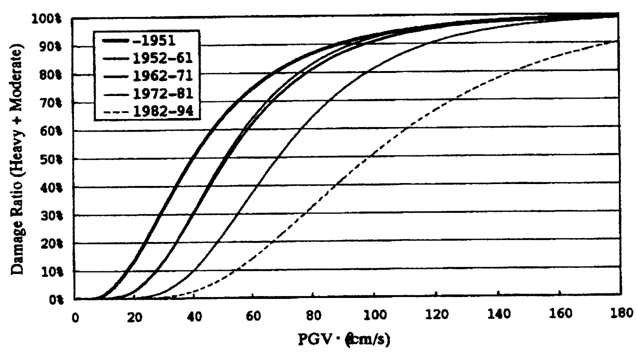

Figure 5: Interim fragility curves of wood-frame buildings with respect to PGV for different construction periods

damage data associated with the detailed building information.

First, (interim) fragility curves of wood-frame buildings were constructed using the damage ratio of buildings in each block level of Nada Ward and the estimated PGV distribution shown in Fig. 4 (a). The damage ratios of buildings were first calculated for each block (containing about scores to a few hundred buildings). However, after classifying the buildings within a block using the category in Table 1, the number of buildings in each block with the same category becomes small. Hence the several neighboring blocks having a certain range of the estimated strong motion indices were synthesized when calculating the damage ratios.

In selecting the neighboring blocks to combine the damage data, the extent of damage and the subsurface soil condition of the blocks were considered. For each construction period of wood-frame buildings, 20 combined blocks were used with the approximate number of buildings in each block as: 360 buildings for period equal or before 1951, 220 buildings for period 1952-61, 200 buildings for period 1962-71, 120 buildings for period 1972-81, and 100 buildings for period 1982-94. Such regional grouping was adopted to obtain reliable damage statistics that correspond to the estimated PGV.

For a strong motion index x, the cumulative probability $P_R(x)$ of the occurrence of damage equal or higher than rank R is assumed to be log-normal as follows:

$$P_R(PGV) = \Phi\,((\ln PGV - \lambda)/\zeta) \qquad (1)$$

In which Φ is the standard normal distribution and λ and ζ are the mean and the standard deviation of $\ln PGV$. The two parameters of the distributions, λ and ζ, were determined by the least square method on lognormal probability paper.

Figure 5 shows the interim fragility curves for wood-frame buildings in Nada Ward for different construction periods based on the building survey data of Kobe City. As demonstrated in Fig. 5, the interim fragility curves for wood-frame buildings are dependent on the period of construction. However, no such information was available for the building damage data of BRI. Hence, in estimating the distribution of PGV from the BRI data, we implicitly assumed that the construction periods of one or two-storied residential buildings had similar distribution in all the studied area. But this assumption is obviously not true. Some districts consist of old buildings and some others consist of new buildings.

Considering these issues, the distribution of PGV was re-estimated using the interim fragility curves shown in Fig. 5. From the damage ratio of buildings for one construction period in a block, one PGV value in the block can be estimated. Using the five interim fragility curves corresponding to the different construction periods, the five PGV values are obtained. Similarly, the two damage levels (heavy, heavy + moderate) give two PGV values for a block. These estimated PGV values were averaged for the re-evaluation of PGV. Figure 4 (b) shows the distribution of re-evaluated PGV.

4. FRAGILITY CURVES OF BUILDINGS IN JAPAN

In the similar manner, the fragility curves for all of the buildings based on the re-estimated PGV were constructed with regard to structural types and construction periods. Table 2 summarizes the results of the regression analysis. With regard to R_h and R_m in Table 2, the square of correlation coefficients (R^2) for wood-frame building are largest. This fact can be explained by 1) the PGV was re-estimated from the mean value of damage ratio for wooden buildings; and 2) the number of wood-frame buildings is largest among structural type, thus they gave the most stable statistics. R^2 values for other type of structures are lower than those for wood-frame buildings. But they are, in general, very high.

Table 2: Parameters of fragility curves for Japanese buildings

		Heavy (R_h)			Heavy + Moderate(R_m)		
		λ	ζ	R^2	λ	ζ	R^2
Wood-frame (W)	-1951	4.36	0.41	0.96	3.66	0.67	0.88
	1952-61	4.44	0.35	0.98	3.97	0.49	0.95
	1962-71	4.45	0.34	0.98	4.02	0.46	0.97
	1972-81	4.73	0.38	0.97	4.25	0.39	0.98
	1982-1994	5.12	0.50	0.88	4.61	0.47	0.97
	All	4.51	0.41	0.98	4.07	0.51	0.98
Reinforced Concrete (RC)	-1971	5.12	0.65	0.95	4.72	0.69	0.93
	1972-81	5.33	0.58	0.94	4.85	0.61	0.84
	1982-94	6.00	0.79	0.90	5.33	0.79	0.92
	All	5.50	0.71	0.97	4.99	0.72	0.92
Steel (S)	-1971	4.64	0.62	0.72	4.25	0.71	0.79
	1972-81	4.97	0.49	0.94	4.49	0.55	0.80
	1982-94	5.64	0.73	0.89	5.01	0.73	0.82
	All	5.14	0.63	0.75	4.69	0.67	0.69
Light Gauge Steel (LS)	-1971	4.70	0.55	0.93	4.41	0.50	0.91
	1972-81	5.82	0.97	0.73	4.95	0.86	0.78
	1982-94	6.19	1.10	0.86	5.28	0.87	0.85
	All	5.03	0.56	0.94	4.73	0.60	0.97

Figure 6 shows the fragility curves for the four structural types. In each figure, wood-frame buildings show the smallest seismic capacity and RC structures show the largest seismic capacity. The functions for steel-frame and light-gauge steel-frame structures look very similar.

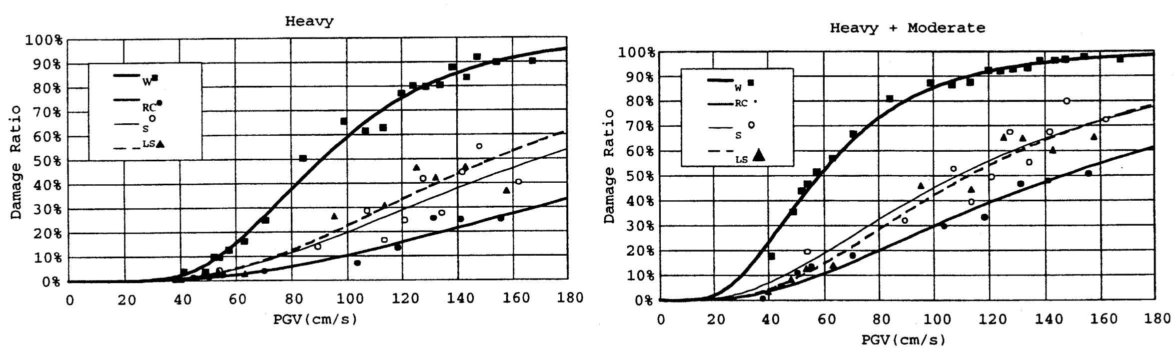

(a) Heavy damage (b) Heavy + Moderate damage

Figure 6: Fragility curves with respect to PGV for different structural types

Figure 7 shows the fragility curves for reinforced concrete and steel buildings with different construction periods. It is clearly seen in the figures that the older buildings are more vulnerable than the newer buildings. For these engineered structures (S and RC), the revision of the seismic design code in each construction period may have a significant effect for the improvement of seismic resistance. However, for other structural types, especially for wood-frame buildings, it is concluded that the aging of buildings is mostly responsible for this observation, based on the plot of building damage ratios year by year (of construction).

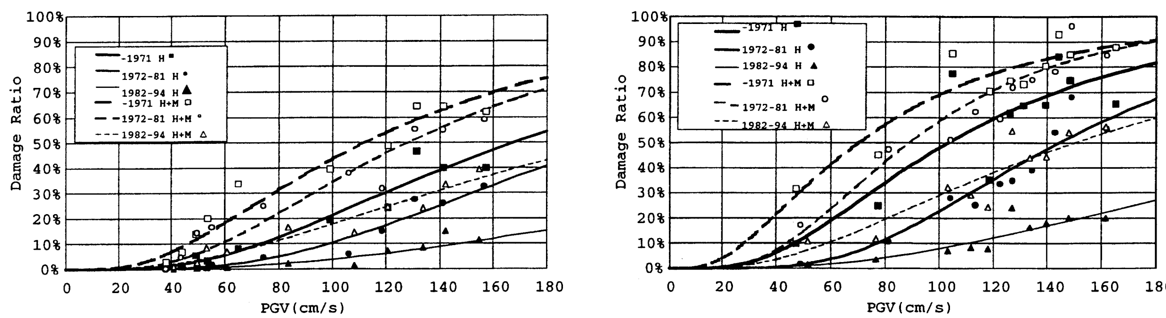

(a) RC buildings (b) Steel buildings

Figure 7: Fragility curves for RC and steel buildings

The fragility curves developed here may be further improved by introducing the damage data from neighboring cities in the 1995 Kobe Earthquake (e.g. Yamaguchi and Yamazaki 2000) and the results of numerical simulation for building damage.

5. CONCLUSIONS

The 1995 Hyogoken-Nanbu (Kobe) Earthquake caused unprecedented damage in Kobe and its surrounding area. A number of building damage surveys were carried out for different purposes. The results of these surveys contain highly valuable information on building fragility and ground motion estimation. In this paper, the building damage data for Nada Ward of Kobe surveyed by Kobe City Government were employed to construct fragility curves that consider the structural type and construction period. The resultant fragility curves show that the structural type and construction period are important parameters to determine the occurrence probability of damage.

In developing the empirical fragility curves, the distribution of strong motion indices estimated using the recorded ground motion and other building damage survey data were used. Since the estimated PGV was affected by the inventory characteristics of each district block, the PGV distribution was re-evaluated using the obtained fragility curves that consider the construction period of wood-frame buildings. Using the re-evaluated PGV distribution, refined fragility curves considering more detailed characteristics of buildings were developed. The final fragility curves may be useful for damage assessments and early damage estimation systems in Japan.

6. ACKNOWLEDGEMENTS

The damage survey data used in this paper were provided by the Architectural Institute of Japan, the City Planning Institute of Japan, Building Research Institute, and Kobe City.

7. REFERENCES

Architectural Institute of Japan and City Planning Institute of Japan. 1995. *Report of emergency damage survey of the 1995 Hyogoken-Nanbu earthquake.*

Building Research Institute. 1996. *Final report of damage survey of the 1995 Hyogoken-Nanbu earthquake.* (In Japanese).

Japan Meteorological Agency. 1997. *Report on the Hyogo-ken-Nanbu earthquake, 1995.* Technical Report of JMA 119. (In Japanese).

Kobe City. 1996. *Statistical year book 1996.* (In Japanese).

Miyakoshi, J., Y. Hayashi, K. Tamura, and N. Fukuwa. 1998. Damage ratio functions of building using damage data of the 1995 Hyogo-Ken Nanbu Earthquake. *Proceedings of the 7th International Conference on the Structural Safety and Reliability* Vol. 1, pp. 349–54.

Murao, O., and F. Yamazaki. 1997. Analysis on building damage in Nada Ward due to the Hyogoken-Nanbu earthquake. *Proceedings of the 24th JSCE Earthquake Engineering Symposium* Vol. 2, pp. 1261–64. (In Japanese).

Murao, O., and F. Yamazaki. 1999. Comparison of building damage evaluation by local governments after the 1995 Hyogoken-Nanbu earthquake. *Journal of Architecture, Planning and Environmental Engineering* 515: 187–94. (In Japanese).

National Land Agency. 1997. *White Paper for disaster prevention 1997.* (In Japanese).

Shabestari, K. T., and F. Yamazaki. 1998. Attenuation relation of JMA seismic intensity based on JMA-87-type accelerometer records. *Bull. of Earthquake Resistant Structure Research Center* 31: 13–21. Institute of Industrial Science, University of Tokyo.

Sugiura, M., and F. Yamazaki. 1998. Fragility curves for buildings based on damage data in Takarazuka due to the Hyogoken-Nanbu earthquake. *Proceedings of the 10th Japan Earthquake Engineering Symposium* Vol. 2, pp 3385–90. (In Japanese).

Yamaguchi, N., F. Yamazaki, and K. Wakamatsu. 1998. Analysis of building damage in Nishinomiya City due to the Hyogoken-Nanbu earthquake. *Proceedings of the 6th U. S. National Conference on Earthquake Engineering.* Seattle. CD-ROM.

Yamaguchi, N., and F. Yamazaki. 1999. Estimation of strong motion in the 1995 Hyogoken-Nanbu earthquake based on building damage data. *Proceedings of the Asian-Pacific Symposium on Structural Reliability and its Applications*, pp. 478–89. Taipei, Taiwan.

Yamaguchi, N., and F. Yamazaki. 2000. Fragility curves for buildings in Japan based on damage surveys after the 1995 Kobe earthquake. *Proceedings of the 12th World Conference on Earthquake Engineering.* Auckland, New Zealand. CD-ROM.

Keywords: building damage, fragility curve, the 1995 Kobe Earthquake, structural type, construction period, Nada Word, damage survey, inventory, peak ground velocity, GIS.

"SMART" DAMPERS FOR STRUCTURAL RESPONSE REDUCTION

B.F. SPENCER, JR.,[1] J.C. RAMALLO[2] AND G. YANG[3]

ABSTRACT

In the last few decades, there has been a great deal of interest in the use of structural control systems to mitigate the effects of seismic hazards on civil engineering structures. One of the most promising new control systems employs magnetorheological (MR) fluid dampers. MR dampers offer the reliability of passive control devices, yet maintaining the versatility and adaptability of fully active control devices. Such dampers have the inherent ability to provide a simple and robust interface between electronic controls and mechanical components, enabling reliable, fast-acting semiactive vibration control of systems. This paper comprises two parts. The first discusses the design and testing of a monotube, linear MR fluid damper capable of achieving real-time controlled damping forces of 10^5 to 10^6 Newtons. This MR damper design is shown to be mechanically simple and require low power, an important feature for seismic control of structures. The second part of the paper discusses a "smart" base isolation system using devices such as the MR fluid damper that can adapt to and protect against seismic excitation of different characteristics. The adaptable nature of the smart damper system is shown to be effective for extreme earthquakes, without sacrificing performance during the more frequent, moderate seismic events.

1. INTRODUCTION

Conventional seismic design approaches require that structures passively resist environmental forces (*i.e.*, wind, waves and earthquakes) through a combination of strength, deformability, and energy absorption. During strong earthquakes, for example, these structures often deform well beyond the elastic limit, remaining intact only due to their ability to respond inelastically. Much of the input earthquake energy is absorbed by the structure itself through local damage. This is somewhat of a paradox in that the effects of the earthquake (*i.e.*, structural damage) are counteracted by allowing structural damage.

An alternative approach to mitigating the effects of seismic loads is to absorb or reflect a portion of the input energy, not by the structure itself, but by some type of structural control systems. This point of view has resulted in many new and innovative concepts of structural control being advanced that are in various stages of development. Those concepts can be divided into three main categories: passive, active and semiactive control systems.

Passive systems alleviate energy dissipation demand on the primary structure by reflecting or absorbing part of the input energy, therefore reducing possible structural damage. However, passive systems have the limitation that they can not deal with the change of either external loading conditions or usage patterns.

Active systems have the ability to adapt to different loading conditions and to control different vibration modes of the structure. Many important advances have been made in this relatively new

1. Dept. of Civil Engrg. and Geo. Sci., Univ. of Notre Dame, Notre Dame, IN 46556. E-mail: spencer@nd.edu
2. Dept. of Civil Engrg. and Geo. Sci., Univ. of Notre Dame, Notre Dame, IN 46556. E-mail: jramallo@nd.edu
3. Dept. of Civil Engrg. and Geo. Sci., Univ. of Notre Dame, Notre Dame, IN 46556. E-mail: gyang2@nd.edu

research area during the last decade (Housner *et al.* 1997; Spencer and Sain 1997). However, wide-spread implementation of active systems is limited due to reliance on external power supplies and concerns over long-term reliability and maintainability.

Semiactive, or, "smart," damping systems have the capability of adapting to the changes of the external loads, as with the active systems, but without requiring the input of large amounts of energy. In many cases, semiactive systems can achieve control performance that is similar to that of active systems. Control strategies based on semiactive devices combine the best features of both passive and active control systems to offer significant possibilities for near-term acceptance of control technology as a viable means of protecting civil engineering structures against severe earthquake loading.

Because of their mechanical simplicity, high dynamic range, low power requirement, large force capacity and robustness, MR fluid dampers are one of the most promising semiactive devices for structural control. Spencer *et al.* (1997a) and Dyke *et al.* (1998) have conducted a number of pilot studies to evaluate the efficacy of MR dampers for earthquake response reduction. The experimental results indicate that the MR damper is quite effective for a wide class of seismic excitations. To demonstrate that the MR fluids technology is scalable to full-size civil engineering structures, the next section discusses a full-scale seismic MR damper that has been built tested at the Structural Dynamics Control / Earthquake Engineering Laboratory at the University of Notre Dame. Subsequently, an application of this technology is considered wherein a passive isolation system is enhanced by the addition of "smart" dampers (*e.g.*, magnetorheological dampers). The adaptable nature of the smart damper system is shown to be effective for extreme earthquakes, without sacrificing performance during the more frequent, moderate seismic events.

2. FULL-SCALE SEISMIC MR FLUID DAMPER

To prove the scalability of MR fluid technology to devices of appropriate size for large-scale civil engineering applications, a 20-ton MR fluid damper has been designed and built (Spencer, et al. 1997b). For the nominal design, a dynamic range equal to ten was chosen. The damper uses a particularly simple geometry in which the outer cylindrical housing is part of the magnetic circuit. The effective fluid orifice is the entire annular space between the piston outside diameter and the inside of the damper cylinder housing. The damper is double-ended, *i.e.* the piston is supported by a shaft on both ends. This arrangement has the advantage that a rod-volume compensator does not need to be incorporated into the damper, although a small pressurized accumulator is provided to accommodate thermal expansion of the fluid. The damper has an inside diameter of 20.3 cm and a stroke of $\pm$ 8 cm. The electromagnetic coil is wound in three sections on the piston. This results in four effective valve regions as the fluid flows past the piston. The coils contain a total of about 1.5 km of copper wire. The damper contains approximately 5 liters of MR fluid. However, the amount of fluid energized by the magnetic field at any given instant is only ~90 cm^3, which leads to power requirements of less than 50 watts.

Figure 1 shows the experimental setup at the University of Notre Dame for the 20-ton MR fluid damper. The damper was attached to a 7.5 cm thick plate that was grouted to a 2 m thick strong floor. The damper is driven by a 560 kN actuator configured with a 305 lpm servo-valve with a bandwidth of 80 Hz. A Schenck-Pegasus 5910 servo-hydraulic controller is employed in conjunction with a 200 MPa, 340 lpm hydraulic pump.

Figure 2 shows the measured performance for a commanded triangular displacement. The maximum force measured at full magnetic field strength is 201 kN at a piston velocity of 5 cm/sec, which is within 0.5% of the analytically predicted result. Moreover, the dynamic range of the damper is well over the design specification of 10.

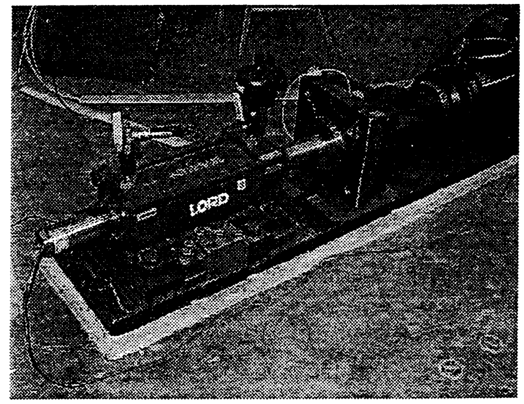

Figure 1: Experimental Setup for 20-Ton MR Fluid Damper

3. SMART SEISMIC ISOLATION SYSTEMS

Recent years have seen a number of occurrences of catastrophic structural failures due to severe, impulsive, seismic events. Under such dynamic events, some researchers (*e.g.*, Hall *et al.* 1995; Heaton *et al.* 1995) have raised concerns as to the efficacy of seismic isolation. Based on observations from the 1994 Northridge earthquake, these researchers suggested that base-isolated buildings are vulnerable to strong impulsive ground motions generated at near-source locations. Moreover, the most recent revisions to the Uniform Building Code (ICBO 1997) have made the requirements for base-isolation systems more stringent compared to the previous versions, potentially rendering the additional complexity and cost of such structures less economically justified (Kelly 1999). The code-mandated accommodation of larger base displacements and the requirement to consider a larger Maximum Capable Earthquake (MCE) has suggested the need for supplemental damping devices (Asher *et al.* 1996). However, additional damping may also increase the response of the superstructure, thus defeating many of the gains for which base isolation is intended (Kelly 1999). To understand the impact of excessive damping, it is important to consider the disrupted operation of (or even damage to) highly sensitive equipment in hospitals, communication centers and computer facilities under various ground acceleration levels (Inaudi and Kelly 1993). For example, internet-based businesses involved in the expanding e-commerce market reported that a single company lost $5 million in sales and $4 billion in stock value after its site shut down for 22 hours in 1999 (*USA Today*, February 11, 2000).

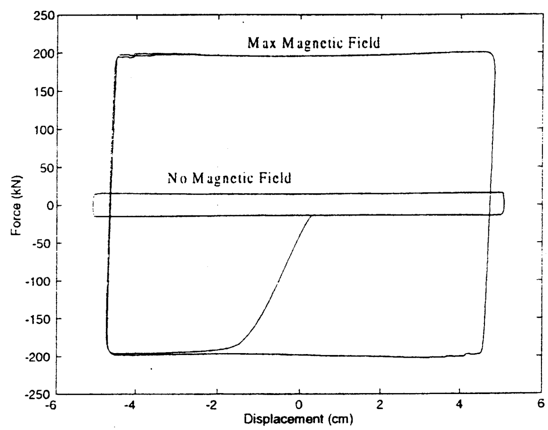

Figure 2: Measured Performance for 20-Ton MR Fluid Damper at 5 cm/sec

As reported by Spencer and Sain (1997), a number of studies have focused on the use of active control devices in parallel with a base-isolation system to alleviate these difficulties. However, active control devices have yet to be fully embraced by engineers working in the field of civil infrastructures, in large part due to the challenges of large power requirements (that may be interrupted during an earthquake), concerns about stability and robustness, and so forth. Alternatively, several researchers have investigated the use of smart dampers for seismic response mitigation (*e.g.*, Feng and Shinozuka 1990; Johnson *et al.* 1999; Nagarajaiah 1994; Symans and Kelly 1999; Yoshida *et al.* 1999; for further references, see Spencer and Sain 1997). Studies of smart base isolation have used several types of control design methodologies such as LQG and H_∞ control (*e.g.*, Yoshida *et al.* 1999), fuzzy control (*e.g.*, Symans and Kelly 1999), *etc.*, and have examined both bridge and building structures. The first full-scale implementation of smart base isolation was recently constructed at Keio University (Yoshida *et al.* 1999).

This section investigates the effectiveness of several base isolation strategies employing either lead-rubber bearings or smart dampers. (*e.g.*, magnetorheological dampers) for earthquakes of various magnitudes and characteristics. To demonstrate the advantages and disadvantages of the various approaches, several historical earthquakes scaled to different magnitudes are used to excite an isolated building structure. Smart damping strategies are shown to be able to achieve more effective response reduction due to their adaptability to various excitations.

3.1. Problem Formulation

The structural model used in this study is a single degree-of-freedom model that has mass and fundamental modal frequency and damping ratio equal to that of the five-story building model given in Kelly *et al.* (1987). With the addition of an isolation layer, the model has two degrees of freedom. The isolation layer is chosen to obtain a fundamental mode with period 2.5 seconds and 1% critical damping (see Fig. 3).

This low-damping, long period, isolation system fits into the "*Class (ii): lightly damped, linear isolation system*" category defined in Skinner *et al.* (1993). Letting $\mathbf{x} = [x_b \;\; x_s]^T$ denote the displacements relative to the ground, the equation of motion of the base-isolated system may be written as

$$\mathbf{M}\ddot{\mathbf{x}} + \mathbf{C}\dot{\mathbf{x}} + \mathbf{K}\mathbf{x} = \Lambda f - \mathbf{M}\mathbf{1}\ddot{x}_g \tag{1}$$

where $\Lambda = [1 \;\; 0]^T$ gives the position of the supplemental damper, f is the force exerted by the damper, and $\mathbf{1}$ is a vector whose elements are all unity. In this study, two types of isolation damping are considered, which can be classified as follows.

***Lead-rubber bearing (LRB)*:** Because use of the bilinear model may result in overestimation of the acceleration levels in isolated buildings, the LRB is modeled herein using the Bouc-Wen model (Wen 1976) with a hysteretic exponent of unity. The properties selected for the isolators are such that under plastic deformation the fundamental mode will have a 2.5 second period and 2% of (viscous) critical damping, properties provided by the rubber component of the bearing. In the selection of the lead-rubber bearings, the influence of two parameters is considered, namely the total yield force Q_y (expressed as a fraction of the total structural weight) and the stiffness ratio $K_{\mathrm{initial}}/K_{\mathrm{yield}}$. The post-yield stiffness is fixed at $K_{\mathrm{yield}} = 2.32$ kN/m to obtain a fundamental period of 2.5 seconds once the lead plug has yielded. Skinner *et al.* (1993) suggested that for design earthquakes having the severity and 'character' of the El Centro earthquake, typical values of the yield force Q_y are on the order of 5% of the total weight of the structure. Therefore, for the El Centro and Hachinohe earthquakes (the 'moderate' earthquakes), a system designated as *LRB1* with $Q_y = 5\%$ of the structural weight and with $K_{\mathrm{initial}}/K_{\mathrm{yield}} = 6$ was selected as the yardstick for comparison to the other supplemental damping devices. However, to achieve similar results for severe seismic events, higher yield levels are necessary. Hence, a second design, called *LRB2* with $Q_y = 15\%$ of the structural weight and with $K_{\mathrm{initial}}/K_{\mathrm{yield}} = 10$ is also studied. This value for Q_y follows the results of Park and Otsuka (1999).

Smart (semi-active) damper: A controllable damper (*e.g.*, variable orifice damper, controllable fluid damper, *etc.*) that may exert only dissipative forces; *i.e.*, $f_{SA}\dot{x}_b \leq 0$ where f_{SA} is the applied force and $\dot{x}_b$ is the velocity across the damper. In previous studies of smart dampers in seismic protection systems (*e.g.*, Dyke *et al.* 1996a-b, Johnson *et al.* 1999, Spencer *et al.* 1999), one control strategy that performed well, a *clipped-optimal control*, assumed an "ideal" active control device, used H_2/LQG control theory to design an appropriate controller for this active device, and then, using a secondary bang-bang-type controller, made the semiactive damper approximate the same forces the active device would have exerted on the structure.

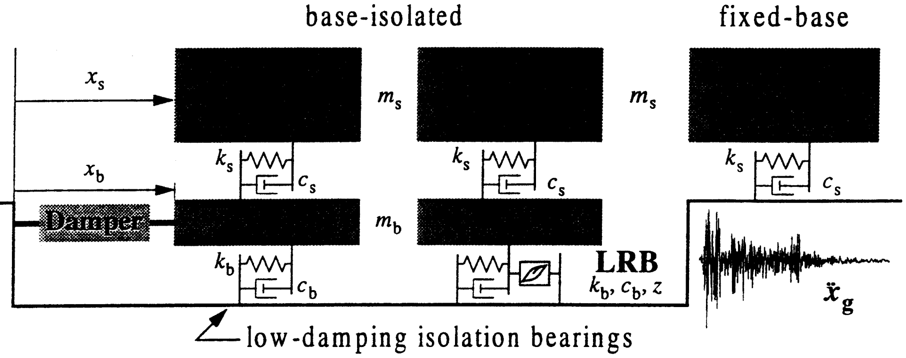

Isolation Parameters	**Structure Parameters**
m_b=6800 kg	m_s=29485 kg
Period 2.5 s $\Rightarrow k_b$=232 kN/m	Period 0.3 s $\Rightarrow k_s$=11912 kN/m
Damping ratio 2% $\Rightarrow c_b$=3.74 kN·s/m	Damping ratio 2% $\Rightarrow c_s$=23.71 kN·s/m

Figure 3: Two degree-of-freedom (2DOF) models

4. SIMULATION RESULTS

The isolation structures considered herein are excited by a suite of ground motions that are intended to encompass moderate (1940 NS El Centro and 1968 NS Hachinohe) and severe (1995 NS Kobe and 1994 NS Northridge (Sylmar County Hospital record)) events. Additionally, the earthquakes are scaled to several magnitudes to better understand the effectiveness of the isolation strategies for different earthquake strengths. The moderate records are scaled in the range from 0.50 to 2.00 times the historical record, and the severe ones from 0.50 to 1.50. Although magnifying the severe earthquakes might seem unnecessary, the results using 1.50 times historical are included to show the behavior of different damping devices under truly extreme events.

Table 1 shows the responses of the structural system with the designed LRB1 (*i.e.,* the LRB with Q_y = 5% of the building weight) under various earthquakes. Table 2 summarizes the percent improvement of LRB2 (the high-yield LRB) and the 'smart' damper over the response of LRB1.

The LRB2 system, due to its higher yield level, is capable of substantial reductions in the peak base drift. Not surprisingly, however, this reduction in base drift comes at the price of increased accelerations and interstory drifts. The base acceleration in the LRB2 system was substantially increased for 8 of the 10 ground motions considered. Moreover, for the reduced scale earthquakes (*i.e.,* those that are likely to occur more frequently), the accelerations increased up to 137% (in the case of El Centro) over the LRB1 system. Structural drifts follow a pattern similar to base acceleration.

The smart damping system achieved reductions in peak base drift that were comparable with the LRB2 system. However, in contrast to the LRB2 system, Table 2 shows that the peak base accelerations were reduced (as compared to the LRB1 system) for all except two of the ground motions considered; in these two cases, the increase in the base acceleration was only a few percent. The peak structural drifts were reduced for all cases considered. In particular, note the excellent performance for the reduced scale ground motions where the smart damping system reduces peak base acceleration from 24% to 42% and reduces the base drifts by up to 41% in comparison with the LRB1 system. Thus, the decrease in the base drift during the large earthquakes does not necessarily come at the expense of larger accelerations and interstory drifts. With regard to the peak forces exerted, the smart damper required a peak force only 11% larger than the LRB2 system.

Table 1: Peak drifts [mm], absolute accelerations [mg], and forces [kN] for LRB1

	El Centro				Hachinohe				Kobe			Northridge		
Scale	**0.50**	**1.00**	**1.50**	**2.00**	**0.50**	**1.00**	**1.50**	**2.00**	**0.50**	**1.00**	**1.50**	**0.50**	**1.00**	**1.50**
Base Drift	41.0	82.9	167.7	300.6	41.9	92.6	168.3	312.1	132.4	265.3	454.0	231.7	556.0	1013.9
Base Accel	68.7	109.0	155.8	234.7	72.8	111.6	153.1	240.2	124.9	233.2	351.3	198.3	410.9	721.9
Struct. Drift	1.6	2.4	3.7	5.8	3.1	5.4	8.3	11.3	3.1	5.4	8.3	4.7	9.9	17.2
Struct. Accel	67.7	99.3	152.0	239.5	69.9	103.0	152.4	246.6	129.2	221.7	340.7	193.6	409.0	707.3
Force	14.38	14.83	14.83	14.83	14.63	14.83	14.83	14.83	14.83	14.83	14.83	14.83	14.83	14.83

Table 2: Percent reduction for different damping mechanisms over LRB1

Earthquake	Scale	Peak Base Drift		Peak Base (Abs.) Acceleration		Peak Structural Drift		Peak Struct.(Abs.) Acceleration		Peak Applied Force	
		LRB2	**Smart Damper**	**LRB2**	**Smart Damper**	**LRB2**	**Smart Damper**	**LRB2**	**Smart Damper**	**LRB2**	**Smart Damper**
El Centro	0.50	4.9	3.2	–137.6	24.2	–125.0	31.3	–117.7	33.1	–193.2	18.6
Hachinohe		15.3	15.8	–91.5	42.2	–61.3	74.2	–89.5	50.2	–181.8	15.9
Kobe		24.3	39.3	–98.0	32.1	–61.3	25.8	–40.4	25.9	–223.6	–98.0
Northridge		50.8	41.6	–12.5	26.8	–8.5	23.4	–0.6	23.6	–223.9	–170.3
El Centro	1.00	13.1	4.3	–97.8	4.4	–91.7	8.3	–101.0	8.8	–218.1	–57.8
Hachinohe		31.3	23.8	–70.6	24.6	–13.0	68.5	–74.9	32.4	–219.4	–65.9
Kobe		35.7	39.4	–65.3	6.1	–13.0	14.8	–35.2	13.7	–224.0	–260.0
Northridge		38.0	42.8	4.0	17.1	10.1	25.3	3.1	25.5	–224.0	–260.0
El Centro	1.50	35.9	29.0	–79.5	–0.4	–40.5	10.8	–58.7	10.5	–223.0	–136.7
Hachinohe		41.9	37.1	–51.7	17.6	–3.6	69.9	–12.6	31.5	–223.7	–148.9
Kobe		26.8	45.1	–42.6	–4.2	–3.6	22.9	–3.9	22.9	–224.0	–260.0
Northridge		35.5	41.3	17.5	16.2	20.3	31.4	–8.7	31.0	–224.0	–260.0
El Centro	2.00	51.7	47.2	–44.4	11.2	–1.7	24.1	9.9	24.3	–223.8	–215.6
Hachinohe		52.8	54.8	–13.8	29.9	–7.1	69.9	20.2	43.6	–224.0	–231.9

5. CONCLUSIONS

Because of their simplicity, low input power, scalability and inherent robustness, MR fluid dampers appear to be quite promising for civil engineering applications. A 20-ton MR damper capable of providing a semiactive damping for full-sized structural applications has been constructed, and experimental characterization of this damper has been conducted at the University of Notre Dame. The results confirm the design and performance of this MR damper.

As an example of the technology, a comparison study of three base isolation systems was performed. The responses to a wide range of ground motions were computed using two passive base isolation systems (LRB1, $Q_y = 5\%$, and LRB2, $Q_y = 15\%$, lead-rubber isolators, primarily intended to withstand moderate and severe ground motions, respectively) and a smart (semi-active) isolation system. The response was measured in terms of peak base and structural (relative) displacements, peak base and structural (absolute) accelerations, and peak applied forces. The selected suite of earthquakes (composed of two moderate and two severe earthquakes) was scaled in magnitude to evaluate the designed supplemental damping systems under ground motions exhibiting different frequency content and/or different magnitudes of applied energy. While for base-drifts, the LRB2 system was capable of important improvements over LRB1 values, the LRB2 system amplifies both the base acceleration and interstory drift, as compared to LRB1. This trade-off between the various responses is well recognized in the literature.

In contrast, the smart damping system, using a controllable passive damper, was able to achieve reductions in the base drift comparable to the LRB2 system over the entire suite of earthquakes, without the associated large increases in the base acceleration and interstory drift. Moreover, the required damping force levels were only 11% greater than those of the LRB2 system. The adaptable nature of the smart damper system allows a structure to be protected against extreme earthquakes without sacrificing performance during the more frequent, moderate seismic events, showing significant promise for the use of smart damping devices in base isolation applications.

6. ACKNOWLEDGMENTS

The authors gratefully acknowledge the partial support of this research by the National Science Foundation under grant CMS 99–00234 (Dr. S.C. Liu, Program Director), the LORD Corporation, and by a fellowship from Consejo Nacional de Investigaciones Científicas y Técnicas (República Argentina).

7. REFERENCES

Asher, J. W., R. P. Young, and R. D. Ewing. 1996. Seismic isolation design of the San Bernardino County Medical Center Replacement Project. *J. of Struct. Design of Tall Buildings* 5:265–79.

Dyke, S. J., B. F. Spencer Jr., M. K. Sain, and J. D. Carlson. 1998. An Experimental Study of MR Dampers for Seismic Protection. *Smart Materials and Struct.* 7:693–703.

———. 1996b. Modeling and control of magnetorheological dampers for seismic response reduction. *Smart Materials and Struct.* 5:565–75.

———. Seismic response reduction using magnetorheological dampers. *Proc. IFAC World Congress* L:145–50.

Feng, Q., and M. Shinozuka. 1990. Use of a variable damper for hybrid control of bridge response under earthquake. *Proc., U.S. Nat. Workshop on Struct. Control Res.* USC Publication no. CE–9013.

Hall, J. F., T. H. Heaton, M. Halling, and D. J. Wald. 1995. Near-source ground motion and its effects on flexible buildings. *Earthquake Spectra* 11(4):569–605.

Heaton, T. H., J. F. Hall, D. J. Wald, and M. Halling.1995. Response of high-rise and base-isolated buildings in a hypothetical Mw 7.0 blind thrust earthquake. *Science* 267:206–11.

Housner, G. W. et al. 1997. Structural control: Past, present, and future. *J. Engrg. Mech., ASCE* 123(9):897–971.

Inaudi, J. A., and J. M. Kelly. 1993. Hybrid isolation systems for equipment protection. *Earthquake Engng. Struct. Dyn.* 22:297–313.

International Conference of Building Officials. 1997. *Uniform Building Code, Earthquake Regulations for seismic isolated structures*, Appendix Chapter 16.

Johnson, E. A., J. C. Ramallo, B. F. Spencer, Jr., and M. K. Sain. 1999. Intelligent base isolation systems. *Proc., 2nd World Conf. on Struct. Control* 1:367–76.

Kelly, J. M., G. Leitmann and A. G. Soldatos. 1987. Robust control of base-isolated structures under earthquake excitation. *J. Opt. Theory and Appl.* 53:159–80.

Kelly, J. M. 1999. The role of damping in seismic isolation. *Earthquake Engrg. and Struct. Dyn.* 28:3–20.

Nagarajaiah, S. 1994. Fuzzy controller for structures with hybrid isolation system. *Proc., 1st World Conf. Struct. Control*, TA2:67–76.

Park, J., and H. Otsuka. 1999. Optimal yield level of bilinear seismic isolation devices. *Earthquake Engng. Struct. Dyn.* 28:941–55.

Skinner, R. I., W. H. Robinson, and G. H. McVerry. 1993. *An introduction to seismic isolation.* Chichester, England: John Wiley & Sons Ltd.

Spencer, B. F. Jr., S. J. Dyke, M. K. Sain, and J. D. Carlson. 1997a. Phenomenological model of a magnetorheological damper. *J. Engrg. Mech., ASCE* 123(3):230–38.

Spencer, B. F. Jr., and M. K. Sain. 1997a. Controlling buildings: A new frontier in feedback. *IEEE Control Sys. Mag.* 17(6):19–35.

Spencer, B. F. Jr., J. D. Carlson, M. K. Sain, and G. Yang. 1997. On the current status of magnetorheological dampers: Seismic protection of full-scale structures. *Proc., Amer. Control Conf.* 458–462.

Spencer B.F. Jr., E. A. Johnson, and J.C. Ramallo. 1999. 'Smart' isolation for seismic control. *Proc., Pioneering Int. Symp. on Motion and Vib. Control in Mechatronics*, 169–74.

Symans, M. D. and S. W. Kelly. 1999. Fuzzy logic control of bridge structures using intelligent semi-active seismic isolation. *Earthquake Engrg. and Struct. Dyn.* 28:37–60.

Wen, Y. K. 1976. Method of random vibration of hysteretic systems. *J. Engng. Mech. Division, ASCE* 102(2):249–63.

Yoshida, K., S. Yoshida, and Y. Takeda. 1999. Semi-active control of base isolation using feedforward information of disturbance. *Proc., 2nd World Conf. on Struct. Control* 1:377–86.

8. KEYWORDS

seismic isolation, base isolation, smart damping, magnetorheological fluid dampers, MR dampers, structural control, semi-active control, smart base isolation

INFORMATION MANAGEMENT FOR URBAN EARTHQUAKE DISASTER MITIGATION

Hiroshi KAGAMI [1]

ABSTRACT

In this paper the outline of the research project of " Information Management for Urban Earthquake Disaster Mitigation" is presented. This project is planed as one of the 8 projects which are designated as principal project in the "Fundamental Research for the Mitigation of Urban Disasters by Near-field Earthquakes". At first, the role and importance of disaster information are discussed and the necessity of its systemization is mentioned. Secondary, problems to be treated are listed in the time and space domain and sub-themes in this project are indicated in order to study in details and to construct information management systems. Finally an outline of each sub-theme is summarized.

1. INTRODUCTION

Direct damage due to a near field earthquake immediately beneath the urban area is significant around the epicenter or the fault although the disaster zone may be confined. However, secondary damage such as earthquake fire spreading depends on official and private emergency responses. Therefore, immediately after an earthquake, it is necessary to collect damage information and appropriate emergency responses should be conducted according to the damage information. However, it is difficult to select an appropriate emergency response under poor and fragmentary damage information. There is the reason why the information management system is needed. The information management system can support apt judgment before and after the event. The earthquake disaster prevention and mitigation activities have to consist on time-series activities such as damage prevention, preparedness, emergency response, restoration, reconstruction and preparedness for the next event. In Japan, main effort has been devoted to the damage prevention but the Great Hanshin-Awaji Earthquake Disaster taught us its limitation.

2. RESEARCH PROJECT

Damage information plays an important role in the disaster management process, such as rescue, damage mitigation, restoration and reconstruction, after a near field earthquake immediately beneath an urban area. Information is exchanged between the disaster zone and responding organizations.

The purpose of this study is to develop information system including collection, analysis, notification and utilization of information. This research project was planned and started for 4 years project with 8 members including the author and 3 more members were added in the forth year of the project. These members are as follows:

[1] *Department of Urban and Environmental Engineering, Graduate School of Engineering, Hokkaido University, Sapporo, Japan. Email: kgm@eng.hokudai.ac.jp*

Principal investigator:

Hiroshi Kagami, Hokkaido University

Research members:

Naotsune Taga: Kyusyu University

Michio Miyano: Osaka City University

Fusanori Miura*: Yamaguchi University

Takashige Ishikawa*: Japan Women's University

Tamotsu Suzuki: Akita Prefectural University

Itsuki Nakabayashi: Tokyo Metropolitan University

Shigeyuki Okada: Hokkaido University

Yoshio Kumagai: Tsukuba University

Kazuyosi Ohnishi: Kobe University

Keishi Shiono*: Nagaoka Technical Collage

(*: members who joined from the fourth year)

At the beginning of this project, the following research scheme has been prepared. Firstly, the information about damage and emergency responses in the Great Hanshin-Awaji Earthquake Disaster is analyzed from the point of view of time series. Secondary, important damage aspects to be systemized are selected and lastly, the way of information management is proposed in each damage aspect.

3. SELECTION OF INFORMATION ITEMS TO BE SYSTEMIZED

In this project, we started to study information management problems with the common understanding of disaster aspects in time and space domain which is indicated in the general report of the Hanshin-Awaji Earthquake Disaster (Kagami, et al., 1999) and following sub-themes are selected.

(a) Emergency response and disaster information management: Naotsune Taga

(b) Information for victims in rebuilding lives: Michio Miyano

(c) Information for disaster weak: Fusanori Miura

(d) Communication system for disaster victims: Takashige Ishikawa

(e) Preventive information in community: Tamotsu Suzuki

(f) Information for urban community reconstruction: Itsuki Nakabayashi

(g) Damage information collected by municipal units: Shigeyuki Okada

(h) Fire information: Yoshio Kumagai

(i) Medical care information after earthquakes: Kazuyoshi Ohnishi

(j) Information of daily living disruption: Keishi shiono

(k) Information for urban reconstruction: Itsuki Nakabayashi

The coverage of these sub-themes are indicated into Figure 1. Horizontal axis corresponds to space domain from household, community, local government to nation. Vertical axis is time series of pre-event, earthquake occurrence, emergency response for direct damage, mitigation activities for secondary damage, and restoration and reconstruction period. Boxes roughly indicate their territory to be covered in time and space domain. Ellipses correspond to 3 new sub-themes added in the final year. As shown in this figure almost important items in time and space domain can be covered by each sub-theme.

Sub-theme (a) is fundamental survey for information management and covers total systems. From another point of view, problems of disaster information can be classified into two types from their standpoint. One is victim and the other is corresponding organization. Sub-themes of b) to f) are problems in victims and those of g) to k) are approached by the standpoint of corresponding

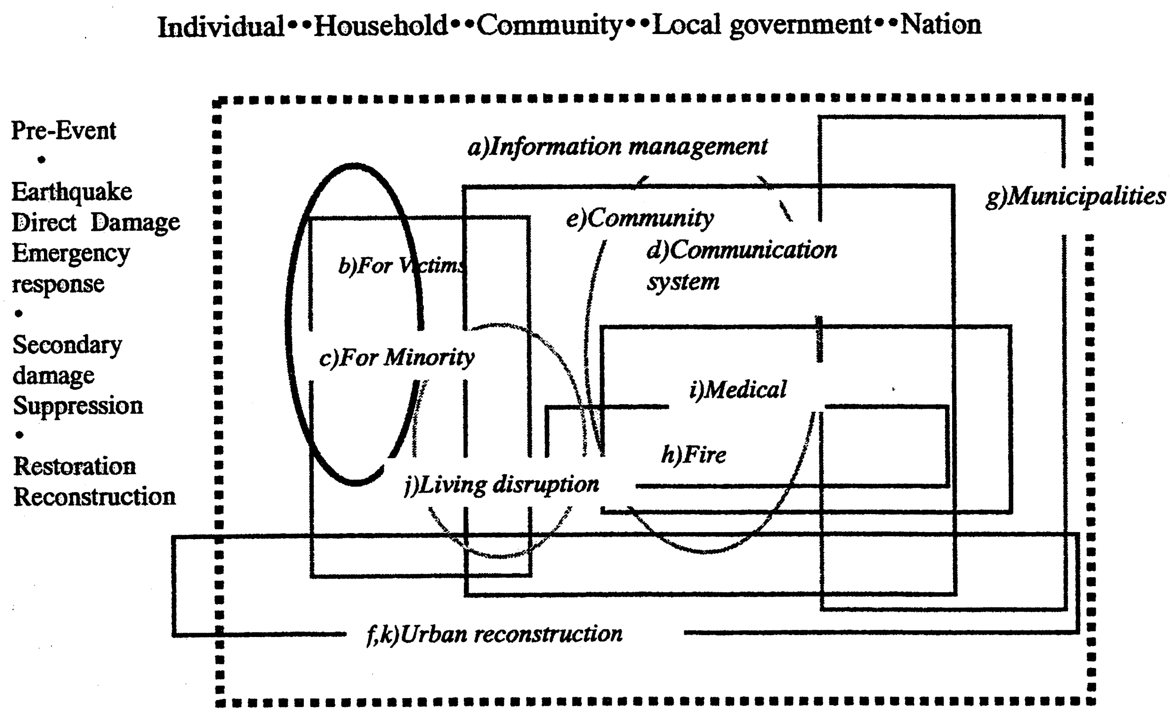

Figure 1. Coverage of each sub-theme in the time and space domain.

authorities. Sub-themes f) and k) will treat same problems of urban reconstruction but standpoints are different as residents and local government.

For each sub-theme the following procedures will be adopted. Figure 2 indicates the flow of construction for information management system. Finally the total system will be made composing these sub-models.

Re-arrangement of disaster information
(Past disasters including the Hanshin-Awaji Earthquake)

↓

Problems to be solved
Needs for information
Collection and transmission

↓

Indication of guideline
Proposal of prototype

Figure 2. Development for information management system for each sub-theme

4. OUTLINE OF EACH SUB-THEME

4.1 Emergency response and disaster information management (N. Taga)

In this study, recent disaster experiences about emergency response just after seismic disaster events have been summarized to apply to mitigation and prevention following successive damages and following matters are pointed out. The importance of emergency response is to make adequate preparedness for sudden happening and to prepare a systematic strategy for collecting necessary information for life saving activities. In case of saving dangerous lives, it is indispensable to promote the co-operation of administrative system with regional residents and for that purpose, it is also of importance to make a daily preparedness and ordinary training and practice in daily business. In order to systematically manage these system for emergency, the systematic information system will be desired and necessary item and articles for its information system are established to do effective function and its is illustrated that the disclosure of related information about regional safety and environment and joint ownership of disaster information with administration and residential people, play an importance.

4.2 Problems with rebuilding lives after the Hanshi-Awaji earthquake disaster (M. Miyano)

In this study, a survey using questionnaire on restration publick housing after the Great Hanshin-Awaji Earthquake Disaster to investigate some problems in the process of rebuilding lives after the earthquake for the people living in restoration public housing was conducted. Some damages in evacuees' lives were separated by the change of their space for living and the process of the lifeline restoration. On the day of the earthquake, the most serious problem was "safety", and it changed to "necessities of life" after one week, "life in future" at the sherters, and they demanded "administration support" when in restoration publick housing. In restoration public housing, the sufferers experienced "difficulties in making ends meet". With the lapse of time, this problem increased.

4.3 Information for disaster weak (N. Miura)

At the Great Hanshin-Awaji Earthquake, there is pointing out that the information transmission did not function enough, and the number of casualty increased. Especially, the damage to so-called disaster weak such as the senior citizen and the physically handicapped person, etc. was severe and it greatly took a long time to get information of the situation of them. From this point of view, a new system which is able to get information about the situation of the disaster weak in short time before the telephone crows is proposed in this study. The system is composed of three subsystems. First, the subsystem by which the system is started when earthquake is perceived, and measurement seismic intensity more than set value is observed. The second one is the subsystem which confirms the safety of the registrants all together. The third one is the system by which the second subsystem is told the registrant's state. The basic idea of the system is explained.

4.4 Communication system for disaster victims (T. Ishikawa)

This study deals with a proposal for new communication system for disaster victims. A case study of communication condition after the Great Hanshin-Awaji Earthquake has clarified that the information which a disaster victim needs is particular and ever-changing, and that there was no two-way system for exchanging information in that disaster. Although it was difficult for people to obtain disaster information after this earthquake, they directly informed others of what they needed to know. This gave us the idea of applying a daily postal service system to disaster communication. This is based on the proposal that people can obtain and send information through a postman when a disaster occurs. The realization and availability of this proposal is supported by the Ministry of Post and Telecommunications and local post offices in the stricken area.

4.5 Preventive information in community (T. Suzuki)

In this study some representative cases in which damage were evidently prevented or mitigated at the time of the Great Hanshin-Awaji Earthquake are examined. The cases are divided into five groups: those which show prior investment, preparation in advance, harmony with nature, the advantage of small scale and multiplex systems, and the solidarity of local society. These examples are then arranged along time and space axes and a cross-sectional view is taken. Finally, a view is taken toward developing social system for information management which will reduce damages of local society in future quakes. Evidences are presented that "soft" system of disaster prevention and damage control may easily be made multi-functional, whereas "hard" facilities tend to be mono-functional, and that the vivid solidarity of each local society, where the residents themselves will hold in common various information relevant to own community, can enhance their ability to survive both the initial damage and its aftermath.

4.6 Information for urban community reconstruction (I. Nakabayashi)

In this study, the direction of information systems for urban reconstruction planning and community-based rehabilitation, so called "Machizukuri" in Japanese, is proposed through the analyses of newspapers by machizukuri organizations and newspapers issued after the Hanshin-Awaji Earthquake. Machizukuri newsletters have played very important role as a local medium to promote the machizukuri project participated with residents.

4.7 Damage information collected by municipal units (S. Okada)

Collecting precisely and fast the relevant information in areas damaged due to earthquakes activates the optimum municipal activities such as emergency calls for municipality staff, orders for evacuation of the affected areas and planning for various restoration. This study discussed some factors controlling the collecting process of earthquake damage information in order to renew the municipal response system after earthquakes. As a result of analyzing a pile of damage reports by local governments in the 1993 Kushiro-Oki, the 1993 Hokkaido Nansei-Oki, and the 1994 Hokkaido Toho-Oki Earthquakes, the investigator found various factors governing the speed of collecting damage information; for example, ground motion severity represented by seismic intensity, the areal size of municipality characterized in terms of population, the limited number of available laborers for surveying damages, and lessons learned from the previous disaster experiences.

4.8 Fire information (Y. Kumagai)

In this theme, Dr. Kumagai dealt with the management of the fire information during an urban disaster due to a near field earthquake. At first, he analyzed the fire spreading and the fire fighting during the Great Hanshin-Awaji Earthquake Disaster in 1995. And then, based on the above analysis, he developed a computer simulation model which was named "The ***F***ire ***I***nformation ***Ma***nagement ***S***ystem : FIMaS". The effectiveness of the FIMaS was checked in Hyohgo-ku, Kobe City through the fire behaviors at the Great Hanshin-Awaji Earthquake Disaster. Also, some cases of simulations were conducted in Hyohgo-ku. Furthermore, the geographical information system : GIS was installed into the FIMaS. Necessary water sources in each district were estimated by the FIMaS and the fire fighting at a coming earthquake disaster were simulated in the Tokyo-Ward-Area.

4.9 Medical care information after earthquake (K. Ohnishi)

This research treats a medical information strategy, as it functions in a confused situation immediately after the Hanshin-Awaji Earthquake. Focusing on information on regional medical treatment in the event of disaster, an analysis of required medical treatment information was conducted in the study.

For this purpose after assembling the data concerning medical response in hospitals or clinics, not only acute case but chronic cases which include artificial dialysis patients behavior and/or search and rescue activities in community on the event, the discussion was deepened based on the results of the questionnaire research answered by residents and/or community carpenters in the stricken areas of Kobe-Hanshin. Following issues are needed in a medical treatment system at a seismic disaster for stricken residents through this study.

4.10 Information of daily living disruption (K. Shiono)

Two kinds of numerical sources, with and without cumulative nature, for evaluating daily living disruption following earthquakes were developed and utilized in a comparative study among seven municipal areas affected in the 1995 Hanshin-Awaji Earthquake. While household scores were determined based on the household-by-household questionnaires, regional scores were given as the average of household scores. Relationship between the regional scores and evacuation rates were examined, and remarkable correlation was found. It was proved that the regional scores of dairy living disruption are a useful independent variable to the estimation of short-term shelter need.

4.11 Information for urban reconstruction (I. Nakbayashi)

This study deals with information problems in reconstruction period and revealed that in the process of urban reconstruction planning in Kobe-city, the survey of damage assessment in a week after the earthquake was important for the nomination of urban reconstruction planning areas. In the community rehabilitation projects, newsletters issued by Mchizukuri organization were also important to reach agreements among residents and to progress the projects. Information system must be built synthetically from urban reconstruction to livelihood recovery of each resident.

5. CONCLUDING REMARKS

This project have been carried out for four years with 11 members who have been devoted in various field. In case of huge near field earthquake, related disaster aspects are existing very wide areas in time and space domain as shown in the Hanshin-Awaji Earthquake Disaster. Our project has been started based on a common understanding that these damage aspect should be considered as information problems in order to find out appropriate countermeasures for mitigation of damages. Eleven sub-themes have been chosen and carried out independently but we had many discussions each other. We prepared three steps for developing new information systems to these sub-themes. Some themes can be reached to proposal of new system but some ones remained to the second step of identification of system demand base on information needs. This caused by the differences in difficulty and coverage of aspects among sub-themes. We believe that further systemization will be done based on our results.

6. KEYWORDS

Information management, Near field earthquake, Earthquake disaster mitigation, The Grate Hanshin-Awaji Earthquake Disaster, Indirect damage, Emergency response, Reconstruction period, Damage information, Disaster victims

7. REFERENCES

Kagami, Hiroshi, Masatake Naganoh, and Yoshio Kumagai, eds. 1999. *Function and structure of urban safety system against earthquake disaster: report on the Hanshin-Awaji earthquake disaster.* General Issues Vol. 3, 605pp. (In Japanese with English abstract and captions).

PROVIDING REAL-TIME AND NEAR REAL-TIME EARTHQUAKE GROUND MOTION DATA ASSOCIATED WITH DAMAGING URBAN EARTHQUAKES

James F. DAVIS[1]

ABSTRACT

Advances in earthquake monitoring instrumentation and communications during this last decade are making it feasible to provide ground motion data to users in real and near real time. Established in 1997, TriNet is a consortium between the operators of the California Strong Motion Instrumentation Program (CSMIP) of the Division of Mines and Geology (CDMG) and the Southern California Seismic Network (SCSN) of the USGS and Caltech to provide ground motion data from southern California to users in the emergency response, engineering and seismological communities. Between 1997 and 2001 TriNet will instrument 150 broadband and 450 strong motion stations in urban southern California. The TriNet consortium has developed ShakeMap™ software that provides an electronic spatial display of a variety of observed ground motion parameters within a few minutes after significant earthquakes. The ShakeMap is periodically updated with additional processed data during the following few hours after the earthquakes. TriNet successfully provided ShakeMap displays on the Internet following the October 1999 M7.1 Hector Mine earthquake. TriNet operators in southern California are joining with the USGS (Menlo Park) UC Berkeley (Seismological Lab) and CDMG to establish the California Integrated Seismic Network (CISN). CISN will provide ShakeMap images seamlessly for any California events. CISN seeks to establish a parity in the number of recording stations in northern and southern California Institutions collaborating in CISN are coordinating in the provision of archive data to engineering and seismology investigators. CDMG is exploring the uses of ShakeMap ground motion patterns to both the emergency responders and the engineering communities in the period shortly after events and in the longer term.

1. BENEFITS TO ENGINEERING OF STRONG MOTION EARTHQUAKE RECORDS

The benefit of regional observation of variations in ground motion patterns associated with damaging earthquakes is well established. Ground shaking produced by the 1994 M6.7 Northridge earthquake was relatively well recorded by the California Strong Motion Instrumentation Program (SMIP) stations operated by the California Division of Mines and Geology (CDMG). SMIP records documented variations in the ratio of vertical to horizontal accelerations locally in some near-field areas and greater than expected accelerations in portions of the San Fernando Valley and in Santa Monica. Especially high free field values were recorded at the Cedar Hill Nursery in Tarzana. Interpretation of the data has increased understanding of the influences of near-field conditions topography basin configuration and special amplification on observed ground motion. However, strong motion instruments were not located in many areas that suffered the most severe damage. The Northridge earthquake proved the need for a much denser distribution of "reference" recording stations in urban California to improve the correlation of input ground motion and observed structural performances in future earthquakes. The CSMIP Advisory Committee has recommended at least one station be located in every zip code.

[1] *California State Geologist, Department of Conservation, Division of Mines and Geology*

2. DEVELOPMENT OF TRINET

The USGS Pasadena and Caltech operate the Southern California Seismic Network (SCSN) which at the time of the Northridge earthquake consisted of 20 digital broadband stations and over two hundred weak motion recorders. The short period records of the Northridge main shock and large aftershocks were clipped off scale and the large volumes of data saturated computer processing capacity. The large volume of data also challenged CDMG because, at the time of the Northridge earthquake, most of the CSMIP observations were analog records on film.

During its oversight of the response to the Northridge earthquake, the Governors Office of Emergency Services (OES) concluded that ground motion information was useful in the preliminary prioritization of areas where assistance would be most needed. Such a use of ground motion information puts a premium on its early availability. Furthermore, OES also used the preliminary ground motion data as input to its damage loss estimation model that was being developed at the time. OES had been planning to create scenarios of future earthquake damage to be used in preparedness exercises. OES relied upon the calculated damage estimate obtained by modeling in its request for disaster assistance from the Federal Emergency Management Agency (FEMA). The request was made the day of the earthquake without waiting for the on-the-ground survey of damage that otherwise would be necessary. OES also used the ground motion pattern to assist in the preliminary identification of areas where property owners would be eligible for federal assistance.

Because of its interest in using ground motion information as a tool in managing its response for future earthquakes, OES encouraged CDMG and Caltech to apply for a FEMA mitigation grant to enhance monitoring capability in southern California. CDMG and Caltech submitted a joint proposal to establish TriNet with FEMA funding that would augment the USGS post-Northridge investment in upgrading monitoring. The TriNet mission is to mitigate losses from future southern California earthquake by digitally recording, transmitting and processing real-time and near-real-time ground motion data for use in emergency response development of resources and in evaluation of safety of occupancy of damaged structures. Subsequently, the ground motion data will be used in engineering research that can lead to building code improvements.

3. TRINET PRODUCTS

The TriNet partnership will install 150 broadband and 450 strong motion stations in southern California during the FEMA mitigation grant period (1997-2001). Records from these stations are being archived and are available to be employed in seismological and engineering research. TriNet is also broadcasting an electronic display of ground motion patterns as "ShakeMap" ™ at its website using the data processed during the first few minutes after significant earthquakes. The display is regularly updated with subsequently processed data during a period of one to several hours following the event. TriNet patterns have developed the software that is necessary to create the ShakeMap display based upon contouring any of a number of ground motion parameters through extrapolation between observations. There will also be a capability for rapid distribution of wave data between TriNet institutions to assure redundancy in data processing capabilities.

4. PLANS FOR THE CALIFORNIA INTEGRATED SEISMIC NETWORK (CISN)

The success of TriNet institutions in working together has stimulated an effort to increase the number of urban monitoring stations in northern California and to integrate rapid distribution of ground motion information throughout the state. Northern California collaborators including CDMG, CSMIP, UC Berkeley Seismological Laboratory and USGS, Menlo Park are working towards this end together with the southern California TriNet institutions. The time frame of full implementation can be reduced by additional funding to increase station density and data transmission and broadcasting capabilities in northern California and to supplement operational costs in southern California after the FEMA grand completion in 2001.

5. RECENT EXPERIENCE

During 1999, $M \geq 4.5$ earthquakes have provided opportunities to test and perfect rapid ShakeMap analysis and distribution. The October 16, 1999 $M \sim 7.1$ Hector Mine earthquake is the first important sized "internet earthquake".

6. CONCLUSIONS

The success of TriNet in southern California is stimulating efforts to create a seamless state-wide monitoring and rapid data distribution capability which OES is advocating as an important emergency response tool. The Advanced National Seismic System (ANSS) proposed by the USGS suggest that TriNet can be the model for revitalized regional monitoring throughout the United States. ShakeMap capabilities are desired by emergency responders in other important areas of earthquake risk in the country. If this national capability is achieved the improved capabilities for emergency response and engineering design requirements in building codes will contribute significantly to lower levels of future earthquake loss.

7. REFERENCES

Hauksson, E., L. M. Jones, A. Shakal. 2000. *TriNet international handbook of earthquake engineering seismology.* International Association of Seismology and Physics of the Earth's Interior.

Seismic Safety Commission Staff. 1996.

Seismic Safety Commission, State of California. *Northridge earthquake: Turning loss to gain.*

U.S. Geological Survey, Southern California Earthquake Center and California Division of Mines and Geology Scientists 2000. *Preliminary report on the October 16 M 7.1 Hector mine, California earthquake.* Seismological Research Letters. November.

8. KEY WORDS

TriNet, strong motion, near field, ground motion, emergency management, building codes.

UTILIZATION OF REAL-TIME EARTHQUAKE INFORMATION IN RESPONDING TO AN URBAN EARTHQUAKE IN CALIFORNIA

Richard K. EISNER, FAIA[1]

ABSTRACT

Assessment of the magnitude, location, and extent of damage and casualties is essential for effective emergency response. In recent earthquake in the United Sates and Japan, delays in assessing and comprehending the magnitude and extent of damage delayed state and national response and masked areas of extensive damage. Delays are a result of government organizational issues, the catastrophic nature of urban earthquakes, communication difficulties and the difficulty in collecting damage data immediately after a large earthquake. Recent development of dense seismic networks in seismically active urban regions, real-time network monitoring, combined with mapping and loss modeling technology, now provide emergency managers with the ability to rapidly assess the extent and location of damage within minutes of an earthquake, and initiate response.

1. DILEMMAS FOR EMERGENCY MANAGEMENT AFTER EARTHQUAKE

In the aftermath of large urban earthquakes it is difficult for emergency managers and responders to assess the overall extent of damage, identify areas of extensive damage, and determine the external resources that will be required to support local response. Rapid delivery of external aid is critical in these events as they can rapidly overwhelm local first responders. Frequently, local government officials are themselves victims, or are constrained by communications failures or a shortage of staff. In the Loma Prieta earthquake (1989) the extensive damage in the cities of Santa Cruz and Watsonville was not known for hours after the event, severely hampering initial response and delaying delivery of state assistance. After the Northridge earthquake (1994), the extent of damage in the San Fernando Valley was not know for several hours until filed reconnaissance could be completed. Similarly, damage in the city of Santa Monica was unreported and therefore unknown for several hours, delaying outside assistance. After the Great Hanshin-Awaji earthquake (1995), communication disruptions and difficulties in assessing damage delayed national response for several hours.

2. USE OF SEISMIC NETWORK DATA FOR EMERGENCY RESPONSE

Two initiates begun prior to the Northridge earthquake now offer state and regional emergency managers the tools necessary to make time critical decisions without being dependent of direct communication with local governments, and prior to receipt of "ground-truth" assessments of actual damage from the impacted area. In the early 1990s, the United States Geological Survey (USGS) in Menlo Park, the University of California Berkeley Seismological Laboratory and the California

[1] *Regional Administrator, Governor's Office of Emergency Services, State of California, USA,*
E-mail: rich_eisner@oes.ca.gov
[2] *EQE International, Irvine, California*

Institute of Technology (CalTech) in Pasadena, began providing near real-time magnitude and epicenter date via pagers to emergency managers in California. This information was critical to state emergency managers in confirming the location and potential for damage and loss immediately after the Northridge earthquake (1994) as it was several hours before daylight arrived and detailed reports of the extent of damage were available. The Northridge earthquake also provided the first test of both 'real-time seismology' and the evolving technology of computer modeling of earthquake losses. Based on the magnitude and epicenter data, a private engineering consulting firm[2], provided the Governor's Office of Emergency Services with both maps of the spatial distribution of damage and initial estimates of damage and losses. While these estimates were inexact, these computer-based estimates of damage were used by the state and federal governments as the official Initial Damage Estimate (IDE) for the Northridge earthquake and provided the basis for federal disaster assistance.

3. DEVELOPMENT OF HAZUS LOSS ESTIMATING TECHNOLOGY

In 1993, the Federal Emergency Management Agency (FEMA) initiated the development of a standardized methodology for estimating earthquake damage. The methodology evolved into a software program, *Hazards United States* (HAZUS™)[3] that is capable of providing estimates of damage, casualties, displaced persons, volume of debris and economic losses based on input of either magnitude and location of an earthquake or the input of maps of ground shaking (PGA, PGV). HAZUS99™ is capable of automatically inputting the magnitude and location data from the combined USGS/CalTech/UC Berkeley seismic networks, and automatically generating an initial estimate of damage and losses. This tool, incorporating geologic and building inventory information, will provide regional and state officials with an overall assessment of earthquake events within minutes of the quake, enabling resource needs assessments, acquisition and staging of resources and personnel, and an expedited response.

4. THE ROLE OF EMERGENCY MANAGEMENT AGENCIES

The roles of emergency response agencies vary with their location within the government hierarchy. Local governments (cities and counties) provide direct first response while state and federal agencies play a secondary role of providing resources to local governments. Table 1, below describes the varying roles of each level of government and the utility of using real-time seismic date and modeling as a decision support tool.

Data availability and quality will vary with time after an urban earthquake. Within minutes of large earthquake, location and magnitude data will be available from the Redi-Cube[4] pagers and displays

[3] HAZUS™, National Institute of Building Sciences, 1090 Vermont Avenue, NW, Washington, DC 20005

Table 1: Roles of Emergency Management Agencies

Level of Government	Primary Role	Primary Functions	Data Needs
• City/Municipal	• First Responders • Assessing and Reporting	• Life Saving, Fire Fighting, Search and Rescue, Care and Shelter	• Pattern of Damage Within Jurisdiction, • Site Specific Data
• County/ • Operational Area	• Assessing and Reporting • Coordination Among Cities • First Response to Rural areas	• Brokering Resources Within Operational Area • Coordinating OpArea Resources	• Pattern of Damage Within OpArea, • Resource Gaps
• State Region	• Assessing Overall Situation • Coordination Within Region • Coordination of State Response • Identification of Need for Federal Resources	• Brokering Resources Within Region • Coordinating Inter-regional Resources	• Regional Pattern of Damage • Estimates of Damage and Loss • Overall Economic Impact • Estimates of Restoration
• Federal	• Provide Resources Requested by State	• Coordinating Federal Agency Resources	• Overall Damage and Loss • Economic Loss

at state and local emergency management agencies. The earthquake would have already initiated local response. State emergency managers will initiate loss estimates using HAZUS™ with the Redi-Cube data. These initial loss estimates will be necessarily constrained by data available. As additional data becomes available, more refined loss estimates will be processed as described in Table 2 below.

5. CONCLUSIONS

It is recognized that ShakeMap™ depictions of ground motions, as well as loss estimates based on HAZUS™, are only approximations of actual events. Loss estimation models are limited by the detail of geology and quality of building inventory data they contain, how they interpolate between instrument data points, assumptions about soil-structure interaction and assumptions about the

[4] *Data provided by the UC Berkeley, CalTech and USGS networks in California*
[5] *Currently only available from TriNet for Southern California*

fragility of buildings. They will, however, provide a critical "quick picture" of an evolving event and enable emergency manage agencies to initiate response and support operations without having to wait for detailed assessments and requests for assistance after an earthquake.

6. KEY WORDS

HAZUS™, TriNet, ShakeMap™, Emergency Management, Loss Estimation

Table 2: Refinement of HAZUS Loss Estimates

Time Frame	**Data Available**	**Output**
0 to 3 Minutes	• Magnitude and Epicenter • No Assigned Fault	General Display of PGA and PGV using geology database and attenuation models
3 to 10 Minutes	• Magnitude and Epicenter • Initial ShakeMap™ [5]	Maps of Instrument Data of Shaking and "Calibrated" Map
10+ Minutes	• Assigned Fault • Refined ShakeMap™	Initiation of Full Loss Estimation Using ShakeMap™ in lieu of Modeled Ground Shaking

DISASTER MANAGEMENT FUNCTIONS FOR TRANSPORTATION AND TELECOMMUNICATION SYSTEMS

Hiroyuki KAMEDA[1] and Yasunori IIDA[2]

ABSTRACT

The project is aimed at development of engineering and socio-economic methodologies for realizing appropriate level of disaster management functions of transportation and telecommunication systems. Emphasis is placed on realizing network redundancy and strategic decisions for seismic strengthening of system components, operation of traffic control systems and information management under disaster emergency. Socio-economic approach is incorporated regarding policy making as to investment in disaster mitigation for transportation and telecommunication systems under near-field urban earthquakes as "low frequency-high impact disasters".

1. PROJECT OVERVIEW

The project is aimed at development of engineering and socio-economic methodologies for realizing appropriate level of disaster management functions of transportation and telecommunication systems under earthquake emergency. For this purpose, a multi-disciplinary research team comprising experts in lifeline earthquake engineering, transportation systems planning, and social system analysis is working in the development of methodologies through reconnaissance of actual disaster, network analysis, simulation of disaster processes, development of GIS based information management systems, and econometric analysis. General framework of the project is illustrated in Figure 1.

The roster of the team is as follows:

Principal Investigators:

Hiroyuki Kameda, Disaster Prevention Res. Inst., Kyoto Univ. (1996–98)
Yasunori Iida, Dept. of Civil Eng., Kyoto Univ. (1999)

Member Researchers:

Yasunori Iida, Dept. of Civil Eng., Kyoto Univ. (1996–98)
Shiro Takada, Faculty of Eng., Kobe Univ.
Eiji Kawakami, Dept. of Civil Eng., Saitama Univ.
Kiyoshi Kobayashi, Dept. of Civil Eng., Kyoto Univ.
Nobuoto Nojima, Dept. of Civil Eng., Gifu Univ.
Hiroshi Wakabayashi, Faculty of Urban Science, Meijo Univ.
Takanobu Suzuki, Dept. of Civil Eng., Toyo Univ. (1997–)
Hitoshi Ieda, Dept. of Civil Eng., Univ. of Tokyo (1999)
Satoshi Tanaka, Disaster Prevention Research Inst., Kyoto University (1999–)

[1] *Disaster Prevention Research Institute, Kyoto University, Kyoto, Japan*
[2] *Department of Civil Engineering, Kyoto University*

Collaborating Researchers:

Hiroyuki Kameda, Disaster Prevention Research Inst., Kyoto Univ. (1999–)

Eizo Hideshima, Dept. of Architecture and Civil Eng., Nagoya Institute of Technology

Fumitaka Kurauchi, Dept. of Civil Eng., Kyoto Univ.

Kakuya Matsushima, Dept. of Civil Eng., Kyoto Univ.

Hiroyuki Kameda was appointed to the Program PI for the US-Japan Cooperative Research for Urban Earthquke Disaster Mitigation, which began in fiscal year 1999. Because of rules of the funding mechanism of Monbusho, the Japan side sponsor, the PI for this project for 1999 was replaced by Yasunori Iida.

2. RESEARCH TOPICS

Following research topics are studied. The titles in parentheses show the output from the activities, which are presented in the following pages.

(1) Effects of Transportation System Loss on Urban Life Functions:

Using a questionnaire survey on the Great Hanshin-Awaji Earthquake Disaster, effects of the quake on the daily life of the citizens living in the area are studied. Issues of transportation are compared with those of other lifeline disruptions. (Nojima and Kameda)

(2) Networks Reliability of Transportation Systems under Earthquake Emergency

Theoretical background for development of redundant networks is studied as a major tool for realizing transportation systems with high disaster manageability. Its effectiveness is tested with case studies for various urban regions. (Kawakami/ Wakabayashi/ Nojima and Sugito)

(3) Method for developing the seismic fragility function

Methodologies for developing the seismic fragility function that takes both physical and functional aspects into account are proposed. (Tanaka and Kameda)

(4) Analysis on the Street-Blockade

Street-blockades in residential regions are investigated and the methodology to evaluate the likeliness of street-blockade, the dangerousness of particular region, and the effect of various countermeasures. (Ieda)

(5) Traffic Management and Control under Disaster Emergency

Methodologies for traffic management and control are studied under the specific conditions of disaster emergency, including traffic demand for emergency operation and capacity of damaged networks. (Iida and Kurauchi)

(6) Disaster Management Functions of Telecommunication Systems and Their Reliability Assurance

Recovery process of telecommunication systems in the Great Hanshin-Awaji Earthquake is examined considering cases of NTT, PC communication and disaster communication networks.

On this basis, hardware as well as software types of earthquake countermeasures are studied. (Suzuki/ Takada, Hassani and Kitada)

(7) Econometric Analysis of Investment for Disaster Mitigation

On the basis of socio-economic discussion on disaster loss and safety assurance, a theoretical basis will be developed for economic valuation of risks in social systems and social willingness-to-pay for disaster mitigation measures. (Kobayashi and Matsushima)

3. DEVELOPMENT OF A SUBJECT CHART

Under the multi-disciplinary framework of this project, an exhaustive list of keywords related to the functional reliability of transportation and telecommunication systems were developed and reviewed by the all project members. They have been arranged in a form of block chart to facilitate understanding relationship between the general framework and individual subjects. Its results are shown in Figure 2.

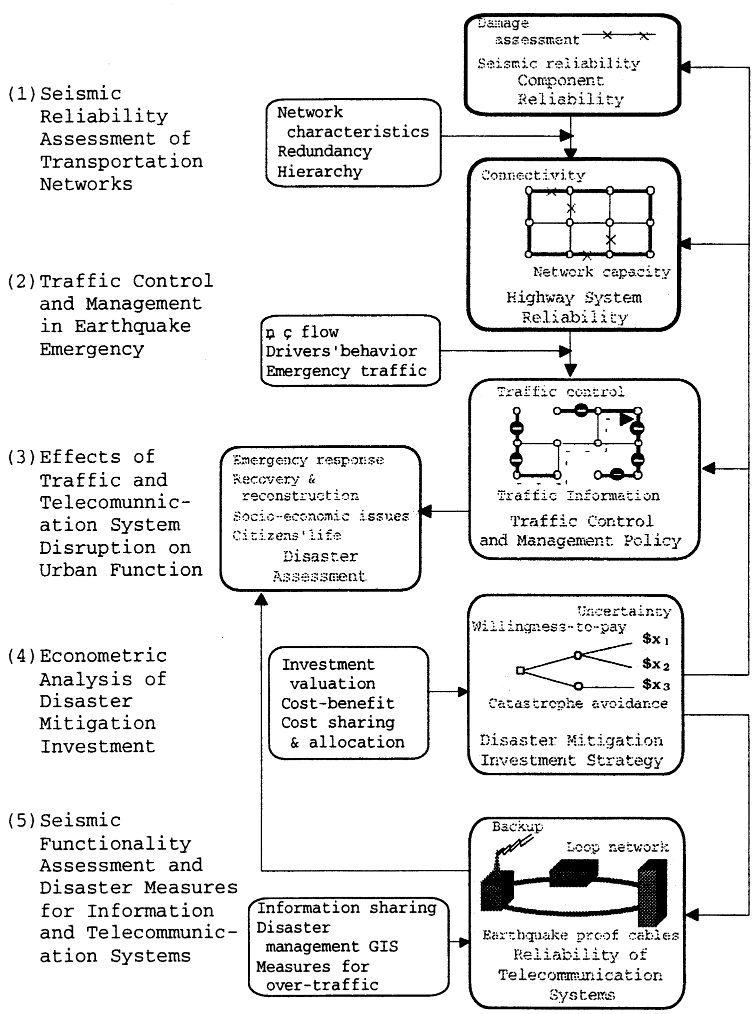

Fig. 1. Research Framework for Disaster Management Functions for Transportation and Telecommunications Systems

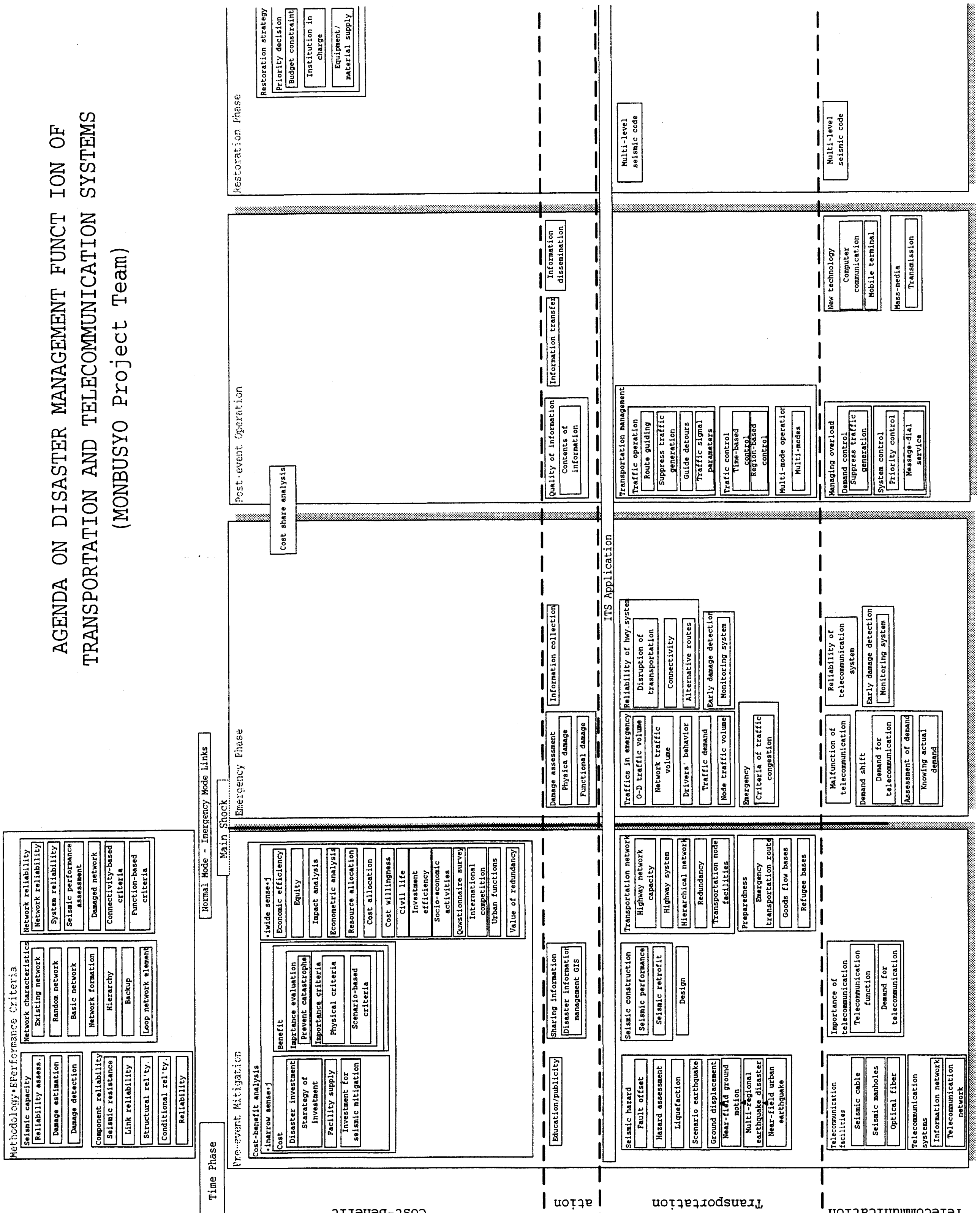

Fig. 2 Block Chart of Key Words

INVENTORY MANAGEMENT IN AN URBAN AREA: THE UC BERKELEY EXPERIENCE

Mary C. COMERIO*

ABSTRACT

The Disaster Resistant Universities Initiative is intended to motivate and enable the nation's largest research universities to reduce and manage their vulnerability to hazards in their locals. Not only are universities unique organizations that serve their communities, states, and nation, but the federal government has an investment in them—annually, federal agencies fund about $15 billion in university research. The Federal Emergency Management Agency (FEMA) has begun a two-part program to support universities' attempts to reduce their potential losses in foreseeable disasters. At U. C. Berkeley, we are developing and implementing prototype loss estimation methods and strategic risk management plans that other universities can use in their own efforts. In Washington D. C. FEMA is working with Congressional staff and a coalition of other universities to establish new funding over the next ten years. The research component of the Disaster Resistant Universities (DRU) project quantifies the losses and economic consequences of disasters on major research universities. Faculty from Architecture, Structural Engineering, and Economics, together with professional engineering and economic consultants, have developed a loss estimation model specific to campus settings in which losses are measured based on six factors. These include soil conditions, infrastructure, structural and nonstructural building conditions, space use and number of occupants. Using the capital loss projections with data on capital flows, the team has estimated the impact of campus losses in three earthquake scenarios. In addition to traditional economic modeling, the methodology includes a specific component for assessing the impacts on significant research units and on human capital. This paper will describe the campus loss model and its results.

INTRODUCTION

One of the most significant developments in earthquake loss estimation is the comprehensive HAZUS software package, which was funded by the Federal Emergency Management Agency (FEMA), and has been tested in numerous cities and regions. HAZUS is one of the best tools available for estimating losses at the regional level, but, like all standardized tools, it does not meet the needs of many specific applications. Universities, for example, are unique and specialized in terms of their physical facilities, which serve both research and teaching, and in terms of their economic function within a community. Universities are also self-contained communities with housing facilities, food

**Mary C. Comerio, Professor and Vice Chair, Department of Architecture, U. C. Berkeley*

services, small businesses (from retail stores to printing presses), hospitals, etc. Universities frequently have too many buildings to conduct complete building by building assessments of hazards and potential losses. Yet a campus is small enough to take into account how the loss of specific portions of individual buildings will affect the ability of the University to operate.

The University of California, Berkeley is a worldwide leader among universities in research, education, and public service. The central campus houses 40,000 students, faculty, and staff in more than 100 academic departments and organized research units. The central campus has 114 buildings on 177 acres, with about 5 million net square feet of classrooms, libraries, offices, research laboratories and other specialized facilities. In the 1998 fiscal year, the campus operating budget was approximately $998 million and sponsored research awards totaled $362 million (of which, more than two thirds comes from federal agencies). Overall, the University's Risk Management Office has estimated the insured value of the campus at $4.7 billion (compared with a total replacement value for buildings of approximately $8.8 billion).

ESTIMATING LOSSES IN THREE EARTHQUAKE SCENARIOS

The research for the Disaster Resistant Universities Initiative, described in this paper, creates a specialized method of evaluating the extent of potential losses and the subsequent economic impact of those losses on the region and on the nation. Our research builds on the 1997 structural survey of all university buildings. In this survey, structural conditions were evaluated in terms of the ten-point performance index in the Structural Engineers Association of California, Vision 2000 methodology for performance based design (Hamburger et al. 1995; SEAOC, 1996). In the 1997 Preliminary Seismic Evaluation (PSE), the engineers found that 27 percent of the useable space on campus was in "poor" or "very poor" structural condition (equivalent to a 1-3 Vision 2000 rating).

Each building was evaluated in terms of its performance in three earthquake scenarios: an Occasional, Rare, and Very Rare event. The scenarios are defined as follows:

> A Level 1 Occasional Earthquake was defined as one with ground motion of moderate severity that is likely to occur as a result of an earthquake on any of the active faults in the Bay area (50 percent probability of being exceeded in 50 years, or a 72-year return period).
>
> A Level 2 Rare Earthquake was defined as a severe event (magnitude 7.0) expected to occur on the nearby northern segment of the Hayward Fault (10 percent probability of being exceeded in a 50-year period or a 475 year return period).
>
> A Level 3 Very Rare Earthquake was defined as one with extremely severe ground motion—magnitude of 7.25 on the Hayward Fault (5 percent probability of being exceeded in a 50-year period or a 975-year return period).

In the current research project, we worked with the same team of structural engineers (Degenkolb, Forell-Elsesser, and Rutherford and Chekene), coordinating with Professor Vitelmo

Bertero, to evaluate the non-structural building conditions and to enhance the previous structural assessments of campus building with additional analysis. We also worked with Geomatrix Consultants, geotechnical engineers, to identify the site soil classifications, to evaluate previously developed earthquake ground motion response spectra, and to select acceleration time histories for use in this study.

BUILDING CONDITIONS

The building by building data collected in the 1997 structural survey of buildings became the basis for the expanded loss estimation model. We improved our basic understanding of the structural performance of ninety larger campus buildings, using a preliminary pushover analysis of each building (or building sub-area if multiple systems were present).

To describe the performance of the non-structural components in the major use areas of campus building, our approach was to evaluate six major building components. These included the cladding and glazing on the building exterior; the architectural finishes; the Mechanical, Electrical, and Plumbing (MEP) systems; the contents; and the potential for water damage to the building interior. These components were evaluated in each of the major use areas within each campus building: classrooms, laboratories, offices, libraries, and special/other (e.g. recreation and/or performance spaces), as well as residential buildings, and parking structures.

For each building, a list of space-use classifications was made from a campus facilities database, and this list was used to create an evaluation form listing the building components. The consulting engineers then rated the replacement value of each component as High, Medium, or Low and rated the non-structural performance of the component using the one to ten performance index. For example, the cladding and glazing in each building were rated as High, Medium, or Low as a measure of their replacement cost value and given a numerical performance index for each of the three earthquake scenarios. Similarly, architectural finishes, MEP, contents, and potential water damage were rated for classrooms, laboratories, and other sub-areas in each building.

For example, one five-story concrete shear wall building, built in 1950, 57 percent of the assignable space is in laboratories, 32 percent in offices, 4 percent in classrooms, and the remainder is in special/other uses, in this case primarily storage. In the structural analysis, it is rated 5, 4, 3 in the Level 1, 2, and 3 earthquakes, respectively. By the rating system used in the 1997 PSE, this building is considered "fair." As such, the building is not one of the buildings that would have warranted further analysis. Adding performance ratings for the non-structural components allowed us to make a more refined estimate of damage and losses. In the non-structural evaluation, for example, cladding was rated as Low (not costly to replace), with performance ratings of 7, 5, 4. Glazing was rated as Medium, with performance ratings also at 7, 5, 4. Each of the spaces was reviewed in terms of architectural finishes, MEP, contents, and potential water damage. In the laboratory areas, only contents were rated High, because of the presence of highly specialized and expensive equipment. In the lab areas, the non-structural ratings were:

System	Level 1	Level 2	Level 3
Architectural Finishes	7	5	4
MEP	6	4	3
Contents	7	5	4
Potential Water Damage	6	4	2

The numerical ratings were based on standardized definitions for each component, from Complete Damage at 1, to No Damage at 10, with descriptive examples for each rating value. Definitions and application rules were developed for each category. For example, MEP at 8, 6, 4 was used as a standard rating for modern buildings with well-braced pipes and lights. A rating of 7, 5, 3 was used for modern buildings with poorly braced pipes and lights, and 6, 4, 3 was used for older buildings with poorly braced pipes and lights. A rating of 2 was used only if a particular vulnerability was observed. From these ratings, it is clear that the greatest vulnerability in the laboratories is damage to the mechanical, electrical, and plumbing systems, as well as the potential for water damage and loss of contents. This is, in fact, a typical condition in most spaces in most buildings.

The engineering team also estimated the time needed for repairs in each building in each scenario. The lab building described above was estimated to need six months for repairs in the occasional scenario, and twenty-four months in either the rare or very rare scenario. This "downtime" estimate took into account that certain kinds of repairs could be done with campus staff, in a few weeks or months, with some areas of the building open for use. However, with more severe damage, in which the building's structural condition would require an engineering evaluation and repairs would require drawings, peer reviews, etc., repair times might take months or longer. Under such conditions, it is likely that all or part of a building would be completely unusable until work was complete. The downtime estimates and the building component performance evaluations were the key data sets to be used in the loss estimation model.

TRANSLATING BUILDING PERFORMANCE RATINGS TO LOSS CURVES

As the building data was assembled, the engineering team translated the structural and non-structural ratings into loss curves. A great deal of research already completed (ATC-13, HAZUS, etc.) equates the damage observed in previous earthquakes with a percentage of structural loss. In the HAZUS methodology, slight damage is set as 2 percent of complete, moderate damage is 10 percent of complete, and extensive damage is 50 percent of complete, but the damage cost for each building type is ultimately calculated using a probabilistic distribution of damage within that building type.

Similarly, in this research, we assigned a percent structural damage to each of the ten point ratings, and then used a probabilistic method for distribution within each rating. Thus, a building assigned a structural rating of 5 (with 30 percent damage) in a particular earthquake scenario has a 21 percent probability of actually sustaining 30 percent structural damage, a 16 percent probability of 50 percent damage (rating 4), an 18 percent probability of 10 percent damage (rating 6), etc.

Separate loss curves were developed for the non-structural building components (Architectural Finish, MEP, Contents, Cladding, and Glazing), based on data available from recent earthquakes and on the judgment of the engineering team. In cases where the team assigned percentage losses to only even rating numbers, regressions were run on ratings against percentage using several different functional forms. No probabilistic distributions were used for the non-structural building components because there was not sufficient data to justify that level of mathematical sophistication.

The percent losses for Potential Water Damage were created as an addition to losses in Contents and Architectural Finishes. However, this is more complex than a simple add-on. The degree to which water damage adds to the cost of losses depends on the amount of other damage. If losses to structure, architectural finishes, or contents in a particular building in a particular occupancy were severe, then the damage percentages and associated costs would be at or near 100 percent of replacement. In this case, water damage rated at 2 (severe) should not take losses over 100%. In contrast, if structural, architectural finishes, and contents damage were moderate (> 4), and the water damage was rated 2 (severe), the percent loss added to architectural finishes and contents would be higher to reflect the added increment in repair costs.

REPLACEMENT COST ESTIMATES

We conducted a detailed review of new construction and seismic retrofit expenditures on projects at U. C. Berkeley during the last ten years, and of construction costs for numerous comparable university buildings around California. The replacement cost spreadsheets were developed for the seven main building types in the study—classroom, laboratory, office, library, special use, residential, or parking. The replacement costs were based on Type I and II mid-rise campus buildings, with costs expressed for low, medium and high quality of construction in current dollars in California, reflecting the cost of construction at any campus in California. From the base costs, a group of multipliers were developed to reflect adjustments needed for locally specific work. These included:

- The cost of work on the Berkeley campus.
- The anticipated cost of work under the 1997 UBC for near-field seismic construction.
- The additional cost for repairing components over the cost of the same components in new construction.
- The university related soft costs for design and management.

In addition, multipliers were added to accommodate unique structural or building components that might be present, such as high rise buildings, historic buildings, super complex buildings, or hospitals. A deduction multiplier was used for small wood frame buildings.

For each building type the building costs were organized into the same categories as the building sub-components so that each cost component could be multiplied by the percent loss of the component in each sub-area. In general, the loss estimate is characterized as a percentage loss of each building component, based on replacement cost values for the building type. It is assumed that even a building used predominantly as a library will have some offices or classrooms in it. The cost sheet for libraries reflects that typical condition, and the library costs are divided among structure, cladding, glazing, architectural finishes, MEP, and fixed contents. Values for non-fixed contents, such as furniture, equipment, computers, library books, art, etc., were added to each building estimate, based on annual university reports on the value of equipment and building contents. The formulas for calculating exterior building components, structure, and interior building components vary slightly because of the use of the distribution function in the structural calculation and the need to compute the interior components based on different ratings for different uses.

Structural Loss sample formula: (1)
Structural % Loss x distribution function x OGSF x Cost of Component by Building Type

Exterior Component Loss sample formula (cladding and glazing): (2)
Component % Loss x OGSF x Cost of Component by Building Type

Interior Component Loss sample formula (architectural finish, MEP, fixed contents) (3)
Component % Loss + (Potential Water Damage % Loss) x ASF x (ASF/OGSF) x Cost

The sum of all these components plus the special feature factors and the non-fixed contents gives the values of the losses as repair costs. Before proceeding to a final estimate, it was necessary to account for the fact that all the damage percentages associated with an event and a building may go to 100 percent if the damage to the structure went over a certain threshold. We examined the results of three potential thresholds, 40 percent, 50 percent, and 60 percent, plus a scenario with no step function (i.e., simply using the losses as calculated). Another sensitivity analysis was done to evaluate the use of the structural distribution function. Ultimately, we used a financially conservative estimate, including the probabilistic distribution of the structural loss calculations and a 60 percent structural damage threshold for triggering the increase in repair costs to 100 percent replacement.

ESTIMATES OF LOSSES AND TIME NEEDED FOR REPAIRS

Using the 60 percent step as the basis for our calculations, the cost of repairs in an occasional earthquake is about $720 million. In the Level 2 rare earthquake scenario, the costs rise to $1.7 billion. In the Level 3 very rare scenario, the total cost of repairs is estimated to be $2.9 billion. It is important to put these rather precise estimates into a more realistic range of possibilities. The sensitivity analysis suggests that the value of losses for the core campus could range from $500 million to $1 billion in the occasional or moderate earthquake, comparable to the losses in 1994 at California State University at Northridge. The Rare earthquake scenario—a M 7.0 on the Hayward fault—has repair costs ranging from $1 billion to $3 billion. The Very Rare scenario—a M 7.25 on the Hayward fault—could have repair costs that range from a low of $1.5 billion to a high of $4 billion. These estimates are not surprising. Indeed the highest estimates represent 30 to 40 percent of the full replacement value of campus buildings and contents at about $8.8 billion.

We analyzed how the closure of different kinds of buildings—classrooms, laboratories, libraries, offices, etc.,—would affect their operations. In the Occasional earthquake, the impact of building closure is not severe. In every case, except the laboratories, the percentage of space affected is less than 10 percent. Nineteen percent of the laboratory spaces are threatened with closure for more than twenty months. This is clearly a reflection of the poor condition of many of our current laboratory buildings, and of the sensitivity of their contents. In the Rare and Very Rare scenarios, the portion of labratory space needing to be closed ranges from 49 to 64 percent.

SPACE USE AND NUMBER OF OCCUPANTS

Two additional measures were germane to the loss estimate, 1) how buildings were used and 2) how many people used them. To understand of the way space is used on campus, we divided each building into its sub-areas of major use. Overall, there is approximately 5 million net or assignable square feet (ASF) of space in core campus buildings: 6 percent in classrooms, 30 percent in laboratories, 29 percent in offices, 16 percent in libraries, and 19 percent in other spaces, such as the student union, food services, performance space, storage, etc. This allocation of space is not significantly different from other universities.

Counting the number of people in buildings ought to be as easy as measuring space, but, in fact, it requires a methodology that avoids double counting. The Equivalent Continuous Occupancy (ECO) Calculation is an abstract number used to measure the population at risk in any given building during an earthquake. It represents the number of persons theoretically occupying a building on a continual basis—for 24 hours a day, 365 days a year. The ECO provides a means to account for actual varying use. For example, one person present in a building for 8 hours a day, 52 weeks a year would contribute .33 to the ECO for that building. The following shows the calculation of this ECO.

$$\begin{array}{ccccccc} 56/168 & \text{x} & 52/52 & \text{x } 1 & = & .33 & (4) \\ \text{[Hrs of per Week/Total hrs per Week]} & \text{x} & \text{[Wks per Yr/Total Wks per Yr]} & \text{x Persons} & = & \text{ECO} & \end{array}$$

Accounting for all building occupants in all spaces of a building, a total ECO for each building can be calculated. This total building ECO is the number of persons who may be occupying a building at any given hour of any given day, distributed on an annual basis.

CONCLUSION

The University of California, Berkeley remains highly vulnerable to earthquake losses, despite the extraordinary efforts to improve the life safety of hazardous buildings. This vulnerability can be attributed to three key factors:

1. The potential for nonstructural and contents damage.
2. The potential for business interruption.
3. The potential for loss of research, students, and faculty.

This research provides the university with a methodology for evaluating risk and devising priorities for risk reduction in policies that recognize the importance of limiting damage in teaching, research, and library space, and limited damage to critical infrastructure in order to insure continued operations after a large earthquake.

REFERENCES

H. J. Degenkolb & Associates. 1978. *Investigation of seismic hazards.* University of California Campuses, Berkeley Campus Summary Notes.

Earthquake Engineering Research Institute. 1997. *Earthquake Spectra* 13(4): Theme Issue on Loss Estimation.

Hamburger, R. E., A. B. Court, J. R. Soulages. 1995. Vision 2000: A framework for performance based engineering of buildings. In *Proceedings SEAOC Annual Convention,* Indian Wells, California.

National Institute of Building Sciences. 1997. *HAZUS Technical Manual.* Washington D.C.: FEMA and NIBS.

Peat Marwick. 1989. *University of California at Berkeley, economic impact study, final report.* San Francisco: Peat Marwick.

Rutherford & Chekene. 1993. *Hearst Memorial Mining Building, seismicity and ground motion study.* Berkeley, Calif.: University of California.

University of California, Berkeley. 1997. *Preliminary seismic evaluation.* Planning Design and Construction, U.C. Berkeley.